5′-triphosphate RNA requires base-paired structures to activate antiviral signaling via RIG-I

Andreas Schmidt[a,1], Tobias Schwerd[a,1], Wolfgang Hamm[a,1], Johannes C. Hellmuth[a], Sheng Cui[b], Michael Wenzel[a], Franziska S. Hoffmann[a], Marie-Cecile Michallet[c], Robert Besch[d], Karl-Peter Hopfner[b], Stefan Endres[a], and Simon Rothenfusser[a,e,2]

[a]Division of Clinical Pharmacology, Department of Medicine, Ludwig-Maximilian University Munich, 80336 Munich, Germany; [b]Center for Integrated Protein Sciences, Department of Chemistry and Biochemistry, Gene Center, Ludwig-Maximilian University Munich, 81377 Munich, Germany; [d]Department of Dermatology and Allergology and [e]Section Gastroenterology and Endocrinology, Medizinische Klinik Innenstadt, Ludwig-Maximilian University Munich, 80337 Munich, Germany; and [c]Department of Biochemistry, University of Lausanne, CH-1066 Epalinges, Switzerland

Edited by Charles A. Dinarello, University of Colorado Health Sciences Center, Denver, CO, and approved May 26, 2009 (received for review January 29, 2009)

The ATPase retinoid acid-inducible gene (RIG)-I senses viral RNA in the cytoplasm of infected cells and subsequently activates cellular antiviral defense mechanisms. RIG-I recognizes molecular structures that discriminate viral from host RNA. Here, we show that RIG-I ligands require base-paired structures in conjunction with a free 5′-triphosphate to trigger antiviral signaling. Hitherto unavailable chemically synthesized 5′-triphosphate RNA ligands do not trigger RIG-I-dependent IFN production in cells, and they are unable to trigger the ATPase activity of RIG-I without a base-paired stretch. Consistently, immunostimulatory RNA from cells infected with a virus recognized by RIG-I is sensitive to double-strand, but not single-strand, specific RNases. In vitro, base-paired stretches and the 5′-triphosphate bind to distinct sites of RIG-I and synergize to trigger the induction of signaling competent RIG-I multimers. Strengthening our model of a bipartite molecular pattern for RIG-I activation, we show that the activity of supposedly "single-stranded" 5′-triphosphate RNAs generated by in vitro transcription depends on extended and base-paired by-products inadvertently, but commonly, produced by this method. Together, our findings accurately define a minimal molecular pattern sufficient to activate RIG-I that can be found in viral genomes or transcripts.

immunostimulatory RNA | melanoma differentiation-associated protein 5 | retinoid acid-inducible gene-I-like helicases | virus infection | interferon production

Viral infections are sensed by pattern-recognition receptors (PRRs) of the innate immune system that recognize pathogen-associated molecular patterns (PAMPs), and trigger antiviral gene programs, including the production of IFN type-I (1). Viral RNA serves as a PAMP and can be recognized by toll-like receptor (TLR)-3, TLR-7/8, double-stranded (ds)RNA-activated protein kinase (PKR), and the retinoid acid-inducible gene (RIG)-I-like helicase (RLH) family members RIG-I, melanoma differentiation-associated protein 5 (MDA-5), and laboratory of genetics and physiology (Lgp)2 (2–4). There is evidence that RIG-I signals on infection by many RNA viruses, including important human pathogens (5, 6). After ligand-mediated activation critically involving ATPase activity and the C-terminal regulatory domain (RD) RIG-I binds via its amino-terminal caspase-activation and recruitment domain (CARD) to the adaptor protein Cardif (MAVS, VISA, Ips-1) that then triggers the NFκB and IRF signaling pathways (7). The exact nature of the PAMP that allows RIG-I to discriminate viral from host RNA in the cytosol is highly controversial. Kim et al. (8) have shown that RNA produced by in vitro transcription (IVT) bearing a 5′-triphosphate end is able to trigger IFN production in cells. Thereafter, our laboratory and others have reported that an essential feature of the viral RNA ligand of RIG-I is a free 5′-triphosphate that is absent from host cytoplasmic RNA due to eukaryotic RNA metabolism (9, 10). Using 5′-triphosphate RNAs produced by IVT, these studies concluded that both single-stranded (ss) and dsRNAs activate RIG-I as long as they carry the 5′-triphosphate (8–10). The RD of RIG-I has subsequently been characterized as the structural entity that binds 5′-triphosphate and, thus, aids in defining ligand specificity (11, 12). However, the concept that the 5′-triphosphate modification in cytosolic RNA represents the complete PAMP recognized by RIG-I was challenged recently by several prominent studies, suggesting that (*i*) 3′-monophosphate RNAs, as produced by RNase L, might be RIG-I ligands (13); (*ii*) a 5′-triphosphate end is dispensable if the RNA ligand is double stranded and carries either 5′-monophosphates or is long enough (12, 14); and (*iii*) RIG-I ligands require uridine- or adenosine-rich sequences (15). These reports raise the question whether the 5′-modification with (tri)phosphate is sufficient, merely required, or in some cases dispensable for physiological RIG-I ligands. For this report, we have investigated the structural requirements to activate RIG-I-mediated antiviral signaling using defined ligands including synthetic 5′-triphosphate RNA.

Results

Ligand-Induced ATPase Activity Is Triggered by a Feature Other than the 5′-Triphosphate Moiety. Previous studies have shown that short 5′-triphosphate RNAs of 19 to 21 bases generated by IVT are potent RIG-I ligands that induce IFN in human monocytes independently of TLRs (8–10). To identify a minimal pattern sufficient to trigger RIG-I signaling, we analyzed different versions of a 19-mer model-RNA named 2.2 (Table S1). The chemically synthesized 5′-OH version of ss2.2 sense (s) RNA, its complementary antisense (as) strand, and their annealed base-paired version (ds2.2) failed to induce IFN-α when transfected into human monocytes (Fig. 1*A*). However, as expected from previous studies, IVT (5′-triphosphate) 2.2 RNA induced strong IFN production either as ssRNA (ss2.2s) or as dsRNA (ds2.2) (Fig. 1*A*). Of note, in our hands, chemically synthesized ds or ss 3′- or 5′-monophosphorylated RNAs did not show significant immunostimulatory activity when we transfected them into human monocytes using the 2.2 sequence or a 25-mer sequence published to be active in mouse cells by Takahasi et al. (Fig. S1*A*) (12). However, they were active when transfected into human PBMCs containing plasmacytoid dendritic cells, indicating that these RNAs can be recognized by a different

Author contributions: A.S., T.S., W.H., J.C.H., S.C., K.-P.H., S.E., and S.R. designed research; A.S., T.S., W.H., J.C.H., S.C., M.W., and F.S.H. performed research; M.-C.M., R.B., and K.-P.H. contributed new reagents/analytic tools; A.S., T.S., W.H., J.C.H., S.C., M.W., F.S.H., R.B., S.E., and S.R. analyzed data; and A.S., S.E., and S.R. wrote the paper.

The authors declare no conflict of interest.

This article is a PNAS Direct Submission.

Freely available online through the PNAS open access option.

[1]A.S., T.S., and W.H. contributed equally to this work.

[2]To whom correspondence should be addressed. E-mail: simon.rothenfusser@med.uni-muenchen.de.

This article contains supporting information online at www.pnas.org/cgi/content/full/0900971106/DCSupplemental.

IMMUNOLOGY

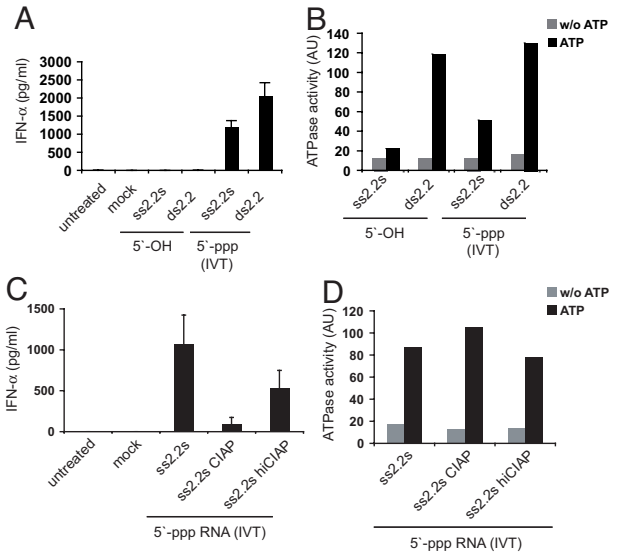

Fig. 1. In vitro transcribed ssRNA has a feature other than the 5′-triphosphate necessary for RIG-I activation. (*A*) Primary human monocytes were stimulated with ss- and dsRNAs that were chemically synthesized (5′-OH) or generated by IVT (5′-ppp). After 36 h, IFN-α was quantified in the supernatant by ELISA. (*B*) The same set of RNA ligands was assayed for their ability to induce ATPase activity in recombinant purified full-length RIG-I protein. Each condition was done in the presence and absence of ATP. (*C*) Untreated or CIAP-treated 5′-ppp-ssRNA (IVT) was tested for immunostimulatory capacity on monocytes as in *A*. RNA treatment with heat-inactivated (hi)CIAP was used as a control. (*D*) Fluorescence signal of the ATPase assay was measured after incubation of full-length RIG-I protein with RNA oligonucleotides from *C*.

PRR like TLR7 (Fig. S1*B*) (16, 17). When we examined IVT ss2.2s and ds2.2 RNAs, they both induced ATPase activity of purified RIG-I in vitro, whereas ss 5′-OH-RNA did not (Fig. 1*B*). Double-stranded 5′-OH-RNA, even though unable to induce IFN, clearly triggered ATPase activation (Fig. 1*B*). To check whether the 5′-triphosphate modification in IVT RNAs is sufficient to trigger ATPase activity of RIG-I, we dephosphorylated IVT ss2.2s RNA with calf-intestine alkaline phosphatase (CIAP), and examined its immunostimulatory activity and ability to induce ATPase activity in RIG-I. Surprisingly, even though dephosphorylated ss2.2s RNA largely lost its immunostimulatory activity, indicating that its 5′-triphosphate modification has been quite efficiently removed (Fig. 1*C*), it retained its full ability to induce RIG-I ATPase activity (Fig. 1*D*). Together, these results confirmed the importance of the 5′-triphosphate modification for activation of RIG-I, and suggested that IVT ss2.2s RNA has a feature other than the 5′-ppp modification that triggers the ATPase activity of RIG-I and is missing in the synthetic 5′-OH-version of ss2.2s RNA.

RNAs Generated by IVT with T7 Polymerase Contain Unexpected Hairpin-Forming By-Products That Activate RIG-I. These results prompted us to examine the RNA products of our IVT reactions in more detail. Denaturing polyacrylamide gels showed that synthetic ss2.2s and ss2.2as RNAs could be observed at sizes according to their expected length (Fig. 2*A*). However, the RNA preparations produced by IVT contained pronounced amounts of products significantly longer than expected in addition to varying amounts of RNA of the expected size (Fig. 2*A*). When we reisolated IVT ss2.2as RNA from bands of the expected size and transfected it into primary human monocytes, no IFN production was seen (Fig. 2*B*). However, when the same amount of RNA isolated from a band of the unexpected size was tested, it induced amounts of IFN comparable with those induced by unpurified IVT ss2.2as RNA. Consistent with these results, only reisolates from the unexpected band were able to induce RIG-I ATPase activity (Fig. 2*C*). Comparable results were observed with ss2.2s RNA. Together, these results showed that the immunostimulatory activity of RNA produced by IVT resulted exclusively from unexpected, potentially base-paired RNA species.

It has been described that phage RNA polymerases such as T7, which is commonly used to produce IVT RNAs, possess an RNA-dependent RNA polymerase activity in addition to being a DNA-dependent RNA polymerase (18, 19). Therefore, RNA with self-complementarity at the 3′-end generated from a DNA-template can serve as a self-primed RNA-template that is elongated in a second step by the RNA-dependent-RNA polymerase activity of T7, potentially supporting the formation of nontemplated self-complementary products. Similar phenomena have been described for viral polymerases during viral replication as so called "copy-back" mechanisms (20). Due to the low degree of self-complementarity required, this phenomenon was found to be very common in IVT reactions (19). Indeed, using a previously analyzed large panel of permutated DNA-templates categorized into 3 groups according to their yield of expected and extended RNA products (type A, only the expected RNA; type B1.1, up to 2% extended products; type B2.1, up to 90% extended products; see ref. 19), we found that only in vitro transcribed RNAs that form high amounts of extended products were potent IFN inducers (Fig. S2*A*). Similarly, 100-mer poly(A) RNA generated by IVT as described by Saito et al. (15) was inactive in our hands if devoid of extended by-products (Fig. S2 *B* and *C*).

To prove that the unexpected bands derived from the 2.2 sequence do contain self-complementary structures, we sequenced clones of cDNA libraries constructed from RNA isolated from the expected and unexpected bands of IVT ss2.2s and ss2.2as. Indeed, whereas sequencing of RNAs from the expected band only identified sequences encoded by the respective DNA-template, the clones isolated from the unexpected bands contained sequences with 3′-extensions complementary to the original DNA-templated sequence; these extensions facilitate stable hairpin formation according to the prediction by the Mfold webserver (21). Two examples, clones 1 and 9, are shown in Fig. 2*D*. When we transcribed these sequences in vitro (for purity, see Fig. S3), they were able to induce significant amounts of IFN-α in human monocytes (Fig. 2*E*). The levels were comparable with those induced by ss2.2s IVT RNA or an optimized IVT hairpin artificially designed by fusion of the sense and antisense strand of the 2.2 sequence (hp2.2s/as). Interestingly, the amount of IFN induced by these RNAs seemed to correlate with the size of the stem structure. To investigate whether RIG-I mediates the recognition of these 5′-triphosphate hairpin RNAs, we silenced potential PRRs involved in 1205Lu melanoma cells using siRNA. Indeed, silencing of RIG-I, of its signaling adapter Cardif, and of both RIG-I and MDA-5 abolished IP10 production after stimulation with IVT 2.2 RNAs and clone 1 highlighting the requirement of RIG-I for recognition (Fig. 2*F*). These data were confirmed by experiments using mouse dendritic cells lacking Cardif and using HEK 293 cells overexpressing RIG-I (Fig. S4 *A* and *B*). Silencing MDA-5 alone led to a moderate decrease in IP10 production for these RNAs, suggesting that MDA-5 is not essential, but might be involved in a full signaling response. Depletion of PKR did not decrease IP10 production in any of the conditions tested. Together, these data show that small RNAs that carry both a base-paired hairpin structure and a 5′-triphosphate group in its proximity are potent RIG-I ligands. We propose that many observations that have been made with respect to RIG-I ligands using enzymatically synthesized RNAs might at least in part be due to unexpected RNAs that contain base-paired secondary structures in addition to the 5′-triphosphate end.

RNAs Require a Free 5′-Triphosphate and Base-Paired Stretches to Activate RIG-I. To investigate RIG-I activation in a system where the effect of base-pairing and 5′-triphosphate can be clearly separated,

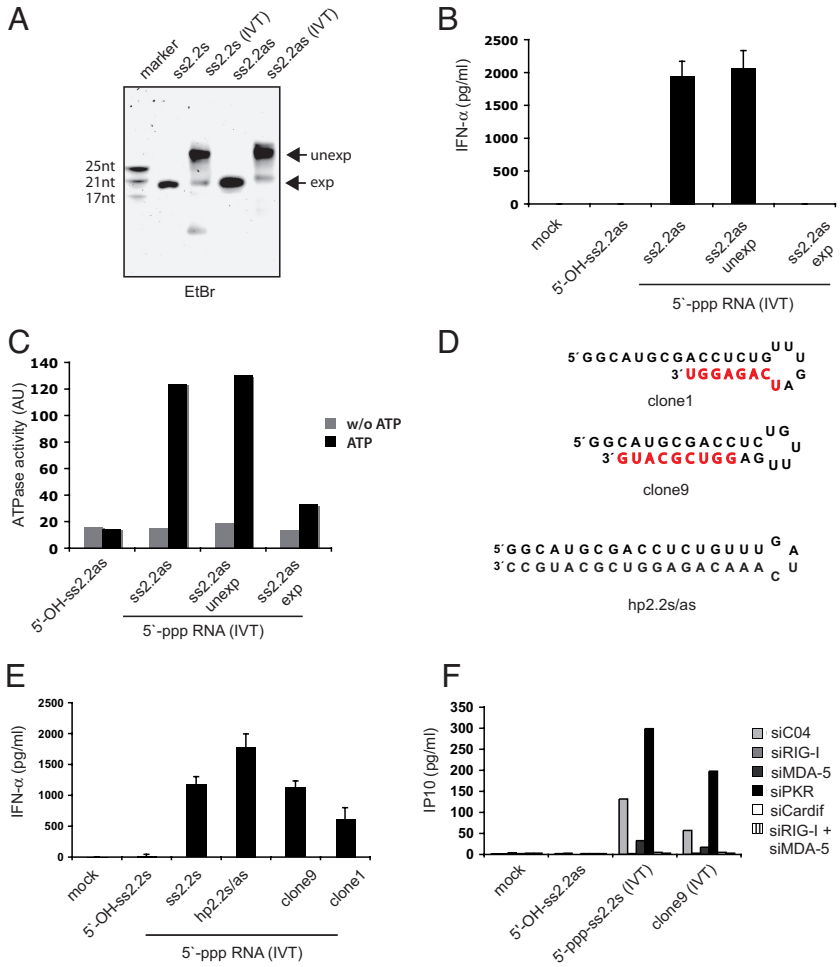

Fig. 2. 5′-triphosphate RNAs generated by IVT contain base-paired by-products that activate RIG-I. (*A*) Chemically synthesized 5′-OH-ssRNAs and 5′-ppp-ss2.2 RNAs generated by IVT were analyzed by denaturing gel electrophoresis and ethidium bromide (EtdBr) staining. Products of the expected (lower arrow in all samples), and unexpected (upper arrow in lanes containing 5′-ppp-RNA generated by IVT) size were reisolated for further analysis. (*B*) Reisolated IVT products were compared with 5′-OH-ss2.2as RNA and unpurified 5′-ppp-ss2.2as (IVT) RNA, for their ability to induce IFN-α production in human monocytes. (*C*) Stimulation of ATPase activity of recombinant, full-length RIG-I protein with reisolated and control RNAs. (*D*) Clones 1 and 9 are 2 RNA-sequences identified by 5′-ppp-ss2.2 RNA (IVT) small RNA cloning and sequencing. Nucleotides not encoded by the DNA template are indicated in red. Also, the sequence of a designed hairpin RNA (hp2.2s/as) based on the 2.2 model sequence is displayed. Secondary structures (minimum free energy) of clone 1, clone 9, and hp2.2s/as are as predicted by the Mfold software (21). (*E*) RNAs of clone 1, clone 9, and hp2.2s/as were generated by IVT and transfected into human monocytes. Production of IFN-α was measured by ELISA after 36 h. (*F*) The 1205Lu human melanoma cells were treated with the indicated siRNAs for 48 h and subsequently transfected with the indicated RNAs; 12 h after stimulation, supernatants were subjected to IP10 analysis by ELISA.

we resorted to defined, chemically synthesized 5′-triphosphate RNA (syn-ppp-ss2.2s). Of note, the production of 5′-triphosphate RNAs by nonenzymatic chemistry is a challenge, and these reagents were not available so far. We consistently found that syn-ppp-ss2.2s RNA, which like the expected IVT product of 2.2s cannot form stable secondary structures, was unable to induce IFN in cells (Fig. 3*A Left*). However, annealing of a complementary 5′-OH strand (5′-OH-ss2.2as) before transfection rescued IFN production, indicating that a base-paired structure was necessary and, together with a 5′-triphosphate, sufficient to trigger RIG-I (Fig. 3*A Left*). Thus, formation of a loop structure was dispensable in this system. Still, a chemically synthesized 5′-triphosphate hairpin RNA (syn-ppp-2.2hp) designed to incorporate base-paired secondary structure and 5′-triphosphate into one molecule lead to high-level IFN induction in human monocytes (Fig. 3*A Right*). Importantly, the corresponding 2.2 hairpin RNA lacking a 5′-triphosphate did not induce IFN (Fig. 3*A Right*). Signaling of chemically synthesized 5′-triphosphate RNAs showed the same RIG-I-dependence seen before with ligands generated by IVT (Fig. 3*D*; Fig. S4 *A* and *B*). Assaying RIG-I ATPase activity of the chemically produced ligands showed that only base-paired, but not unstructured 5′-triphosphate RNA, can induce ATP hydrolysis (Fig. 3*B*). This difference in activity was not due to a higher stability of base-paired RNA, because neither ssRNA nor dsRNA showed degradation under assay conditions (Fig. S4*C*). These results support our hypothesis and provide proof that the 5′-triphosphate end is not sufficient to mediate RNA-induced RIG-I activation and cannot trigger ATPase activity on its own.

To define the structural requirements for RIG-I activation in more detail, we hybridized successively longer 5′-OH-RNAs complementary to the 3′- or 5′-end of syn-ppp-ss2.2s RNA, and tested their ability to induce IFN production in monocytes and ATPase activity of recombinant RIG-I. When oligonucleotides of 5-, 10-, or 15-nts length were hybridized to syn-ppp-ss2.2s RNA from the 3′-end, no IFN production was observed (Fig. 3*C*); only fully complementary RNA (Fig. 3*A*) or an 18-mer hybridized to the 3′-end of syn-ppp-ss2.2s RNA could rescue IFN production (Fig. 3*C*). However, when 5-, 10-, or 15-nts complementary RNA were hybridized to the 5′-end of syn-ppp-ss2.2s RNA, 10 nts were sufficient to rescue IFN induction, suggesting that the extent of base-pairing as well as its relative position to the 5′-triphosphate-end are important determinants of immunostimulatory activity (Fig. 3*C*). Assaying the same set of RNAs for ATPase activity showed that ATP-hydrolysis depended on a base-paired stretch of >5 nts, but was independent of its relative position to or the presence of the 5′-triphosphate (Fig. 3*E*). Interestingly, complementary strands producing a short 3′-overhang at the 5′-triphosphate-bearing end of the oligonucleotide supported RIG-I ATPase activity, but did not induce IFN. The short overhang in direct proximity to the 5′-triphosphate group seemed to interfere with its correct recognition, highlighting the importance of a free 5′-triphosphate for signaling activity (Fig. S5 *A* and *B*). Together, these results show that a 5′-triphosphate modification on RNA is not sufficient to activate RIG-I signaling. They support a model in which a minimal pattern that can be recognized by RIG-I is a rather small stretch of base-paired RNA in addition to a 5′-triphosphate group. Of note, this finding does not seem to be an effect that is observed exclusively with short RNAs below 20 bases. A 70-mer RNA designed not to form secondary structures (Table S1) is

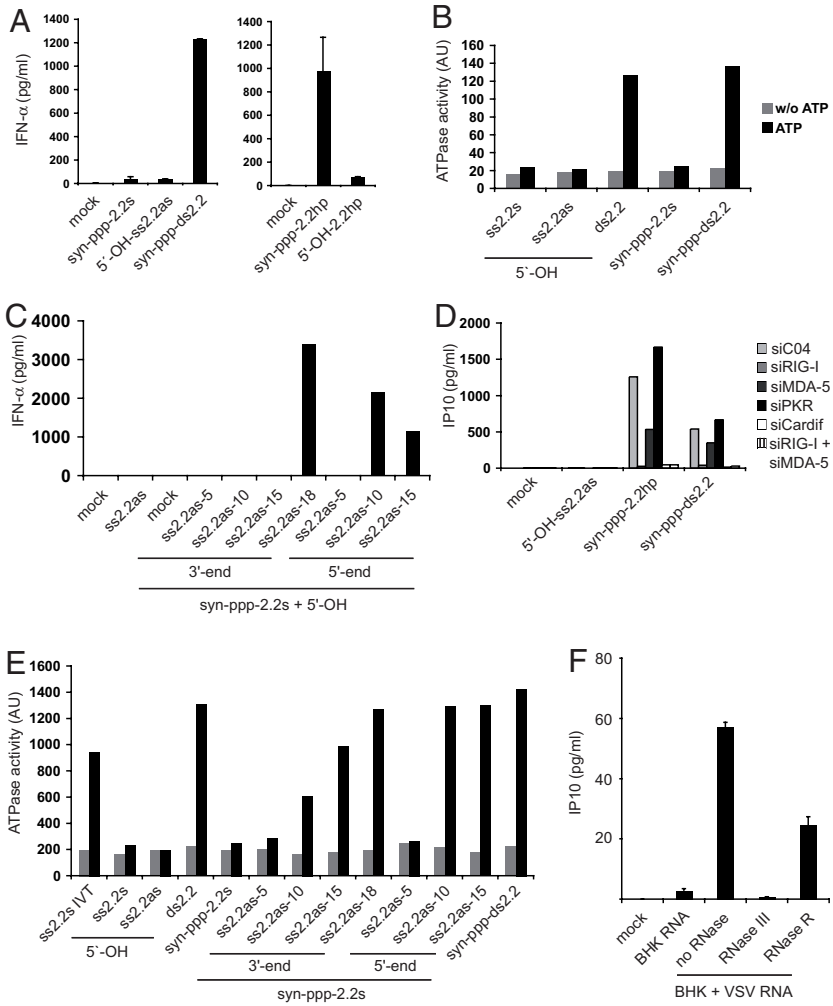

Fig. 3. A small base-paired stretch and the 5′-triphosphate are necessary and sufficient to activate RIG-I. (*A*) Chemically synthesized 5′-triphosphate 2.2 RNA (syn-ppp-2.2s) either alone or after hybridization (syn-ppp-2.2ds) to 5′-OH-ss2.2as RNA (*Left*) and chemically synthesized 2.2 hairpin RNA with (syn-ppp-2.2hp) or without (5′-OH-2.2hp) a 5′-triphosphate (*Right*) was transfected into human monocytes. IFN-α secretion was analyzed after 36 h. (*B*) Activation of ATP hydrolysis by full-length RIG-I protein was studied with chemically synthesized RNAs bearing either a 5′-OH group or a 5′-ppp group. (*C*) syn-ppp-2.2s RNA was hybridized to complementary OH-RNA of variable length. The length gradually increased from either the 3′- or the 5′-end. IFN-α production was assessed in human monocytes as in *A*. (*D*) 1205Lu human melanoma cells were stimulated with chemically synthesized RNAs after treatment with the indicated siRNAs for 48 h. IP10 levels were measured after 12 h by ELISA. (*E*) RNA oligonucleotides used in *C* were examined for their induction of RIG-I ATPase activity in full-length protein. (*F*) 1205Lu cells stimulated with total RNA isolated from BHK cells infected or not with VSV for 16 h at a multiplicity of infection of 0.2. RNA isolates from VSV-infected BHK cells were treated with equal activities of the RNases III or RNase R before transfection. IP10 levels were determined by ELISA 14 h after stimulation.

unable to induce IFN as an in vitro transcript. However, in line with our previous data, cytokine production and ATPase activity can be rescued by addition of a complementary strand (Fig. S6). Stressing the importance and requirement of the 5′-triphosphate modification for optimal activation of RIG-I, two chemically produced base-paired 70- and 40-nt RNAs lacking a 5′-triphosphate did not lead to detectable cytokine production in human 1205Lu cells (Fig. S6).

To investigate the importance of base-pairing in the setting of viral infection, we isolated total RNA from BHK cells infected with vesicular stomatitis virus (VSV), a virus known to be recognized by RIG-I (22). When we transfected 1205Lu cells with the RNA isolated from uninfected cells, no cytokine production was observed, because cellular RNA is not recognized by RIG-I. However, when we transfected RNA from virus-infected cells, IP10 production triggered by viral RNA ligands in the preparation could be observed. In line with our model, we found that the ds specific RNase III abolished signaling by these ligands, whereas the ss specific RNase R only had a minor effect on the activity of the RNA preparation (Fig. 3*F*). Specificity of the RNases was confirmed using synthetic ss or ds oligonucleotides (Fig. S7). Together, these results indicate that base-pairing is an important additional feature of the RIG-I ligands that generate the signal after viral infection.

Both Features of the PAMP Contribute to RIG-I Dimerization. Next, we wanted to examine the molecular basis of RIG-I activation by ligands carrying the bipartite PAMP. Dimerization of RIG-I molecules has been proposed to have a crucial role in promoting RIG-I signaling (11). Thus, we sought to examine the association state of RIG-I molecules in the presence of defined, synthetic RNA ligands in vitro. Recombinant purified RIG-I protein formed complexes with chemically synthesized RNAs when they were base-paired or carried a 5′-triphosphate group as assayed by native PAGE analysis (Fig. S8*A*). For a more detailed analysis, we performed gel filtration analysis of purified full-length RIG-I incubated with different synthetic RNAs. As expected, RIG-I incubated with ssRNA carrying a 5′-OH group (5′-OH-ss2.2s RNA) showed no change in the elution volume compared with RIG-I protein analyzed in the absence of RNA (Fig. 4*A*; Fig. S8*B*). When we incubated RIG-I with synthetic ss 5′-triphosphate RNA or a base-paired 5′-OH RNA, both induced an elution volume shift of RIG-I indicative of dimerization (Fig. 4*A*; Fig. S8*B*). Interestingly, when we incubated RIG-I protein with ligands that were base-paired and carried a 5′-triphosphate (synthetic or IVT), the shift in elution volume was more pronounced. Together, these results demonstrate that both features of the PAMP, base-pairing and 5′-triphosphate, independently contribute to the structural changes in RIG-I leading to its higher order assembly in vitro. They also suggest that the bipartite PAMP leads to a structural change different from that induced by the single features that possibly reflects the conformation of the signaling competent complex in vivo.

RIG-I Binding to Base-Paired 5′-Triphosphate RNA Is Mediated by Distinct Binding Sites. The structure of the RIG-I carboxyl-terminal RD (RIG-I RD or CTD) has been solved recently by X-ray crystallography and NMR spectroscopy, and a binding groove for the 5′-triphosphate and dsRNA structures was identified in the

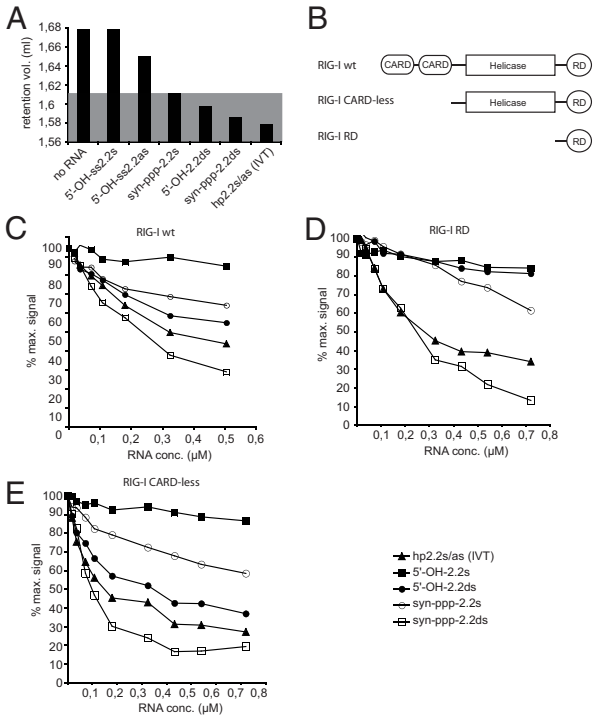

Fig. 4. Double-stranded 5′-triphosphate RNAs have multiple binding sites on RIG-I and induce dimerization of RIG-I. (*A*) Different RNAs were examined for their ability to induce homodimerization of recombinant full-length RIG-I protein. The protein-RNA mixture was loaded onto a gel filtration column, and the absorbance at 280 nm was determined. RIG-I elution volume peaks of the different mixtures are represented as columns. The gray area indicates the range of values interpreted as dimeric RIG-I-RNA complexes. (*B*) Schematic representation of the recombinant RIG-I proteins used in *C*, *D*, and *E*. (*C*) Recombinant RIG-I full-length protein prebound to fluorescently labeled 5′-ppp-hp2.2s/as RNA (IVT) was incubated with increasing amounts of unlabeled competitor RNAs. Fluorescence anisotropy was determined multiple times after each addition and equilibration. Binding and competition of the unlabeled RNAs is seen as a progressive loss of anisotropy signal. Background values were subtracted, and the anisotropy value of labeled RNA bound to RIG-I in the absence of a competitor was set as 100%. (*D*) The RNAs used in *C* were assayed by using recombinant RIG-I RD domain. (*E*) The RNAs used in *C* were assayed by using recombinant RIG-I protein lacking both CARD domains.

RIG-I RD domain (11, 12). To gain further insight into how the structural features of the bipartite RIG-I PAMP, base-paired stretch and 5′-triphosphate end, are recognized by RIG-I, we used a competitive binding assay based on fluorescence anisotropy. Different purified RIG-I proteins (Fig. 4*B*) prebound to fluorescently labeled IVT hp2.2s/as RNA were incubated with increasing amounts of unlabeled synthetic ligands, and the loss of the anisotropy signal was measured. As expected, 5′-OH ssRNA could not compete for binding with IVT hp2.2s-as RNA on full-length RIG-I (Fig. 4*C*). However, when we added RNAs bearing a base-paired stretch or a 5′-triphosphate end or both (5′-OH-ds2.2s, syn-ppp-ss2.2s or syn-ppp-ds2.2), a pronounced loss of fluorescence anisotropy could be observed, indicating that these RNAs compete with IVT hp2.2s-as RNA for binding to RIG-I (Fig. 4*C*). Consistent with our model, loss of anisotropy was more pronounced with a ligand that contained both features of the PAMP (syn-ppp-ds2.2 and IVT hp2.2s-as RNA). When we competed from recombinant purified RIG-I RD protein in a very similar experiment, we found that, as with the full-length protein, a synthetic ligand that carried a base-paired stretch and a 5′-triphosphate was a superior competitor over a molecule bearing a 5′-triphosphate only, indicating that there is a contribution of base-paired stretches to binding the RD domain (Fig. 4*D*). However, the observation that a base-paired molecule that lacked a 5′-triphosphate could not compete showed that this contribution is small and the binding to the RD-domain is mainly determined by the 5′-triphosphate (Fig. 4*D*). Interestingly, when we used full-length RIG-I or protein that lacked the CARDs, but contains the helicase and RD domains, base-paired RNA lacking the 5′-triphosphate component was a better competitor than 5′-triphosphate RNA missing a base-paired stretch (Fig. 4*E*). Comparing the competition patterns of these 3 constructs provides molecular evidence that the helicase domain interacts strongly with the base-paired part of the molecule, and that this interaction constitutes a significant part of the overall binding of RNA ligands to RIG-I. Together, our observations are in line with a model in which the 5′-triphosphate end serves as an initial selective binding motif that associates with the RD domain, and formation of a stable and productive signaling complex occurs in a subsequent step, involving interaction of the base-paired part of the molecule with the helicase domain.

Discussion

We have studied the ligand requirements of RIG-I-mediated antiviral signaling using defined model ligands, including hitherto unavailable synthetic 5′-triphosphate RNA and RNA from virus-infected cells. We conclude that only the combination of a ds stretch of RNA, together with a 5′-triphosphate end, defines a sufficient PAMP recognized by RIG-I. Of note, the minimal extent of base-pairing that we find necessary for RIG-I activation is small (in the range of 5 to 10 bases). The observation that viral infections recognized by RIG-I are specifically characterized by the lack of high amounts of long (>20 bp) dsRNA in infected cells hints that our short model ligands might indeed be in the size range of natural viral ligands of RIG-I (10, 23). In vitro transcribed RNAs have been widely used to probe both the ligand requirements for RIG-I signaling in cells and the mechanisms of RIG-I activation in vitro. Our results clearly show that IVT products must be used with caution when conclusions about ligand requirements for RIG-I signaling are drawn (24). In our study, the functional analysis of IVT products revealed that nontemplated hairpin RNAs generated through the RNA-dependent RNA polymerase activity of T7 were the immunostimulatory RNA species. Interestingly, the self-templated copy-back activity of T7 presumably responsible for those RNA-species has also been demonstrated for the viral RNA polymerases of hepatitis C virus (HCV) and Sendai virus, which are both well described activators of RIG-I (20, 25, 26). It has been observed that RLHs, in particular MDA-5, are able to recognize the dsRNA analog poly(I·C) in the cytoplasm (22, 27, 28). However, for true dsRNA made by chemical synthesis, data are scarce. A recent publication that advocates the dispensability of the 5′-triphosphate end for dsRNA-recognition by RIG-I and differential recognition of long dsRNAs by RIG-I or MDA-5 shows that a chemically synthesized dsRNA of 70 nt without 5′-triphosphate leads to IFN responses that are minimal (>100-fold less) compared to stimulation with a natural RIG-I-dependent ligand (14). Together with our results that showed no activation of RIG-I by chemically produced dsRNA of up to 70 bases in the absence of a 5′-triphosphate, these findings in our view argue against the possibility that RIG-I is activated purely by dsRNA in a physiologically relevant way. The footprint of the ATPase-domain of SF2-family helicases is ≈6 to 7 base pairs (29). How structurally similar helicases distinguish RNAs by length in a range several 100 times larger than their footprint is not clear. Also, a current study shows differential recognition of poly I:C by RIG-I and MDA-5 in a much lower size range (30). Few reports exist that show direct recognition of particular viral RNAs by RIG-I in the setting of infection with a living virus (5, 31). In cases where data of this kind is available, these RNAs (the leader RNAs of negative-stranded RNA viruses and the EBERs of EBV) are comparably small, and contain hairpin-like structures in addition to and in proximity of a 5′-triphosphate end. In line with those data, we found that RNA

isolated from virus-infected cells remains immunostimulatory when treated with a ss specific RNase, but not when base-paired RNA is digested. Recently, it was suggested that viral RNA requires A- or U-rich stretches to activate RIG-I (15). The mechanism of sequence-specific ligand recognition has not been investigated in this context. We did not systematically test the influence of sequence content on RIG-I activation. However, the different short sequences we found to be active were neither A nor U rich (<50% A plus U). Therefore, the ligand features that have been identified by Saito et al. (15) may certainly be highly relevant in the context of HCV recognition, but do not seem to present a generalized structural motif that explains RIG-I ligand recognition. Our biochemical binding and competition data suggest that 5′-triphosphate end and base-paired stretch, the 2 parts of the PAMP, bind distinct sites on RIG-I. Even though the functional cellular assays clearly prove that only a bipartite ligand induces changes in RIG-I that lead to a signaling-competent complex, at the moment, we can only speculate on the nature of these changes. A parallel study showing that RIG-I translocates along dsRNA after binding the 5′-triphosphate provides a further important piece in the puzzle (32). In the future, the structural analysis of RIG-I protein with synthetic RNA ligands will provide us with more information on RIG-I activation mechanisms.

Materials and Methods

RNAs. RNAs (unmodified, monophosphate, and siRNA) and DNAs were purchased from Metabion. Eurogentec kindly produced the chemically synthesized 5′-triphosphate RNA (for details, see *SI Methods*). In vitro transcribed RNAs were synthesized by using the Megashortscript kit (Ambion). DNA templates were generated as previously described (9). RNAs were extracted with phenol/chloroform, precipitated with ethanol, and passed through a Mini Quick Spin Column (Roche). The treatment of IVT RNA with CIAP was carried out as in Hornung et al. (9). Small interfering RNA was applied to 1205Lu cells at 30 nM with Lipofectamine RNAiMax (Invitrogen) as a transfection reagent. After 48 h, the culture medium was exchanged, and cells were stimulated. For a detailed list of all RNA oligonucleotides used for stimulation, see Table S1. For DNA templates and primers, see Table S2, and for the siRNAs, see Table S3.

Cell Stimulation and Cytokine Measurement. Unless indicated otherwise, all primary cells and cell lines were stimulated at 200 ng/mL RNA using Lipofectamine 2000 according to the manufacturer's manual. The 1205LU cells were transfected with Lipofectamine RNAiMax. R848 was from 3M Pharmaceuticals. IFN-α was measured 36 h after stimulation in the supernatant of human monocytes, PBMCs, and murine dendritic cells using the IFN-α module set from Bender MedSystems and PBL, respectively. Human IP10 was analyzed 12 h after stimulation in the culture medium of 1205LU cells using the opteia set from BD. Induction of the IFN-β promoter was detected with a reporter assay in HEK 293 cells as described in Rothenfusser et al. (3); 24 h after transfection, the cells were stimulated with the indicated RNA oligonucleotides for 12 h.

Recombinant Protein and ATPase Activity Assay. The ATPase activity of recombinant, purified RIG-I-protein was measured using the ADP Quest HS Assay (DiscoveRx). Full-length RIG-I was expressed in insect cells and purified as described previously (11). The reaction mixture was prepared on ice in a total volume of 10 μL, containing 1 ng/μL purified RIG-I-protein, 1 ng/μL purified RNA oligonucleotide, and 100 μM ATP. Reactions were initiated by the addition of ATP and incubated for 2 h at 37 °C.

Isolation and Purification of RNA from Polyacrylamide Gels. Stained RNA bands of interest were cut out on a UV table. The gel slices were fragmented, and the RNA was eluted by adding elution buffer (0.5 M ammonium acetate/1 mM EDTA/0.2% SDS) for 12 h at 37 °C. Subsequently, the eluted RNA was extracted and precipitated as described above.

Size-Exclusion Chromatography. All experiments were carried out at room temperature, using a GE Ettan LC system equipped with a Superose 6 PC 3.2/30 (GE Healthcare) size-exclusion column. The size-exclusion column was equilibrated with buffer containing 30 mM Tris·HCl, pH 7.5/150 mM NaCl/2 mM DTT/10 μM $ZnCl_2$. After sample injection, UV absorption at both 260 and 280 nm wavelength was recorded. The column was calibrated with Gel Filtration Standard (Bio-Rad) before use.

Fluorescence Anisotropy Measurement. Fluorescence anisotropy experiments were performed with a FluoroMax-P fluorimeter (Horiba Jobin Yvon); 1 mL of buffer (30 mM Tris·HCl, pH 7.5/150 mM NaCl/5 mM 2-mercaptoethanol/10 μM $ZnCl_2$) and indicated amounts of fluorescently labeled RNA (in vitro transcribed hp2.2s/as RNA with incorporated Alexa Fluor 488–5-UTP) were preequilibrated in a quartz cuvette at 12 °C. Recombinant protein and competitor RNAs were added in a stepwise manner and mixed by gentle pippetting. Preequilibration was used until anisotropy signals were stabilized. The anisotropy data were collected using an excitation wavelength of 495 nm and monitoring the emission at 516 nm. A maximum number of 10 repeats were performed until <2% deviation of the signal was reached.

ACKNOWLEDGMENTS. We thank M. Linke and M. Ruesenberg from Eurogentec for organizing the synthesis of 5′-ppp-RNAs, Gerhard Steger for insightful discussions on RNA structure, and Julia Vorac and Simone Willms for excellent technical assistance. This work was supported by Deutsche Forschungsgemeinschaft Grants DFG RO 2525/3-1 (to S.R.), DFG GK 1202 (to T.S., W.H, J.C.H., S.R., R.B., and S.E.), and LMUexcellent (Center for Integrated Protein Science Munich 114, research professorship), Sonderforschungsbereich-TR 36, and EN 169/7-2 (to S.E.). This work is part of the thesis of T.S., W.H., and J.C.H. at the Ludwig-Maximilian University Munich.

1. Akira S, Uematsu S, Takeuchi O (2006) Pathogen recognition and innate immunity. *Cell* 124:783–801.
2. Andrejeva J, et al. (2004) The V proteins of paramyxoviruses bind the IFN-inducible RNA helicase, mda-5, and inhibit its activation of the IFN-beta promoter. *Proc Natl Acad Sci USA* 101:17264–17269.
3. Rothenfusser S, et al. (2005) The RNA helicase Lgp2 inhibits TLR-independent sensing of viral replication by retinoic acid-inducible gene-I. *J Immunol* 175:5260–5268.
4. Yoneyama M, et al. (2004) The RNA helicase RIG-I has an essential function in double-stranded RNA-induced innate antiviral responses. *Nat Immunol* 5:730–737.
5. Samanta M, Iwakiri D, Kanda T, Imaizumi T, Takada K (2006) EB virus-encoded RNAs are recognized by RIG-I and activate signaling to induce type I IFN. *EMBO J* 25:4207–4214.
6. Sumpter R, Jr, et al. (2005) Regulating intracellular antiviral defense and permissiveness to hepatitis C virus RNA replication through a cellular RNA helicase, RIG-I. *J Virol* 79:2689–2699.
7. Hiscott J, Lin R, Nakhaei P, Paz S (2006) MasterCARD: A priceless link to innate immunity. *Trends Mol Med* 12:53–56.
8. Kim DH, et al. (2004) Interferon induction by siRNAs and ssRNAs synthesized by phage polymerase. *Nat Biotechnol* 22:321–325.
9. Hornung V, et al. (2006) 5′-Triphosphate RNA is the ligand for RIG-I. *Science* 314:994–997.
10. Pichlmair A, et al. (2006) RIG-I-mediated antiviral responses to single-stranded RNA bearing 5′-phosphates. *Science* 314:997–1001.
11. Cui S, et al. (2008) The C-terminal regulatory domain is the RNA 5′-triphosphate sensor of RIG-I. *Mol Cell* 29:169–179.
12. Takahasi K, et al. (2008) Nonself RNA-sensing mechanism of RIG-I helicase and activation of antiviral immune responses. *Mol Cell* 29:428–440.
13. Malathi K, Dong B, Gale M, Jr, Silverman RH (2007) Small self-RNA generated by RNase L amplifies antiviral innate immunity. *Nature* 448:816–819.
14. Kato H, et al. (2008) Length-dependent recognition of double-stranded ribonucleic acids by retinoic acid-inducible gene-I and melanoma differentiation-associated gene 5. *J Exp Med* 205:1601–1610.
15. Saito T, Owen DM, Jiang F, Marcotrigiano J, Gale M (2008) Innate immunity induced by composition-dependent RIG-I recognition of hepatitis C virus RNA. *Nature* 454:523–527.
16. Diebold SS, Kaisho T, Hemmi H, Akira S, Reis e Sousa C (2004) Innate antiviral responses by means of TLR7-mediated recognition of single-stranded RNA. *Science* 303:1529–1531.
17. Hornung V, et al. (2005) Sequence-specific potent induction of IFN-alpha by short interfering RNA in plasmacytoid dendritic cells through TLR7. *Nat Med* 11:263–270.
18. Cazenave C, Uhlenbeck OC (1994) RNA template-directed RNA synthesis by T7 RNA polymerase. *Proc Natl Acad Sci USA* 91:6972–6976.
19. Nacheva GA, Berzal-Herranz A (2003) Preventing nondesired RNA-primed RNA extension catalyzed by T7 RNA polymerase. *Eur J Biochem* 270:1458–1465.
20. Behrens SE, Tomei L, De Francesco R (1996) Identification and properties of the RNA-dependent RNA polymerase of hepatitis C virus. *EMBO J* 15:12–22.
21. Zuker M (2003) Mfold web server for nucleic acid folding and hybridization prediction. *Nucleic Acids Res* 31:3406–3415.
22. Kato H, et al. (2006) Differential roles of MDA5 and RIG-I helicases in the recognition of RNA viruses. *Nature* 441:101–105.
23. Weber F, Wagner V, Rasmussen SB, Hartmann R, Paludan SR (2006) Double-stranded RNA is produced by positive-strand RNA viruses and DNA viruses but not in detectable amounts by negative-strand RNA viruses. *J Virol* 80:5059–5064.
24. Schlee M, et al. (2009) Approaching the RNA ligand for RIG-I? *Immunol Rev* 227:66–74.
25. Leppert M, Kort L, Kolakofsky D (1977) Further characterization of Sendai virus DI-RNAs: A model for their generation. *Cell* 12:539–552.
26. Zhong W, et al. (1999) Nucleoside triphosphatase and RNA helicase activities associated with GB virus B nonstructural protein 3. *Virology* 261:216–226.
27. Gitlin L, et al. (2006) Essential role of mda-5 in type I IFN responses to polyribonosinic:polyribocytidylic acid and encephalomyocarditis picornavirus. *Proc Natl Acad Sci USA* 103:8459–8464.
28. Yoneyama M, et al. (2005) Shared and unique functions of the DExD/H-box helicases RIG-I, MDA5, and LGP2 in antiviral innate immunity. *J Immunol* 175:2851–2858.
29. Durr H, Flaus A, Owen-Hughes T, Hopfner KP (2006) Snf2 family ATPases and DExx box helicases: Differences and unifying concepts from high-resolution crystal structures. *Nucleic Acids Res* 34:4160–4167.
30. Ranjith-Kumar CT, et al. (2008) Agonist and antagonist recognition by RIG-I, a cytoplasmic innate immunity receptor. *J Biol Chem* 284:1155–1165.
31. Plumet S, et al. (2007) Cytosolic 5′-triphosphate ended viral leader transcript of measles virus as activator of the RIG I-mediated interferon response. *PLoS ONE* 2:e279.
32. Myong S, et al. (2009) Cytosolic viral sensor RIG-I is a 5′-triphosphate-dependent translocase on double-stranded RNA. *Science* 323:1070–1074.

LETTERS

STING regulates intracellular DNA-mediated, type I interferon-dependent innate immunity

Hiroki Ishikawa[1], Zhe Ma[1] & Glen N. Barber[1]

The innate immune system is critical for the early detection of invading pathogens and for initiating cellular host defence countermeasures, which include the production of type I interferon (IFN)[1–3]. However, little is known about how the innate immune system is galvanized to respond to DNA-based microbes. Here we show that STING (stimulator of interferon genes) is critical for the induction of IFN by non-CpG intracellular DNA species produced by various DNA pathogens after infection[4]. Murine embryonic fibroblasts, as well as antigen presenting cells such as macrophages and dendritic cells (exposed to intracellular B-form DNA, the DNA virus herpes simplex virus 1 (HSV-1) or bacteria *Listeria monocytogenes*), were found to require STING to initiate effective IFN production. Accordingly, *Sting*-knockout mice were susceptible to lethal infection after exposure to HSV-1. The importance of STING in facilitating DNA-mediated innate immune responses was further evident because cytotoxic T-cell responses induced by plasmid DNA vaccination were reduced in *Sting*-deficient animals. In the presence of intracellular DNA, STING relocalized with TANK-binding kinase 1 (TBK1) from the endoplasmic reticulum to perinuclear vesicles containing the exocyst component Sec5 (also known as EXOC2). Collectively, our studies indicate that STING is essential for host defence against DNA pathogens such as HSV-1 and facilitates the adjuvant activity of DNA-based vaccines.

Nucleic acid species inadvertently generated by microbes after infection are potent inducers of cellular innate immune defences important for protection of the host[1–3]. Although considerable progress has been made into unravelling how RNA viruses induce type I IFN, required for triggering the production of anti-viral genes, little is known at the molecular level about the induction of IFN by DNA pathogens such as herpes simplex virus I (HSV-1) or by intracellular bacteria or parasites[5–10]. Toll-like receptor 9 (TLR9) is known to recognize CpG DNA to trigger IFN production in plasmacytoid dendritic cells (pDCs), and Z-DNA binding protein 1 (ZBP1, also known as DAI) was recently shown to be able to stimulate IFN transcription, but was found to be largely redundant in studies using DAI-deficient cells and mice[11–13]. Recently, a DNA receptor AIM2 was found to be important for ASC (also known as PYCARD)-dependent inflammasome mediated production of IL1β, but was not required for type I IFN production[14–18]. Thus, other innate signalling pathways that recognize intracellular non-CpG DNA species must exist to facilitate type I IFN production.

We previously demonstrated for the first time a role for STING (also referred to as TMEM173, MPYS and MITA), an endoplasmic reticulum (ER) resident transmembrane protein, in facilitating the production of type I IFN[4,19,20]. To evaluate the importance of STING in mediating DNA-induced innate immune responses, we used wild type (+/+) or $Sting^{-/-}$ low passage number mouse embryonic fibroblasts (MEFs) and compared the induction of type I IFN (IFNβ) in response to a variety of DNA ligands. Our results indicated that STING was essential for inducing IFNβ in response to transfected viral DNA (adenovirus, Ad5; herpes simplex virus, HSV-1 and -2), purified *Escherichia coli* DNA, calf thymus (CT) DNA, and interferon stimulatory DNA (ISD; double-stranded 45-base-pair oligonucleotides lacking CpG sequences) (Fig. 1a). Complete abrogation of IFNβ production was also observed after transfection of synthetic double-stranded DNA (poly(dG-dC)•poly(dC-dG), hereafter referred to as poly(dGC:dGC)) in $Sting^{-/-}$ MEFs, and slight IFNβ production was observed using poly(dAT:dAT), probably due to STING-independent, RIG-I (also known as DDX58)-dependent signalling[21,22]. The loss of STING did not significantly affect poly(I:C)-mediated type I IFN production, which is largely governed by MDA5 (ref. 5). Concomitant analysis further indicated a marked reduction in IL6 production in $Sting^{-/-}$ MEFs compared to controls after similar DNA transfections (Fig. 1a). ISD-mediated production of *Ifnb* and *Ifn2a* messenger RNA was not detectable in $Sting^{-/-}$ MEFs compared to controls (Fig. 1b). Translocation of IRF3 or IRF7 was thus not observed in ISD-transfected $Sting^{-/-}$ MEFs, indicating that STING probably functions in mediating intracellular-DNA-triggered IFN production upstream of TBK1 (Fig. 1c and Supplementary Fig. 1). NF-κB signalling was also defective in $Sting^{-/-}$ MEFs after exposure to transfected ISD (Supplementary Fig. 1). Given this, we next examined the importance of STING in facilitating intracellular-DNA-mediated production of type I IFN in antigen presenting cells. This analysis indicated that $Sting^{-/-}$ macrophages transfected with ISD, or infected with the DNA pathogens HSV-1 or *Listeria monocytogenes*, were greatly defective in their ability to manufacture type I IFN (Fig. 1d). However, the cleavage of pro-caspase 1 and production of active IL1β, which is AIM2-dependent, was unaffected by the loss of STING (Fig. 1e and Supplementary Fig. 1). Thus, STING functions independently of the AIM2 'inflammasome' pathway. Further analysis also indicated that STING was required for efficient DNA-mediated production of type I IFN in granulocyte–macrophage dendritic cells (GM-DCs), as well as pDCs (FLT3-ligand-induced dendritic cells, FLT3-DCs) (Fig. 1f, g). However, exogenous CpG DNA remained able to induce type I IFN in $Sting^{-/-}$ FLT3-DCs compared to controls, indicating that TLR9 functions independently of the STING pathway (Fig. 1g). The induction of IL6 in response to intracellular DNA was also reduced in $Sting^{-/-}$ macrophages (Supplementary Fig. 1). However, HSV-1 and CpG DNA remained able to induce IL6 in $Sting^{-/-}$ macrophages, probably through TLR9-dependent signalling (Supplementary Fig. 1)[11]. Furthermore, we noted that STING seemed to be essential for the production of type I IFN by cytomegalovirus (CMV), vaccinia virus (VVΔE3L) and baculovirus (Supplementary Fig. 1). STING therefore seems critical for intracellular-DNA-mediated production of type I IFN in fibroblasts, macrophages, conventional dendritic cells as well as pDCs.

We next evaluated the *in vivo* importance of STING in facilitating effective host defence against select virus infection. Principally,

[1]Department of Medicine and Sylvester Comprehensive Cancer Center, University of Miami Miller School of Medicine, Miami, Florida 33136, USA.

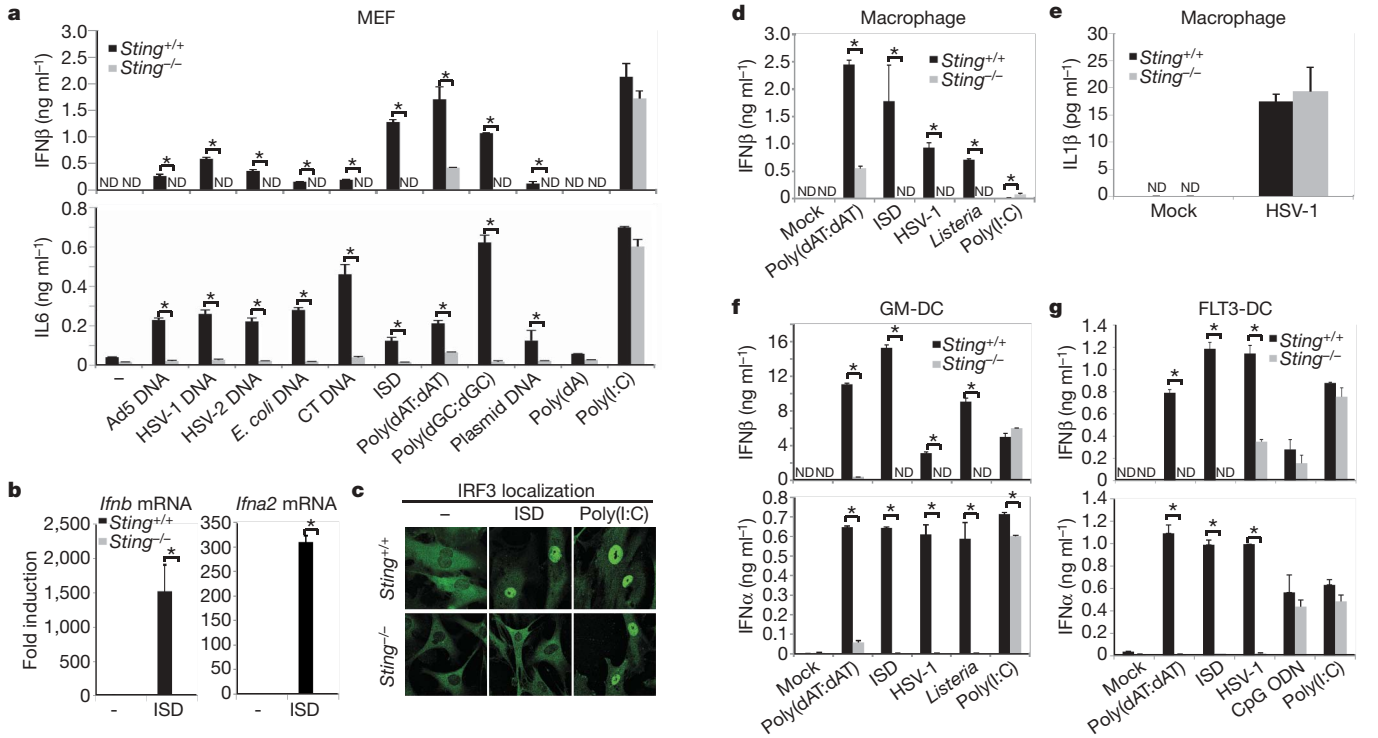

Figure 1 | STING is essential for intracellular DNA-mediated type I IFN production. **a**, MEFs were transfected with 1 μg ml^{-1} of DNA ligands (with Lipofectamine 2000) for 16 h, and IFNβ or IL6 were measured. **b**, MEFs were transfected with ISD for 4 h and *Ifnb* or *Ifna2* mRNA levels were measured. **c**, MEFs treated as in **b** were stained with an antibody for IRF3 translocation. Original magnification, ×40. **d**, Bone-marrow-derived macrophages were transfected with poly(dAT:dAT), poly(I:C) or ISD, or infected with HSV-1 (multiplicity of infection (m.o.i.) 10) or *Listeria* (m.o.i. 10) for 16 h, and IFNβ was measured. **e**, Macrophages were infected with HSV-1 for 16 h and IL1β was measured. **f**, GM-colony stimulating factor (CSF)-induced dendritic cells (GM-DCs) were treated as in **d**, and IFNβ or IFNα was measured after 16 h. **g**, FLT3-stimulated dendritic cells were treated as in **f** (exogenous CpG oligodeoxynucleotides (ODN) (1 μg ml^{-1}) were also used). $*P < 0.05$, Student's *t*-test. Error bars indicate s.d. ND, not determined.

Sting$^{-/-}$ or control mice were infected intravenously (i.v.) with HSV-1 and survival was monitored. The *Sting*-knockout mice died within 7 days of HSV-1 infection (Fig. 2a), whereas 80% of similarly infected wild-type mice survived. Significant amounts of HSV-1 were detected in the brain of infected *Sting*$^{-/-}$ mice, but not in controls at 5 days after infection (Fig. 2b). Analysis of serum from the *Sting*$^{-/-}$-infected animals indicated a profound defect in the production of type I IFN at 6 h after infection, compared to infected control animals (Fig. 2c, d and Supplementary Fig. 2). RANTES and IL6 levels were similarly markedly reduced in *Sting*$^{-/-}$ mice at the same time point (Fig. 2e, f). Moreover, *Sting*$^{-/-}$ mice were found to be more sensitive to HSV-1 after intravaginal administration of HSV-1 (Supplementary Fig. 2). This data indicates that STING is necessary, *in vivo*, for the effective production of type I IFN and is essential for efficient protection against HSV-1 infection.

Because we had previously seen, *in vitro*, a defect in the ability of the negative-stranded virus vesicular stomatitis virus (VSV) to induce type I IFN in the absence of STING, we next examined the *in vivo* importance of STING in protecting against VSV-related disease[4]. We observed that *Sting*$^{-/-}$ animals infected with VSV was also significantly sensitive to lethal infection compared to controls (Fig. 2g). Defects in type I IFN production were seen in *Sting*-knockout mice at early time points (6 h), although less so at 24 h (Fig. 2h, i and Supplementary Fig. 2). Thus, STING is necessary for efficient, early induction of type I IFN production and is required for protection against infection with the negative-stranded virus VSV, possibly by regulating the RIG-I and IPS-1 (also known as MAVS, VISA and CARDIF) pathway[4,6–10].

We did not observe a significant requirement for STING in facilitating poly(I:C) or EMCV (encephalomyocarditis virus, a positive-stranded flavivirus)-mediated IFN transcription, indicating that STING may not influence MDA5 function (Fig. 1a and Supplementary Fig. 2)[4]. However, it is known that some flaviviruses such as hepatitis C virus (HCV) can activate the RIG-I pathway, signalling which seems to be influenced by STING[4,23]. In this regard, databank analysis indicated that the flaviviruses yellow fever virus (YFV) and Dengue virus encode a product NS4B that exhibits strong homology with the amino terminus of STING (amino acids 125–222) (Supplementary Fig. 3). This region was found to be critical for STING function (Supplementary Fig. 3). Various flaviviral NS4B products have been shown to localize to the ER of the cell and to suppress the induction of type I IFN, although the mechanisms remain unclear[24]. Our analysis here indicates that that NS4B was able to inhibit STING activity, probably by direct association (Fig. 2j–l and Supplementary Fig. 3). Thus, STING may be targeted by certain viruses for suppression.

TBK1 has been shown to have an important role in mediating the adjuvant activity of DNA vaccines *in vivo*[12]. TBK1 activation in response to plasmid DNA was found to occur in the absence of the DNA sensors TLR9 or DAI, indicating that other pathways exist to facilitate DNA-mediated immunization[12,25]. To evaluate whether STING was involved in this signalling pathway, *Sting*$^{-/-}$ or control mice were immunized with plasmid DNA encoding the ovalbumin gene. Although we noted normal B- and T-cell subsets in unstimulated *Sting*$^{-/-}$ animals, after immunization *Sting*$^{-/-}$ mice showed significantly less serum ovalbumin (OVA)-specific IgG compared to controls (Fig. 3a and Supplementary Fig. 4). Furthermore, spleen CD8^{+} T-cell frequency and IFNγ secretion was markedly reduced in *Sting*$^{-/-}$ mice after immunization, compared to wild-type mice (Fig. 3b, c). Because immunoglobulin responses to OVA peptide were normal, these data emphasize that the STING-governed DNA sensor pathway is essential for efficient DNA-vaccine-induced T-cell

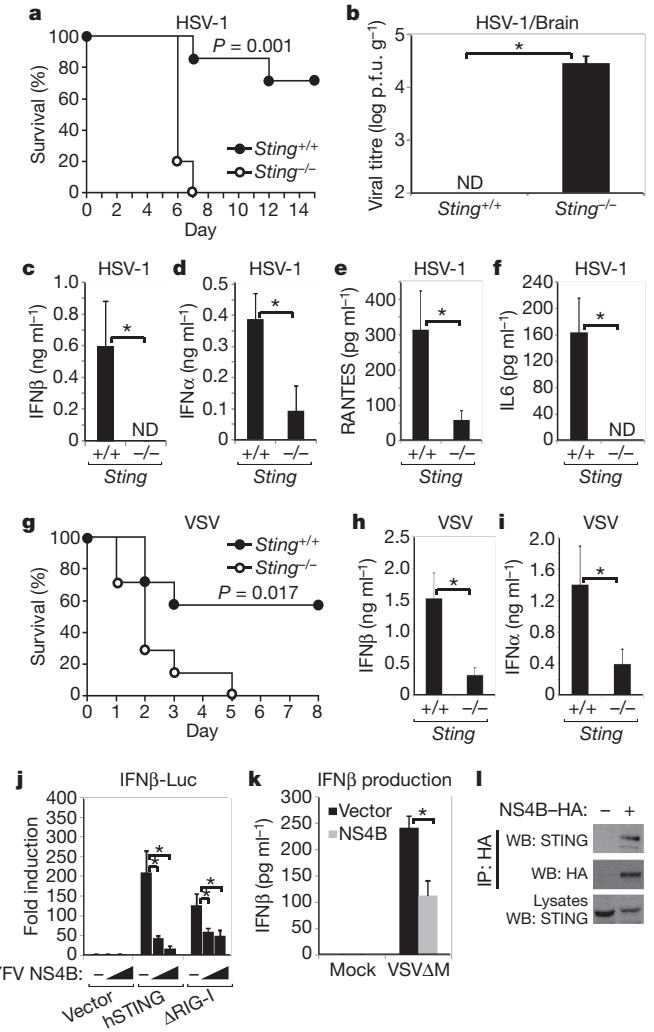

Figure 2 | STING is required for effective *in vivo* host defence. **a**, *Sting*-deficient animals ($Sting^{-/-}$) or littermate controls ($Sting^{+/+}$) ($n = 7$; approximately 8-weeks-of-age) were infected with HSV-1 (1×10^7 i.v.) and survival was monitored. **b**, $Sting^{-/-}$ or control mice were infected with HSV-1 as in **a** and brains were retrieved after 5 days for HSV-1 plaque assays. p.f.u., plaque-forming units. **c**, **d**, Serum from animals ($n = 3$) infected with HSV-1 (1×10^7 i.v.) was analysed for IFNβ (**c**) or IFNα (**d**) production after 6 h. **e**, **f**, Serum from animals infected as in **c** was analysed for RANTES (**e**) and IL6 (**f**) production. **g**, $Sting^{-/-}$ or control mice ($n = 6$) were infected with VSV (5×10^7 i.v.) and survival was monitored. **h**, **i**, Mice ($n = 3$) were treated as in **g** and IFNβ (**h**) or IFNα (**i**) was measured after 6 h. **j**, Increasing amounts of YFV NS4B were co-transfected into 293T cells with human STING or the amino terminus of RIG-I (ΔRIG-I, residues 1–284) and transfected IFNβ promoter-driven luciferase (IFNβ-Luc) was measured after 36 h. **k**, Immortalized MEFs were transfected with YFV NS4B for 24 h, infected with VSVΔM[4] (m.o.i. 1) for 16 h, and IFNβ was measured. **l**, 293 cells were transfected with NS4B–HA for 36 h and after immunoprecipitation (IP) with anti-haemagglutinin antibody, were analysed by western blot (WB) using anti-STING serum. $^*P < 0.05$, Student's *t*-test. Error bars indicate s.d.

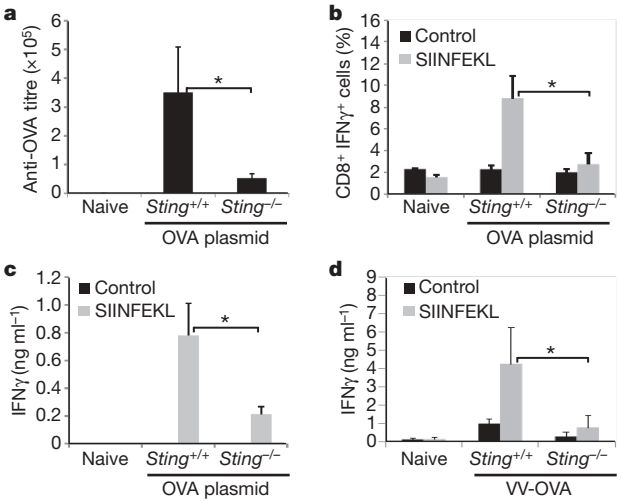

Figure 3 | STING is required for effective DNA-mediated adaptive immune responses. **a**, $Sting^{-/-}$ or control ($Sting^{+/+}$) mice ($n = 5$; approximately 8-weeks-of-age) were immunized twice (100 μg i.m.) by electroporation with a DNA vaccine encoding ovalbumin. Serum was measured for anti-OVA IgG. **b**, **c**, Mice were treated as in **a** and spleen $CD8^+$ $IFN\gamma^+$ cells were measured by fluorescence-activated cell sorting (FACS; **b**), and anti-OVA-specific IFNγ production was measured by ELISA after stimulation of splenocytes using SIINFEKL peptide (**c**). **d**, $Sting^{-/-}$ mice or controls ($n = 4$; approximately 8-weeks-of-age) were infected with vaccinia expressing ovalbumin (VV-OVA; 5×10^6 i.v.) and spleen anti-OVA-specific IFNγ production was measured by ELISA. $^*P < 0.05$, Student's *t*-test. Error bars indicate s.d. All experiments were repeated twice.

responses to antigen (Fig. 3 and Supplementary Fig. 4). Similar studies also indicated that STING had a key role in facilitating T-cell responses to the DNA virus vaccinia expressing ovalbumin (VV-OVA). Our data emphasizes the importance of STING in innate immune signalling processes required for DNA adjuvant activity (Fig. 3d).

We previously demonstrated that STING is an ER resident protein and member of the TRAP (translocon associated protein) complex that can associate with RIG-I and the mitochondrial innate immune signalling adaptor IPS-1 (refs 4, 26). Physical association of mitochondria and the ER, referred to as mitochondria-associated ER membrane (MAM), is important for transmission of Ca^{2+} to the mitochondria and for oxidative metabolism[27]. We thus examined whether STING could associate with MAMs. First, we reconstituted haemagglutinin (HA)-tagged STING into $Sting^{-/-}$ MEFs to follow endogenous STING localization using a haemagglutinin antibody. This analysis confirmed that STING is predominantly associated with the ER as determined by calreticulin marker co-staining (Fig. 4a). Mitotracker co-staining also indicated that STING may co-localize with mitochondria associated with the ER (Fig. 1b). The association of endogenous STING with the ER was also confirmed using anti-STING serum (Supplementary Fig. 5). Fractionation analysis subsequently demonstrated that STING is associated with microsomes, a complex of continuous membranes that comprise the ER, Golgi and transport vesicles (Fig. 4c). Endogenous STING was found to fractionate with MAMs and mitochondria fractions under non-stimulated conditions in MEFs (Fig. 4c). Calreticulin, known to be a chaperone involved in regulating the association of the ER and mitochondria, was observed to fractionate similarly[27]. This data may indicate that STING could associate with IPS-1 by MAM interaction[4]. Interestingly, after HSV-1 infection, STING was shown to become predominantly associated only with microsome fractions (Fig. 4c). To clarify these observations, we infected STING–HA MEFs with HSV-1, or transfected these cells with stimulatory ISD or negative-control single-stranded DNA (ssDNA). These results indicated that in response to HSV-1 infection or ISD transfection, STING translocated from the ER and predominantly congregated to perinuclear, non-ER microsome compartments in the cell (Fig. 4d and Supplementary Figs 5 and 6). Brefeldin A, but not chloroquine, blocked STING trafficking, indicating that STING locates from the ER via the Golgi to vesicles in the perinuclear region (Supplementary Fig. 5). This trafficking, in response to intracellular DNA, was similarly observed for TBK1, which we have previously shown to associate with STING[4] (Fig. 4e). Notably, in the absence of STING, TBK1 failed to relocate to perinuclear regions in response to ISD transfection (Supplementary Fig. 7).

We further observed that in the presence of DNA, STING mostly localized with the early endosome marker protein EEA1 and recycling

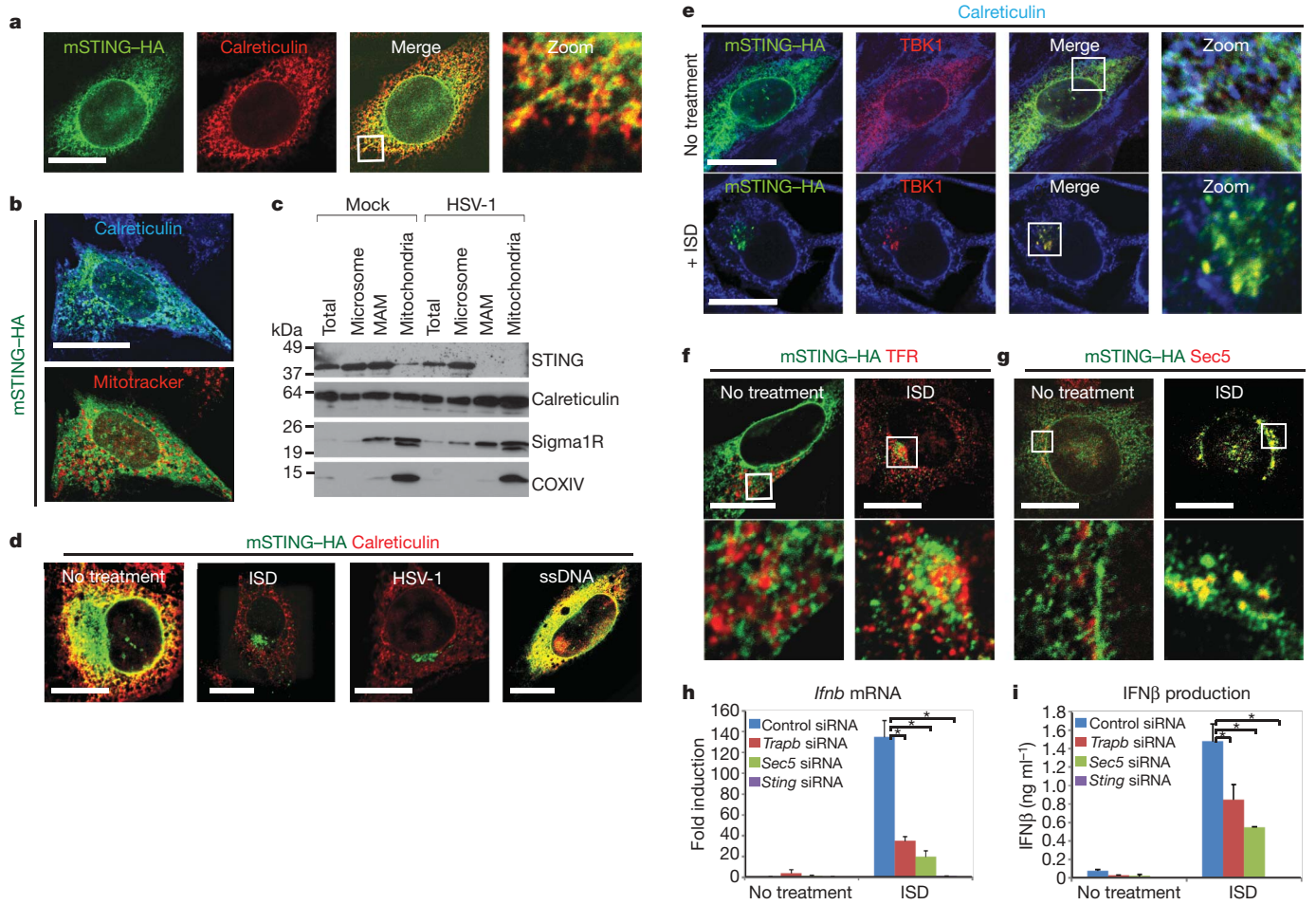

Figure 4 | STING translocates from the ER to Sec5-containing vesicles. **a**, *Sting*$^{-/-}$ MEFs, stably reconstituted with haemagglutinin-tagged mouse STING (mSTING–HA) were stained using haemagglutinin (green) and a calreticulin (red) antibody. **b**, STING–HA MEFs were stained for STING–HA (green), calreticulin (blue) or Mitotracker (red) and three-dimensional reconstruction images were taken. **c**, Immunoblot analysis of fractionation experiments of uninfected or HSV-1-infected (m.o.i. 10; 4 h) MEFs. Endogenous STING was detected using an anti-STING antibody. Calreticulin detects ER, Sigma1R detects MAM, and COXIV detects mitochondria. **d**, Haemagglutinin (green) or calreticulin (red) staining of mSTING–HA MEFs after treatment with transfected ISD (1 μg ml^{-1}), transfected ssDNA (1 μg ml^{-1}) or HSV-1 infection as in **c**. **e**, mSTING–HA MEFs were transfected with or without ISD and cells were stained with haemagglutinin (green), calreticulin (blue) and a TBK1 (red) antibody. **f**, mSTING–HA MEFs were transfected as in **e** and stained with haemagglutinin (green) and a TFR (red) antibody. **g**, mSTING–HA MEFs were transfected as in **e** and stained with haemagglutinin (green) and a Sec5 antibody (red). **h**, **i**, MEFs were treated with RNAi to *Trapb*, *Sting* or *Sec5* for 72 h and transfected with ISD. IFNβ mRNA and protein were measured at 4 and 16 h, respectively. *$P < 0.05$, Student's *t*-test. Error bars indicate s.d. Scale bars, 10 μm.

endosome marker transferrin receptor (TFR; Fig. 4f and Supplementary Fig. 6). TBK1 has also been demonstrated to associate with Sec5, a component of the exocyst 8 subunit complex that facilitates vesicular transport processes[28]. After intracellular DNA stimulation, STING was found to strongly colocalize with Sec5, which has also been demonstrated to associate in perinuclear endosome compartments (Fig. 4g)[29]. The RALB and Sec5 pathway has been previously shown to be required for efficient Sendai-virus-mediated type I IFN production[28]. However, our data here indicates that STING and TBK1 complexes may traffic to endosome compartments to associate with Sec5/exocyst components and facilitate the production of type I IFN in response to intracellular DNA. To evaluate whether Sec5 also modulates the production of IFNβ in response to ISD, we suppressed Sec5 production in normal MEFs using RNA interference (RNAi). This study indicated that in the absence of Sec5, ISD-mediated IFN production was significantly impaired (Fig. 4h, i). A similar effect was observed after knockdown of *Trapb* (also known as *Ssr2*) and *Sec61b*, components of the TRAP complex (Fig. 4h, i and Supplementary Fig. 8). Our data thus indicates that intracellular DNA may induce STING to complex with TBK1 and traffic to Sec5-containing endosome compartments—events that facilitate the production of type I IFN.

In conclusion, we demonstrate that STING is essential for the recognition of intracellular DNA and efficient production of type I IFN in all cell types examined. Loss of STING renders mice susceptible to lethal DNA virus infection (HSV-1). However STING also facilitates host defence responses to negative-stranded viruses such as VSV, plausibly through RIG-I and IPS-1–MAM translocon interactions. Although STING-independent, VSV-mediated type I IFN-induction pathways clearly exist, they do not seem to be sufficient on their own to protect mice against lethal VSV infection. We conclude that in response to intracellular DNA, STING and TBK1 complexes traffic to endosomal compartments to associate with exocyst components including Sec5, resulting in the induction of type I IFN.

METHODS SUMMARY

Details of mice, cells, viruses, plasmids, antibodies and reagents are given in the Methods. ELISA kits were obtained from following sources: murine IFNβ and IFNα (PBL), murine IL6 (R&D systems or Quansys Biosciences), murine IL1β and IFNγ (R&D systems), active NF-κB p65 (Active Motif) murine RANTES (Quansys Biosciences).

DNA vaccine. Mice were immunized with a plasmid encoding OVA by intramuscular (i.m.) electroporation (100 μg per mouse). The booster immunization was given within 4 weeks of the primary immunization.

Measurement of OVA-specific immune response. Spleen cells were extracted 2 weeks after the second immunization and stimulated with synthetic peptide for OVA (H-2Kb SIINFEKL, Proimmune) at 10 μg ml^{-1}. After 3 days, the cell culture supernatants were collected and analysed for the IFNγ titre by ELISA (R&D systems). For intracellular IFNγ staining, stimulated splenocytes were stained using FITC-labelled anti-CD8 antibody (BD). The serum anti-OVA antibody titre was measured by ELISA. Further details are given in the Methods.

Confocal microscopy. For localization of Sec5 and LAMP1, cells grown on coverslips were fixed in 80%/20% methanol/acetone at −20 °C for 5 min. For EEA1 staining, cells were fixed with 4% paraformaldehyde in PBS for 15 min at 37 °C, and were permeabilized in 0.2% Triton X-100. For staining of other proteins, cells were fixed with 4% formaldehyde in DMEM for 15 min at 37 °C, and were permeabilized in 0.2% Triton X-100. For mitochondria staining, living cells were incubated with 300 nM of Mito Tracker Red (Invitrogen) for 45 min at 37 °C.

RNA interference. Chemically synthesized 21-nucleotide short interfering RNA (siRNA) duplexes were obtained from Dharmacon, Inc. The sequences of each siRNA oligonucleotide used in this study are given in the Methods. MEFs were transfected using an Amaxa nucleofector apparatus (program A-023) and Amaxa MEF nucleofector kit 1 according to the manufacturer's instructions.

Full Methods and any associated references are available in the online version of the paper at www.nature.com/nature.

Received 2 August; accepted 3 September 2009.
Published online 23 September 2009.

1. Palm, N. W. & Medzhitov, R. Pattern recognition receptors and control of adaptive immunity. *Immunol. Rev.* **227,** 221–233 (2009).
2. Takeuchi, O. & Akira, S. Innate immunity to virus infection. *Immunol. Rev.* **227,** 75–86 (2009).
3. Beutler, B. A. TLRs and innate immunity. *Blood* **113,** 1399–1407 (2009).
4. Ishikawa, H. & Barber, G. N. STING is an endoplasmic reticulum adaptor that facilitates innate immune signalling. *Nature* **455,** 674–678 (2008).
5. Kato, H. *et al.* Differential roles of MDA5 and RIG-I helicases in the recognition of RNA viruses. *Nature* **441,** 101–105 (2006).
6. Yoneyama, M. *et al.* The RNA helicase RIG-I has an essential function in double-stranded RNA-induced innate antiviral responses. *Nature Immunol.* **5,** 730–737 (2004).
7. Kawai, T. *et al.* IPS-1, an adaptor triggering RIG-I- and Mda5-mediated type I interferon induction. *Nature Immunol.* **6,** 981–988 (2005).
8. Seth, R. B., Sun, L., Ea, C. K. & Chen, Z. J. Identification and characterization of MAVS, a mitochondrial antiviral signaling protein that activates NF-κB and IRF 3. *Cell* **122,** 669–682 (2005).
9. Meylan, E. *et al.* Cardif is an adaptor protein in the RIG-I antiviral pathway and is targeted by hepatitis C virus. *Nature* **437,** 1167–1172 (2005).
10. Xu, L. G. *et al.* VISA is an adapter protein required for virus-triggered IFN-β signaling. *Mol. Cell* **19,** 727–740 (2005).
11. Bauer, S., Pigisch, S., Hangel, D., Kaufmann, A. & Hamm, S. Recognition of nucleic acid and nucleic acid analogs by Toll-like receptors 7, 8 and 9. *Immunobiology* **213,** 315–328 (2008).
12. Ishii, K. J. *et al.* TANK-binding kinase-1 delineates innate and adaptive immune responses to DNA vaccines. *Nature* **451,** 725–729 (2008).
13. Takaoka, A. *et al.* DAI (DLM-1/ZBP1) is a cytosolic DNA sensor and an activator of innate immune response. *Nature* **448,** 501–505 (2007).
14. Muruve, D. A. *et al.* The inflammasome recognizes cytosolic microbial and host DNA and triggers an innate immune response. *Nature* **452,** 103–107 (2008).
15. Roberts, T. L. *et al.* HIN-200 proteins regulate caspase activation in response to foreign cytoplasmic DNA. *Science* **323,** 1057–1060 (2009).
16. Hornung, V. *et al.* AIM2 recognizes cytosolic dsDNA and forms a caspase-1-activating inflammasome with ASC. *Nature* **458,** 514–518 (2009).
17. Fernandes-Alnemri, T., Yu, J. W., Datta, P., Wu, J. & Alnemri, E. S. AIM2 activates the inflammasome and cell death in response to cytoplasmic DNA. *Nature* **458,** 509–513 (2009).
18. Bürckstüümmer, T. *et al.* An orthogonal proteomic-genomic screen identifies AIM2 as a cytoplasmic DNA sensor for the inflammasome. *Nature Immunol.* **10,** 266–272 (2009).
19. Jin, L. *et al.* MPYS, a novel membrane tetraspanner, is associated with major histocompatibility complex class II and mediates transduction of apoptotic signals. *Mol. Cell. Biol.* **28,** 5014–5026 (2008).
20. Zhong, B. *et al.* The adaptor protein MITA links virus-sensing receptors to IRF3 transcription factor activation. *Immunity* **29,** 538–550 (2008).
21. Ablasser, A. *et al.* RIG-I-dependent sensing of poly(dA:dT) through the induction of an RNA polymerase III-transcribed RNA intermediate. *Nature Immunol.* doi:10.1038/ni.1779 (16 July 2009).
22. Chiu, Y. H., Macmillan, J. B. & Chen, Z. J. RNA polymerase III detects cytosolic dna and induces type I interferons through the RIG-I pathway. *Cell* **138,** 576–591 (2009).
23. Saito, T., Owen, D. M., Jiang, F., Marcotrigiano, J. & Gale, M. Jr. Innate immunity induced by composition-dependent RIG-I recognition of hepatitis C virus RNA. *Nature* **454,** 523–527 (2008).
24. Muñoz-Jordan, J. L. *et al.* Inhibition of α/β interferon signaling by the NS4B protein of flaviviruses. *J. Virol.* **79,** 8004–8013 (2005).
25. Spies, B. *et al.* Vaccination with plasmid DNA activates dendritic cells via Toll-like receptor 9 (TLR9) but functions in TLR9-deficient mice. *J. Immunol.* **171,** 5908–5912 (2003).
26. Ménétret, J. F. *et al.* Single copies of Sec61 and TRAP associate with a nontranslating mammalian ribosome. *Structure* **16,** 1126–1137 (2008).
27. Hayashi, T., Rizzuto, R., Hajnoczky, G. & Su, T. P. MAM: more than just a housekeeper. *Trends Cell Biol.* **19,** 81–88 (2009).
28. Chien, Y. *et al.* RalB GTPase-mediated activation of the IκB family kinase TBK1 couples innate immune signaling to tumor cell survival. *Cell* **127,** 157–170 (2006).
29. Spiczka, K. S. & Yeaman, C. Ral-regulated interaction between Sec5 and paxillin targets Exocyst to focal complexes during cell migration. *J. Cell Sci.* **121,** 2880–2891 (2008).

Supplementary Information is linked to the online version of the paper at www.nature.com/nature.

Acknowledgements We thank J. Yewdell for VV-OVA, B. Jacobs for VVΔE3L, K. Frueh for HCMV, M. Kobayashi for baculovirus, H. Horiuchi for the Sec5 antibody, Y. C. Weh for *Tbk1*-knockout MEFs, and S. Nagata, T. Maniatis, J. Hiscott and N. Reich for plasmid constructs. This work was supported by NIH grant AI079336.

Author Contributions H.I. and G.N.B. designed the research and analysed the data. H.I. performed most experiments. Z.M. performed experiments related to YFV NS4B, carried out exocyst RNAi studies and helped with experiments. G.N.B. wrote the paper.

Author Information Reprints and permissions information is available at www.nature.com/reprints. Correspondence and requests for materials should be addressed to G.N.B. (gbarber@med.miami.edu).

METHODS

Mice, cells, viruses and reagents. *Sting*-knockout mice on a 129SvEv × C57BL/6J background have been described previously[4]. MEFs, bone-marrow-derived macrophages and GM-DCs were prepared as described previously[4]. To prepare FLT3-DCs, bone marrow cells were cultured in RPMI 1640 medium supplemented with 10% FBS, 50 μM 2-mercaptoethanol, 10 mM HEPES, pH 7.4, and 100 ng ml^{-1} human FLT3 ligand (Peprotech) for 8 days. 293T cells were obtained from the American Type Culture Collection (ATCC) and were maintained in DMEM medium supplemented with 10% FBS. VSV (Indiana strain), VSVΔM and EMCV were described previously[4]. HSV-1 (KOS strain) and *Listeria monocytogenes* (10403 serotype) were obtained from ATCC. Vaccinia virus encoding chicken ovalbumin (VV-OVA), vaccinia virus E3L deletion mutant (VVΔE3L), human cytomegalovirus (AD169 strain), and baculovirus (*Autographa californica* M nucleopolyhedrovirus) were gifts from J. Yewdell, B. Jacobs, K. Frueh and M. Kobayashi, respectively. Genomic DNA was obtained from following sources: HSV-1, HSV-2, adenovirus type 5 (ATCC); *E. coli*, and calf thymus (Sigma). Poly(dAT:dAT) and poly(I:C) were obtained from Amersham Biosciences. Poly(dGC:dGC) and poly(dA) were obtained from Sigma. CpG ODN (ODN 1585) was obtained from Invivogen. For stimulation of cells, genomic DNA, polydeoxynucleotides or poly(I:C) were mixed with Lipofectamine 2000 (Invitrogen) at a ratio of 1:1 (v/w), and then added to cells at a final concentration of 1 μg ml^{-1}. LPS was obtained from Invivogen. Brefeldin A and chloroquine were obtained from Sigma.

Plasmids. YFV NS4B sequence was amplified by PCR using pYFM5.2 encoding the complete YFV-17D sequence as a template, and was cloned into a pcDNA3 (Invitrogen) plasmid to generate carboxy-terminally haemagglutinin-tagged expression construct. C-terminally haemagglutinin-tagged STINGΔSP (Δ1–36 amino acids) and STINGΔTM5 (Δ153–173 amino acids) were amplified by PCR and cloned into a pcDNA3 plasmid. The expression plasmid containing chicken ovalbumin (OVA) complementary DNA was constructed by cloning of PCR-amplified *OVA* cDNA into pCDNA3. Expression plasmids encoding haemagglutinin-tagged murine STING (mSTING–HA), Flag-tagged ΔRIG-I (amino acids 1–284), ΔMDA5 (amino acids 1–349) and IRF-7 were described previously[4]. p110-Luc (IFNβ-Luc) was obtained from T. Maniatis. pUNO-hsaIRF3 (IRF3SA) and pUNO-hsaIRF7Δ (IRF7SA) were obtained from Invivogen. pCMV-SPORT6 containing murine DAI was obtained from Open Biosystems.

Primers. The following primers were used for cloning: YFV NS4B forward, 5′- GGGGTACCATGAACGAGCTAGGCATGCTGGAG-3′; YFV NS4B reverse, 5′- CCGCTCGAGCCGGCGTCCAGTTTTCATCTTC-3′; STINGΔSP forward, 5′-CCCAAGCTTGCCGCCACCATGCTAGGAGAGCCACCAGAGCAC-3′; STINGΔSP reverse, 5′- CCGCTCGAGAGAGAAATCCGTGCGGAGAG-3′; *OVA* forward, 5′-ATGG GCTCCATCGGCGCAGCAA-3′; *OVA* reverse, 5′-TTAAGGGGAAACACATCTGCC-3′.

Antibodies and ELISA. Rabbit polyclonal antibody against STING was described previously[4]. The antibody against STING-C was generated by immunizing rabbit with recombinant glutathione *S*-transferase (GST)–hSTING-C (amino acids 173–379) produced in *E. coli*. Rabbit polyclonal antibody against Sec5 was a gift from H. Horiuchi. Other antibodies were obtained from following sources: caspase-1 p10 (Santa Cruz Biotechnology), calreticulin (ab14234; Abcam), Sigma1 receptor (ab53852; Abcam), TBK1 (EP611Y, Abcam), COXIV (ab16056, Abcam), rabbit polyclonal HA (ab9110; Abcam), transferrin receptor (H68.4; Invitrogen), mouse monoclonal haemagglutinin (Sigma), Flag (M2; Sigma), IRF3 (ZM3; Zymed), TGN46 (ab16059; Abcam), giantin (ab24586; Abcam), EEA1 (no.2441; Cell Signaling), LAMP1 (NB120; Novus Biologicals) and Sec61β (Upstate). ELISA kits were obtained from following sources: murine IFNβ and IFNα (PBL), murine IL6 (R&D systems or Quansys Biosciences), murine IL1β and IFNγ (R&D systems), active NF-κB p65 (Active Motif), and murine RANTES (Quansys Biosciences).

Real-time PCR. Fluorescence real-time PCR analysis was performed using a LightCycler 2.0 instrument (Roche Molecular Biochemicals) and the following TaqMan Gene Expression Assays (Applied Biosystems): IFNβ (Mm00439546_s1), IFNα2 (Mm00833961_s1) and TRAPβ (Mm00481383_m1). Relative amounts of mRNA were normalized to the 18S ribosomal RNA levels in each sample.

Reporter analysis. 293T cells seeded on 24-well plates were transiently transfected with 50 ng of the luciferase reporter plasmid together with a total of 600 ng of various expression plasmids or empty control plasmids. As an internal control, 10 ng pRL-TK was transfected simultaneously. Then, 24 or 36 h later, the luciferase activity in the total cell lysate was measured.

DNA vaccine. Mice were immunized with a plasmid encoding OVA by i.m. electroporation (100 μg per mouse). The booster immunization was given within 4 weeks of the primary immunization.

Measurement of OVA-specific immune response. Spleens were extracted 2 weeks after the second immunization and 5×10^5 spleen cells were seeded on 96-well plates and then stimulated with synthetic peptide for OVA (H-2Kb SIINFEKL, Proimmune) at 10 μg ml^{-1}. After 3 days, the cell culture supernatants were collected and analysed for the IFNγ titre by ELISA (R&D systems). For intracellular IFNγ staining, stimulated splenocytes were stained using FITC-labelled anti-CD8 antibody (BD). After washing, cells were fixed and permeabilized. Then cells were stained using phycoerythrin (PE)-labelled anti-IFNγ antibody (BD). Flow cytometric analysis was performed on a FACScaliber instrument (BD). The serum anti-OVA antibody titre was measured by ELISA. In brief, 96-well plates were coated with an OVA protein at 1 μg ml^{-1} and then blocked with PBS containing 5% skimmed milk. Plates were washed and overlaid with serially diluted serum for 1 h at room temperature. After washing, antibodies were detected using goat anti-mouse IgG conjugated to horseradish peroxidase (Jackson Immuno Research). After further washing, the plates were stained using 3,3′,5,5′-tetramethylbenzidine (TMB, Sigma) as a substrate. The reaction was stopped with 1 M H_2SO_4 and the absorbance was measured. Antibody titres were expressed as the reciprocal of the endpoint dilution after background subtraction.

Fractionation. MAM, mitochondria and microsomes were isolated from *Sting*$^{-/-}$ MEFs stably transfected with mSTING–HA plasmid as previously described[30]. In brief, cells were washed in PBS and pelleted by centrifugation at 1,000*g* for 10 min. The pellet was resuspended in sucrose homogenization buffer (0.25 M sucrose, 10 mM HEPES, pH 7.4), and cells were lysed by using a dounce homogenizer. Lysed cells were centrifuged at 500*g* for 10 min, and the supernatant was collected. The supernatant was then centrifuged at 10,300*g* for 10 min to separate the crude microsomal (microsome and cytosol) from the crude mitochondrial (MAM and mitochondria) fraction, and the crude microsomal fraction (supernatant) was subjected to ultracentrifugation at 100,000*g* for 60 min. The crude mitochondrial fraction (pellet) was resuspended in ice-cold mannitol buffer A (0.25 M mannitol, 5 mM HEPES, 0.5 mM EDTA) and layered on top of a 30% Percoll in mannitol buffer B (0.225 M mannitol, 25 mM HEPES, 1 mM EDTA). Mitochondria and MAM fractions were separated by ultracentrifugation at 95,000*g* for 65 min. Both isolated fractions were diluted with mannitol buffer B and centrifuged at 6,300*g* for 10 min. The supernatant of MAM centrifugation was further separated by centrifugation at 100,000*g* for 60 min and the pellet was used for the MAM fraction, whereas the pellet of the mitochondria centrifugation was used as the mitochondria fraction. All of the fractions were resuspended in mannitol buffer B.

Confocal microscopy. For localization of Sec5 and LAMP1, cells grown on coverslips were fixed in 80%/20% methanol/acetone at −20 °C for 5 min. For EEA1 staining, cells were fixed with 4% paraformaldehyde in PBS for 15 min at 37 °C, and were permeabilized in 0.2% Triton X-100. For staining of other proteins, cells were fixed by 4% formaldehyde in DMEM for 15 min at 37 °C, and were permeabilized by 0.2% Triton X-100. For mitochondria staining, living cells were incubated with 300 nM of Mito Tracker Red (Invitrogen) for 45 min at 37 °C. Fixed and permeabilized cells were pre-incubated with 0.1% BSA in PBS and were incubated with primary antibodies. Cells were then incubated with secondary antibodies conjugated with FITC, Cy3 or Cy5 (Sigma).

RNA interference. Chemically synthesized 21-nucleotide siRNA duplexes were obtained from Dharmacon, Inc. The sequences of each siRNA oligonucleotide used in this study are follows: murine *Trapb* siRNA, 5′-UGAAAGAGAGGAC GGGUUAUU-3′; murine *Sec5* siRNA, 5′-AGAAGUAUUAGGUCGGAAA-3′, 5′-UCAACGUACUUCAGCGAUU-3′, 5′-CAGCAGAGAUUACACGUCA-3′, 5′-GUGAGUGGCUUGCGCAGUA-3′; murine *Sting* siRNA, 5′-CCAACAGC GUCUACGAGA-3′; murine *Sec61b* siRNA, 5′-GCAAGUACACGCGAUCA UA-3′, 5′-CAUCGCUGCUGUAUUUAUG-3′, 5′-CCACUGUUCGGCAGAGA AA-3′, 5′-GGCGAUUCUACACGGAAGA-3′. Control siRNA was obtained from Dharmacon (D-001206–01-80). MEFs were transfected by using an Amaxa nucleofector apparatus (program A-023) and Amaxa MEF nucleofector kit 1 according to the manufacturer's instructions. L929 cells were transfected using Lipofectamine RNAiMAX (Invitrogen). At 72 h after transfection, cells were used for further experiments.

Statistics. Student's *t*-test was used to analyse data.

30. Mavinakere, M. S., Williamson, C. D., Goldmacher, V. S. & Colberg-Poley, A. M. Processing of human cytomegalovirus UL37 mutant glycoproteins in the endoplasmic reticulum lumen prior to mitochondrial importation. *J. Virol.* **80**, 6771–6783 (2006).

nature immunology

RIG-I-dependent sensing of poly(dA:dT) through the induction of an RNA polymerase III–transcribed RNA intermediate

Andrea Ablasser[1,3], Franz Bauernfeind[1,3], Gunther Hartmann[1], Eicke Latz[2], Katherine A Fitzgerald[2,3] & Veit Hornung[1,3]

RNA is sensed by Toll-like receptor 7 (TLR7) and TLR8 or by the RNA helicases LGP2, Mda5 and RIG-I to trigger antiviral responses. Much less is known about sensors for DNA. Here we identify a novel DNA-sensing pathway involving RNA polymerase III and RIG-I. In this pathway, AT-rich double-stranded DNA (dsDNA) served as a template for RNA polymerase III and was transcribed into double-stranded RNA (dsRNA) containing a 5′-triphosphate moiety. Activation of RIG-I by this dsRNA induced production of type I interferon and activation of the transcription factor NF-κB. This pathway was important in the sensing of Epstein-Barr virus–encoded small RNAs, which were transcribed by RNA polymerase III and then triggered RIG-I activation. Thus, RNA polymerase III and RIG-I are pivotal in sensing viral DNA.

The immune system must trigger an arsenal of defense measures to combat invading microbes. The innate immune system is the first line of defense[1] and functions to control infection directly and relay signals to the adaptive immune system. Several classes of germline-encoded pattern-recognition receptors have been linked to innate defense. These include the Toll-like receptors (TLRs)[2], the C-type lectin receptors[3], the RIG-like helicases[4], members of the Nod-like receptor family[5] and cytosolic DNA sensors[6–8]. Individual pattern-recognition receptors recognize microbial products (also called 'pathogen-associated molecular patterns') from bacteria, viruses, fungi and parasites and trigger signaling pathways that regulate genes encoding molecules of the immune response. These include proinflammatory cytokines such as tumor necrosis factor (TNF), interleukin 1β and type I interferons[1,5]. Accumulating evidence shows that in addition to sensing microbial products, many of these same sensors detect 'danger' signals (or danger-associated molecular patterns) that are released from damaged or dying cells[9].

A common theme in the recognition of pathogen-associated molecular patterns is the sensing of non-self nucleic acids. Viruses, for example, are sensed almost exclusively via their nucleic acid genomes or as a result of their replicative or transcriptional activity[10]. In the cytosol, RIG-I and Mda5 (encoded by *Ddx58* and *Ifih1*, respectively) discriminate between different classes of RNA viruses[11,12]. RIG-I senses the nascent 5′-triphosphate moiety of viral genomes or virus-derived transcripts of negative-sense single-stranded RNA (ssRNA) viruses, whereas Mda5 is activated by long double-stranded RNA (dsRNA), a typical intermediate of the replication of positive-sense ssRNA viruses[13,14]. RIG-I also detects short blunt-ended dsRNA[15]. Both RIG-I and Mda5 engage the mitochondrial adaptor protein IPS-1 (also known as MAVS, Cardif or VISA)[16–19]. IPS-1 subsequently triggers 'downstream' signaling and activation of the kinase IKKα-IKKβ–transcription factor NF-κB pathway or the kinase TBK1–transcription factor IRF3 pathway, which promote the transcription of genes encoding inflammatory cytokines and type I interferon, respectively.

DNA is also a potent activator of innate immunity. In plasmacytoid dendritic cells (DCs), CpG DNA engages TLR9 to turn on transcription of the gene encoding interferon-α (IFN-α). A second DNA-sensing pathway elicits activation of the TBK1-IRF3 signaling pathway and transcription of genes encoding IFN-α and IFN-β, although the underlying mechanisms responsible for these last events are unclear. A candidate sensor, DAI (encoded by *Zbp1*)[7], has been shown to bind synthetic double-stranded DNA (dsDNA) and activate TBK1 and IRF3 to promote the transcription of interferon genes. Knockdown experiments have indicated that DAI is involved in sensing cytosolic DNA in some cell lines[7]. However, DAI-deficient embryonic fibroblasts and macrophages respond normally to cytosolic DNA[20], and DAI-deficient mice mount normal adaptive immune responses, which indicates possible redundancy with additional sensors. A second DNA sensor, AIM2 (absent in melanoma 2), has also been identified. AIM2 binds dsDNA and the adaptor protein ASC to form a caspase-1-activating inflammasome. However, AIM2 does not regulate the transcription of genes encoding type I interferon[8,21–23].

It is likely that in most cell types, DNA viruses trigger the transcription of genes encoding type I interferons through TLR-independent DNA-sensing mechanisms. Although type I interferons are best studied in antiviral immunity, evidence of the involvement of these cytokines in bacterial, fungal and parasitic infection has also emerged. *Francisella tularensis*[24], *Streptococcus agalactiae*[25], *Listeria monocytogenes*[26,27],

[1]Institute for Clinical Chemistry and Pharmacology, University of Bonn, Bonn, Germany. [2]Division of Infectious Diseases and Immunology, University of Massachusetts Medical School, Worcester, Massachusetts, USA. [3]These authors contributed equally to this work. Correspondence should be addressed to V.H. (veit.hornung@uni-bonn.de).

Received 6 June; accepted 13 July; published online 16 July 2009; doi:10.1038/ni.1779

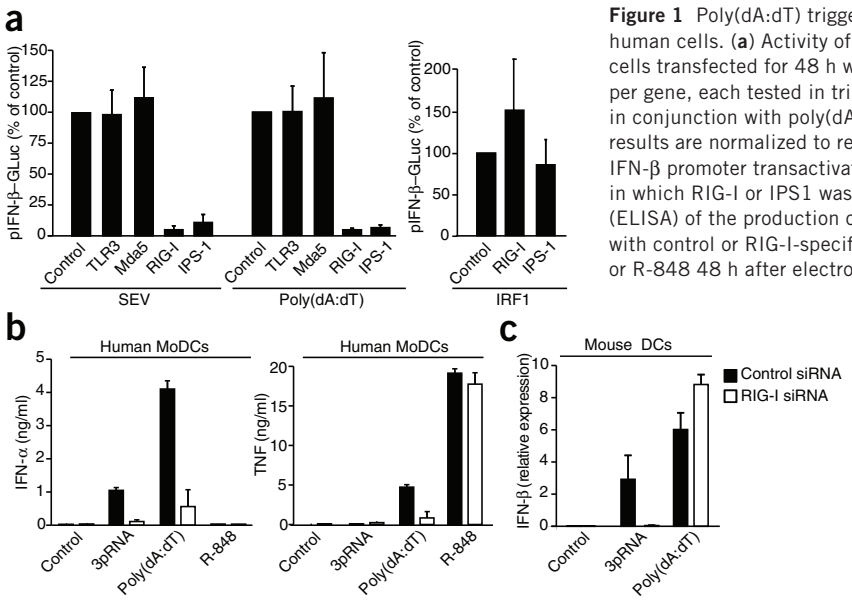

Figure 1 Poly(dA:dT) triggers the induction of type I interferon via RIG-I in human cells. (**a**) Activity of an IFN-β reporter plasmid (pIFN-β–GLuc) in 293T cells transfected for 48 h with siRNA targeting TLR3, RIG-I, Mda5 or IPS-1 (three per gene, each tested in triplicate), then transfected with the reporter plasmid in conjunction with poly(dA:dT) or SEV and assessed after an additional of 24 h; results are normalized to results obtained with control siRNA, set as 100%. Right, IFN-β promoter transactivation in response to overexpression of IRF1 in 293T cells in which RIG-I or IPS1 was silenced. (**b**) Enzyme-linked immunosorbent assay (ELISA) of the production of IFN-α or TNF by MoDCs transfected by electroporation with control or RIG-I-specific siRNA, then stimulated with 3pRNA, poly(dA:dT) or R-848 48 h after electroporation and assessed 24 h later. (**c**) Real-time PCR analysis of IFN-β induction in mouse bone marrow–derived DCs mock transfected (Control) or transfected by electroporation with control or RIG-I-specific siRNA, then stimulated 48 h after electroporation and assessed 5 h later; results are presented relative to the expression of *Hprt1* (encoding hypoxanthine guanine phosphoribosyl transferase). Data are from one representative of two (**a**) or three (**b**,**c**) experiments (mean and s.e.m.).

Mycobacterium tuberculosis[28], *Legionella pneumophila*[29], *Brucella abortus*[30] and *Trypanosomai cruzi*[31] all trigger type I interferon by what seems to be a TBK1- and IRF3-dependent pathway. Neither the host sensor nor the microbial ligands that trigger these responses have been clearly identified, although DNA has been suggested as the likely ligand[25,27]. Endogenous DNA molecules generated during autoimmunity are also probably sensed by this pathway. For example, macrophages from DNase II–deficient mice, which fail to digest DNA from engulfed apoptotic cells, show robust production of type I interferon and inflammatory cytokines through IRF3 activation, which leads to lethal anemia and chronic arthritis[32]. Defining the molecular mechanisms responsible for sensing DNA and the induction of type I interferons and inflammatory cytokines therefore may aid in understanding and treating infectious as well as autoimmune diseases.

Here we identify a novel DNA-sensing pathway involving RIG-I. AT-rich dsDNA served as a template for RNA polymerase III, which normally functions to transcribe 5*S* rRNA, tRNA and other small noncoding RNA through specific promoter regions. AT-rich dsDNA was transcribed by RNA polymerase III into dsRNA with a 5′-triphosphate moiety; this process converted AT-rich DNA into a RIG-I ligand. Moreover, we show that Epstein-Barr virus (EBV)-encoded RNAs (EBERs) was also transcribed by RNA polymerase III and then activated RIG-I and the transcription of genes encoding type I interferons. The RNA polymerase III–RIG-I pathway seems to be functional in both human and mouse cells, but in mouse cells, this pathway seems to be redundant with additional DNA-sensing mechanisms.

RESULTS

Poly(dA:dT) triggers type I interferons through RIG-I

To study the function of known RNA sensors in the detection of the negative-strand ssRNA paramyxovirus Sendai virus (SEV), we transfected human 293T embryonic kidney cells with small interfering RNA (siRNA) targeting TLR3, RIG-I, Mda5 or IPS-1. We used the dsDNA mimetic poly(dA:dT) as a control stimulus, as it has been shown to signal independently of these sensors in the mouse system[33,34]. As expected, SEV-mediated induction of type I interferon was completely abolished in 293T cells that had been treated with siRNA targeting RIG-I or IPS-1. Unexpectedly, poly(dA:dT)-triggered production of type I interferon was also abolished in 293T cells expressing RIG-I- or IPS-1-specific siRNA (**Fig. 1a**). Induction of type I interferon triggered by overexpression of IRF1 was unaffected by knockdown of RIG-I or IPS-1 (**Fig. 1a**). Dominant negative RIG-I constructs or targeting of IPS-1 with the hepatitis C virus–derived protease NS3-4A[19] in 293T cells also completely abolished poly(dA:dT)-triggered induction of type I interferon (**Supplementary Fig. 1a**). Similar findings have been reported before[5]. We found that poly(dA:dT) also activated NF-κB-dependent gene transcription through RIG-I (**Supplementary Fig. 1b**).

In primary human monocyte-derived DCs (MoDCs), RIG-I-specific siRNA also resulted in much lower type I interferon and TNF responses after poly(dA:dT) stimulation (**Fig. 1b**). TNF production in response to the TLR7-TLR8 ligand R-848 was unaffected, however. In agreement with published reports, mouse DCs or macrophages genetically deficient in IPS-1 (data not shown) or transfected by electroporation with siRNA targeting RIG-I were still responsive to poly(dA:dT) in terms of production of type I interferon (**Fig. 1c**). Together, these results indicate that RIG-I and IPS-1 are critical for poly(dA:dT)-triggered induction of type I interferon in human cells but are dispensable for these responses in cells of the mouse immune system.

Poly(dA:dT) activates RIG-I through an RNA intermediate

We next sought to understand how RIG-I, an RNA sensor, could respond to dsDNA. We first compared the kinetics of the interferon response after treatment of human peripheral blood mononuclear cells (PBMCs) with the true RIG-I stimulus 5′-triphosphate RNA (3pRNA) and transfected poly(dA:dT). PBMCs responded with slower kinetics to poly(dA:dT) than to 3pRNA (**Fig. 2a**), which suggested that poly(dA:dT) may activate RIG-I indirectly through the formation of an endogenous, secondary RNA ligand for RIG-I. To address that possibility, we isolated RNA from poly(dA:dT)-transfected 293T cells and tested its ability to stimulate the production of type I interferon in human PBMCs. We pretreated PBMCs with chloroquine to inhibit TLR9-dependent induction of type I interferon (**Supplementary Fig. 2a**) and then transfected the cells with RNA isolated from poly(dA:dT)-transfected or untransfected cells. Indeed, RNA derived from poly(dA:dT)-transfected 293T cells induced the production of type I interferon in PBMCs, but RNA derived from untransfected cells did not (**Fig. 2b**). The magnitude of the interferon response was similar to that obtained by SEV infection (**Fig. 2b**). This response was unaffected by treatment of the 293T cell–derived RNA with DNase I (**Supplementary Fig. 2b**), which indicated that the response was DNA independent. The induction of a stimulatory RNA species by poly(dA:dT) occurred within 4 h of transfection and peaked 9 h after delivery of poly(dA:dT) (**Fig. 2c**).

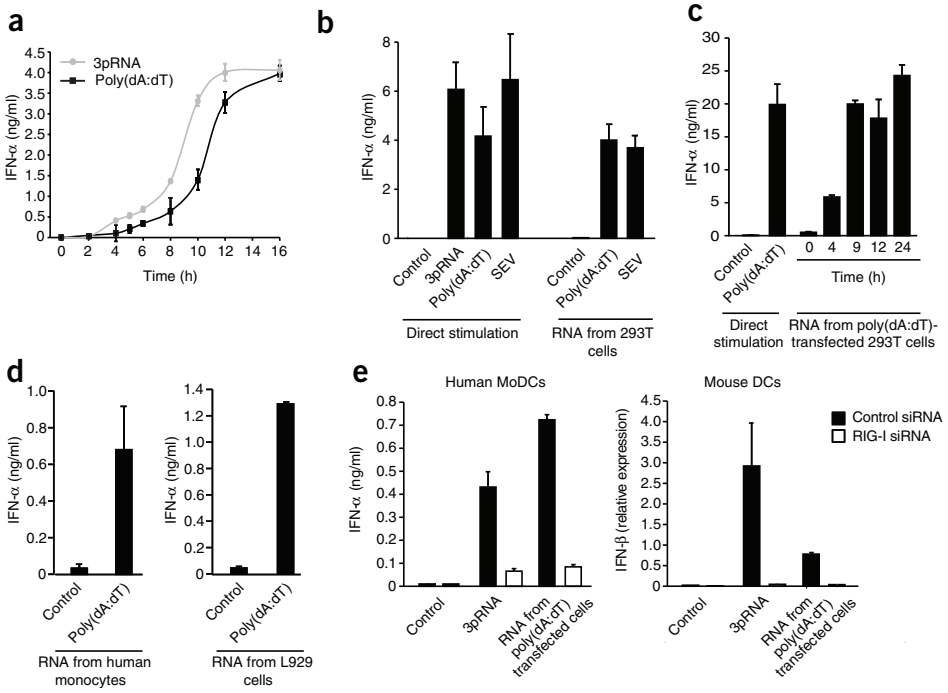

Figure 2 Poly(dA:dT) triggers the formation of endogenous RIG-I-stimulatory RNA. (**a**) ELISA of IFN-α production by human PBMCs transfected with 3pRNA or poly(dA:dT). (**b**) ELISA of IFN-α production by chloroquine-treated PBMCs transfected with RNA isolated from 293T cells stimulated with SEV or poly(dA:dT) (right) or PBMCs stimulated directly with 3pRNA, poly(dA:dT) or SEV (left), assessed 24 h after stimulation. (**c**) ELISA of IFN-α production by chloroquine-treated PBMCs stimulated with RNA isolated from 293T cells 0, 4, 9, 12 or 24 h after poly(dA:dT) transfection, assessed 24 h after stimulation. Far left, directly transfected poly(dA:dT) serves as a positive control; Control, mock-transfected cells (negative control). (**d**) ELISA of IFN-α production by PBMCs stimulated as described in **c** with RNA purified from poly(dA:dT)-transfected monocytes and L929 cells. (**e**) ELISA of IFN-α production (left) and real-time PCR analysis of IFN-β mRNA production (right) by human MoDCs or mouse DCs transfected by electroporation with control or RIG-I-specific siRNA and, after 48 h, stimulated with 3pRNA or RNA from poly(dA:dT)-transfected 293T cells, then assessed 24 h later (IFN-α) or 5 h later (IFN-β; presented relative to *Hprt1* expression). Data are from one representative of two (**a**,**c**,**d**), three (**e**) or four (**b**) experiments (mean and s.e.m.).

The ability of poly(dA:dT) to generate a stimulatory RNA ligand was not restricted to 293T cells, as RNA derived from primary cells (for example, human monocytes) stimulated with poly(dA:dT) induced type I interferon when transfected into human PBMCs (**Fig. 2d**). RNA derived from mouse L929 fibroblasts (**Fig. 2d**) or mouse embryonic fibroblasts (MEFs; data not shown) transfected with poly(dA:dT) also potently induced the production of type I interferon, which indicated that this mechanism was conserved across humans and mice. Knockdown of RIG-I in human MoDCs or mouse DCs resulted in a much lower type I interferon response triggered by RNA derived from poly(dA:dT)-transfected cells (**Fig. 2e**). We obtained similar findings with dominant negative RIG-I or the hepatitis C virus protease NS3-4A in 293T cells (**Supplementary Fig. 2c**). Together, these results indicate that transfection of poly(dA:dT) led to the generation of RNA species in both human and mouse cells, which activated RIG-I.

Having established that transfection of poly(dA:dT) led to the generation of an endogenous RNA ligand for the RIG-I pathway, we next determined whether dsDNA from other sources also triggered the RIG-I pathway by generating an RNA intermediate. We generated dsDNA molecules of various lengths and random sequences by PCR and tested their ability to trigger the production of type I interferon in 293T cells and in primary human PBMCs. We selected dsDNA molecules in the size range of the poly(dA:dT) used for our studies (~20–250 nucleotides; **Fig. 3a**). Notably, whereas poly(dA:dT) triggered type I interferon responses in both PBMCs and 293T cells, PCR-generated dsDNA failed to trigger this response in 293T cells (**Fig. 3b**). In contrast, we found a size-dependent interferon response to dsDNA in PBMCs (**Fig. 3a** and **Supplementary Fig. 3**). Contrary to the results we obtained with poly(dA:dT), the interferon response to PCR-generated dsDNA was not abolished in human MoDCs in which RIG-I was silenced (data not shown). In agreement with those findings, RNA derived from 293T cells transfected with poly(dA:dT) induced an interferon response, whereas RNA generated from PCR-generated dsDNA failed to do so (**Fig. 3c**). Collectively, these results indicate that in human cells, at least

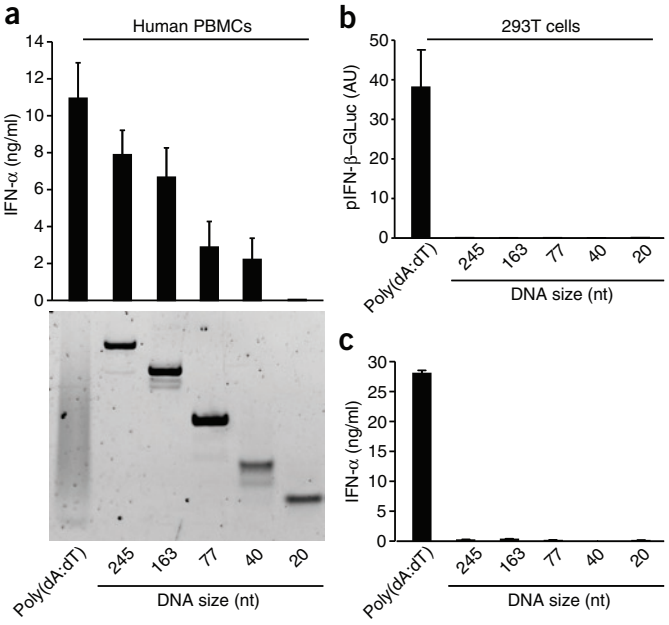

Figure 3 Non-poly(dA:dT) dsDNA triggers the induction of type I interferon through an RNA-independent pathway. (**a**,**b**) ELISA (**a**) or IFN-β reporter analysis (**b**) of the induction of type I interferon in chloroquine-blocked PBMCs or 293T cells transfected with dsDNA of various lengths (derived from pcDNA3 by PCR) and assessed 24 h after stimulation. Below (**a**), nondenaturing PAGE. AU, arbitrary units. (**c**) ELISA of IFN-α production by chloroquine-blocked PBMCs transfected for 24 h with RNA from 293T cells that had been transfected with dsDNA of various lengths. Data are from one representative of four (**a**,**c**) or three (**b**) experiments (mean and s.e.m.).

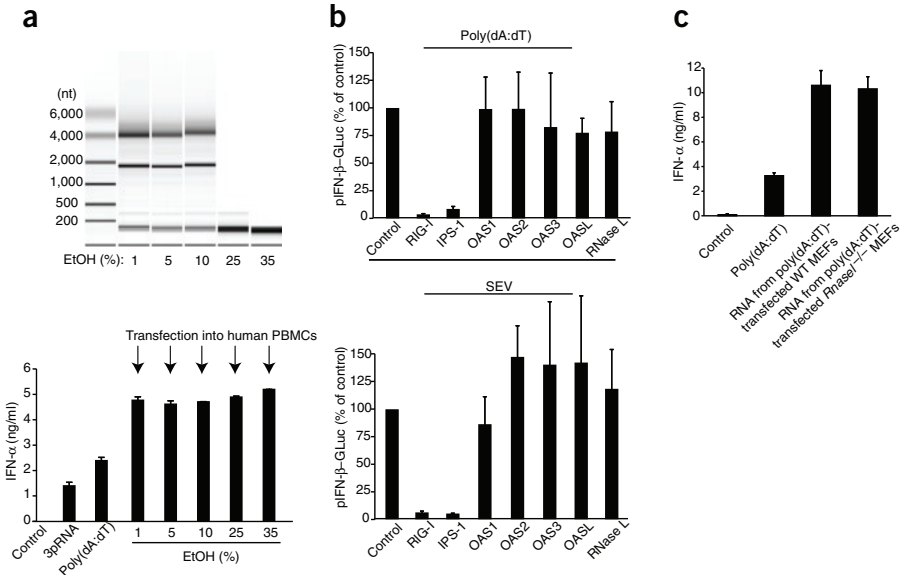

Figure 4 Poly(dA:dT) triggers the formation of a small stimulatory RNA species independently of the OAS–RNase L pathway. (**a**) Agilent RNA 6000 Pico Chip analysis of RNA isolated from poly(dA:dT)-transfected 293T cells and fractionated with various concentrations of ethanol during the initial binding step of the RNA in a silica matrix–based spin-column purification system (top). Below, induction of IFN-α by the RNA in chloroquine-treated PBMCs; direct stimulation with 3pRNA or poly(dA:dT) serves as a positive control. (**b**) IFN-β reporter activity in 293T cells transfected for 48 h with siRNA targeting various genes (horizontal axes; three per gene, each tested in triplicate), then transfected with an IFN-β reporter plasmid in conjunction with poly(dA:dT) (top) or SEV (bottom) and assessed after an additional 24 h; results are normalized to those of control siRNA, set as 100%. (**c**) ELISA of IFN-α production by chloroquine-treated PBMCs transfected with RNA isolated from poly(dA:dT)-transfected wild-type (WT) or *Rnasel*$^{-/-}$ MEFs. Far left, direct transfection of poly(dA:dT) serves as a control. Data are from one representative of four (**a**) or two (**b**,**c**) experiments (mean and s.e.m.).

two independent receptor systems exist to sense dsDNA: an indirect RIG-I pathway for poly(dA:dT), and a second RIG-I-independent pathway for random long dsDNA molecules. Both of these pathways are independent of TLR9.

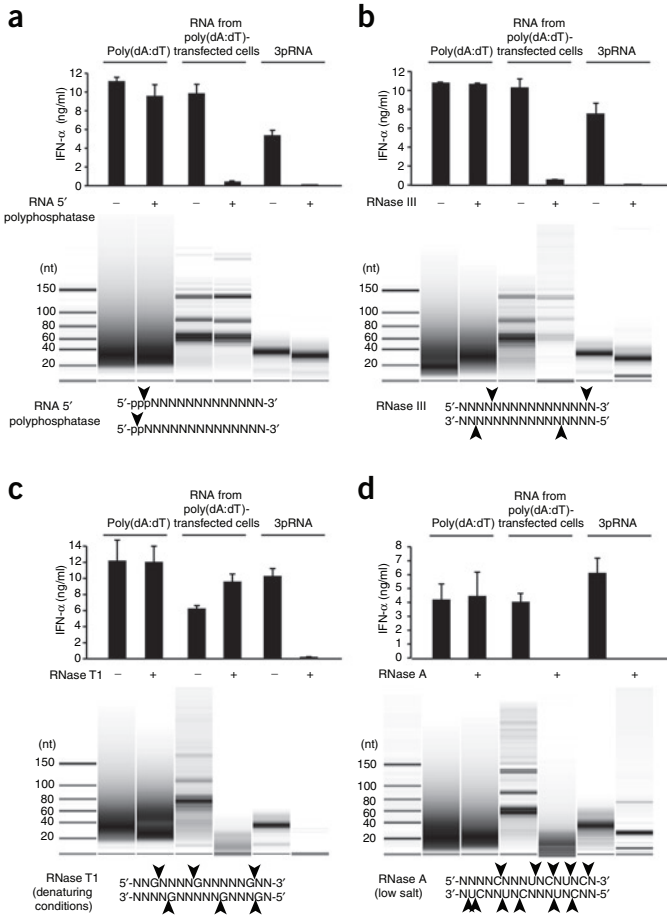

Figure 5 Poly(dA:dT)-induced RNA is a 5′-triphosphate dsRNA species devoid of guanosine. ELISA of IFN-α production by chloroquine-treated PBMCs transfected with RNA isolated from poly(dA:dT)-transfected 293T cells and treated with RNA 5′ polyphosphatase (**a**), RNase III (**b**), RNase T1 in denaturing conditions (**c**) or RNase A at a low salt concentration (**d**), or with poly(dA:dT) or 3pRNA treated the same way, and assessed 24 h later (top). Below, analysis of nucleic acids on an Agilent small RNA chip (bottom, enzymatic activity of enzymes). Data are from one representative of two (**a**,**d**) or four (**b**,**c**) experiments (mean and s.e.m.).

Characterization of the RNA intermediate

To further characterize the poly(dA:dT)-dependent RNA species, we isolated and fractionated RNA from 293T cells that had been transfected with poly(dA:dT). By using different ethanol concentrations during the binding of RNA to a silica column, we were able to crudely fractionate RNA into different sizes. We then tested the ability of these RNA fractions to trigger interferon. The small RNA fraction (less than 200 nucleotides in length) was sufficient to induce type I interferon (**Fig. 4a**). The antiviral endoribonuclease RNase L, which is activated by 2′,5′-linked oligoadenylates derived from 2′,5′-oligoadenylate synthetase (OAS), produces small RNA-cleavage products from self RNA that can initiate interferon production through the RIG-I–IPS-1 pathway. Small RNA molecules of less than 200 nucleotides isolated from RNase L–activated cells have been shown to contain this stimulatory RNA species[36]. We therefore examined the function of the OAS–RNase L system in the interferon response to poly(dA:dT). Transient overexpression of OAS1, OAS2, OAS3 or RNase L did not alter poly(dA:dT)-induced induction of type I interferon (data not shown). Furthermore, overexpression of dominant negative RNase L mutants (data not shown) or targeting of RNase L, OAS1, OAS2, OAS3 or OASL with siRNA (**Fig. 4b**) did not inhibit poly(dA:dT)- or SEV-triggered type I interferon responses. Finally, RNA isolated from poly(dA:dT)-transfected wild-type or *Rnasel*$^{-/-}$ MEFs cells induced similar production of type I interferon (**Fig. 4c**). Thus, poly(dA:dT) transfection induces the formation of stimulatory small RNA independently of OAS and RNase L.

To define the features of the poly(dA:dT)-triggered RNA species important for the interferon response, we took advantage of several RNA-modifying enzymes. To determine if phosphate groups were important features of the RNA, we treated poly(dA:dT) itself,

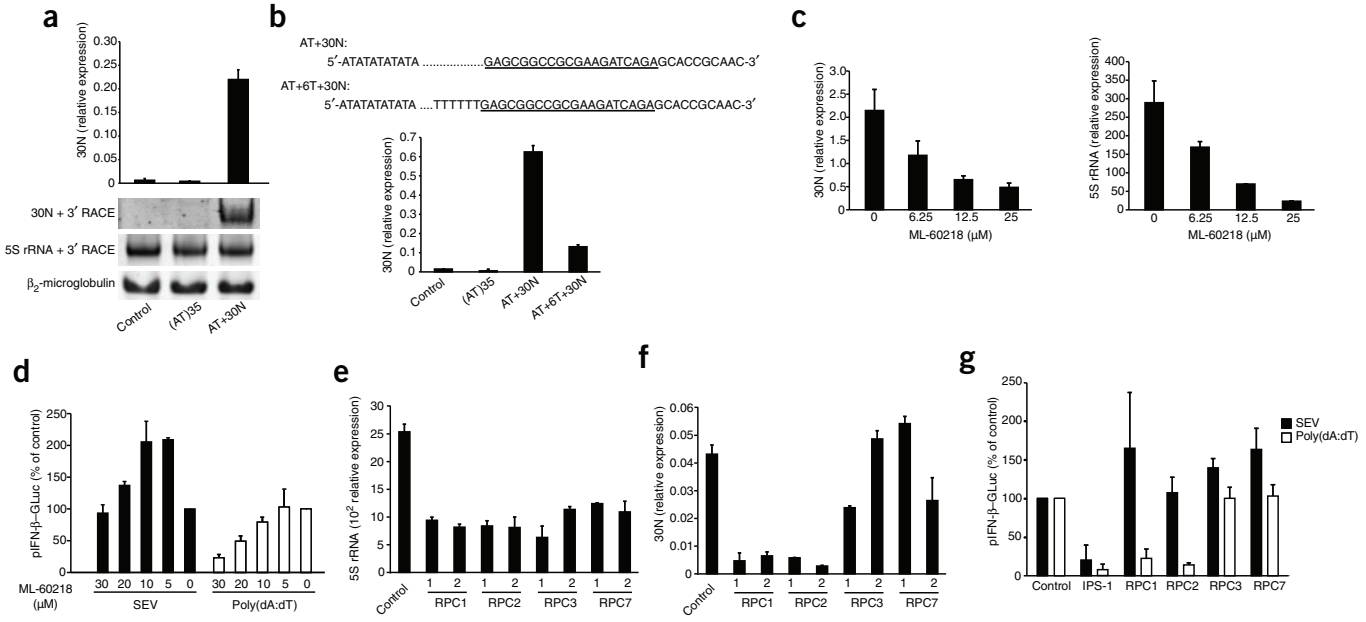

Figure 6 RNA polymerase III transcribes AT-rich DNA and is required for poly(dA:dT)-mediated induction of type I interferon. (**a**) Real-time PCR analysis (as in **Supplementary Fig. 7**) of expression of the 30N tag in 293T cells left untreated or transfected with the dsDNA template (AT)35 or AT+30N, assessed 8 h after transfection and presented relative to the expression of B2M (encoding β_2-microglobulin). Below, standard PCR and PAGE of expression of 5*S* rRNA, the 30N tag or β_2-microglobulin. (**b**) Expression of the 30N tag in 293T cells left untreated (Control) or transfected with (AT)35, AT+30N or AT+6T+30N dsDNA, assessed 8 h after transfection and presented relative to *B2M* expression. Top, AT+30N and AT+6T+30N sequences, with the primer-binding sites for PCR underlined (dotted lines indicate additonal AT sequence). (**c**) Expression of the 30N tag and 5*S* rRNA in 293T cells treated for 2 h with ML-60218 (concentration, horizontal axes) and transfected with AT+30N dsDNA and then assessed 16 h later; results are presented relative to *B2M* expression. (**d**) IFN-β reporter activity in 293T cells treated for 2 h with ML-60218 and then transfected with an IFN-β reporter plasmid in conjunction with poly(dA:dT) or SEV and assessed after 24 h. (**e**,**f**) Transcription of 5*S* rRNA (**e**) and AT+30N (**f**) in 293T cells transfected for 48 h with two individual siRNA molecules (1 or 2) targeting genes encoding RPC1, RPC2, RPC3 or RPC7, then transfected with AT+30N and assessed after an additional 16 h; results are presented relative to *B2M* expression. (**g**) IFN-β reporter activity in 293T cells transfected for 48 h with siRNA specific for IPS-1, RPC1, RPC2, RPC3 or RPC7, then transfected with an IFN-β reporter plasmid in conjunction with poly(dA:dT) or SEV and assessed after an additional 24 h; results are presented relative to results obtained with control siRNA, set as 100%. Data are from one representative of three (**a**,**b**,**g**), two (**c**,**e**,**f**) or four (**d**) experiments (mean and s.e.m.).

poly(dA:dT)-triggered RNA and *in vitro*–transcribed 3pRNA with alkaline phosphatase to remove any 5′ or 3′ phosphates that might be present. Treatment of 3pRNA and poly(dA:dT)-triggered RNA with alkaline phosphatase considerably diminished their stimulatory activity, whereas poly(dA:dT) was unaffected by alkaline phosphatase treatment (**Supplementary Fig. 4**). In addition, RNA 5′-polyphosphatase, an enzyme that specifically removes the phosphate group in the γ-position and β-position of 5′-triphosphate or 5′-diphosphate RNA, completely abolished the induction of type I interferon by *in vitro*–transcribed 3pRNA and poly(dA:dT)-triggered RNA (**Fig. 5a**). Treating the stimulatory RNA with RNase III, an enzyme that degrades long dsRNA into short dsRNA molecules, also abolished the stimulatory ability (**Fig. 5b**). Of note, the *in vitro*–transcribed RNA species were completely sensitive to treatment with RNase III, in agreement with the finding that *in vitro*–transcribed RNA critically requires dsRNA conformation for its RIG-I-stimulatory activity[37]. Consistent with those observations, RNase T1, an endoribonuclease that degrades ssRNA at guanosine residues, did not inhibit the activity of the poly(dA:dT)-triggered RNA species or the *in vitro*–transcribed RNA (data not shown). However, when we used RNase T1 in conditions that denature dsRNA, the *in vitro*–transcribed RNA was rendered completely inactive, whereas the poly(dA:dT)-triggered RNA species was not affected (**Fig. 5c**). This was notable, as in denaturing conditions, RNase T1 treatment almost completely degraded the RNA from poly(dA:dT)-transfected cells (**Fig. 5c**, bottom). In contrast, the endoribonuclease RNase A, which cleaves both ssRNA and dsRNA at uridine and cytidine residues in low-salt conditions, led to complete degradation and loss of activity of both *in vitro*–transcribed RNA and poly(dA:dT)-triggered RNA (**Fig. 5d**). As RNase T1 cleaves ssRNA specifically after guanosine residues, we hypothesized that the stimulatory RNA of interest was devoid of guanosine, at least at critical residues required for the stimulatory activity. Indeed, an *in vitro*–transcribed RNA molecule that consisted only of alternating uridine and adenosine bases was not affected by RNase T1 treatment in denaturing conditions and was still active in terms of induction of type I interferon (**Supplementary Fig. 5**). From these results, we conclude that transfection of poly(dA:dT) triggers the formation of an endogenous, double-stranded, 3pRNA molecule that is devoid of guanosine.

RNA polymerase III in type I interferon induction

The results reported above led us to hypothesize that poly(dA:dT) might itself serve as a template for the transcription of a 5′-triphosphate poly(rA:rU) molecule by a DNA-dependent RNA polymerase. Indeed, poly(dA:dT) has, for example, been used to study promoter-independent transcription by RNA polymerase III (refs. 38,39). Additionally, it has been shown that poly(dA:dT) is transcribed to poly(rA:rU) by RNA polymerase III (ref. 40). We therefore tested the possibility that poly(dA:dT) was transcribed in cells after transfection. *In vitro*–transcribed poly(rA:rU) turned out to be an unsuitable template for specific RT-PCR amplification because of its homopolymeric nature (data not shown). We therefore constructed a synthetic homopolymeric dA:dT template consisting of 35 'units' of dA:dT (AT) plus an additional

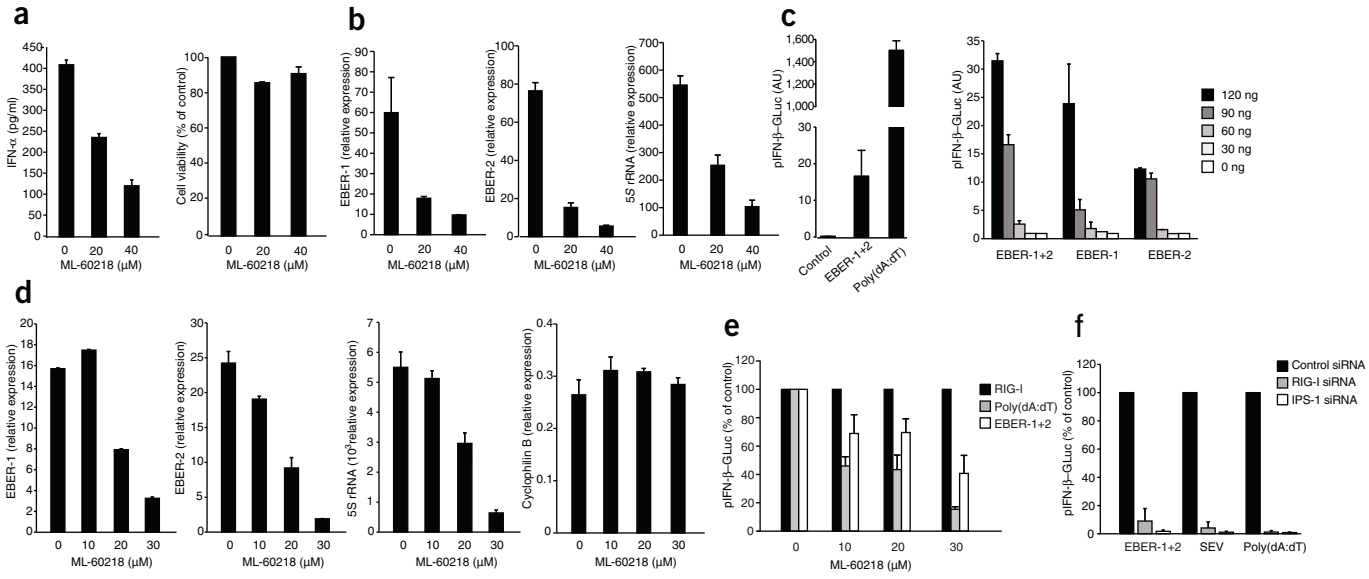

Figure 7 EBER moleucles are transcribed by RNA polymerase III and trigger activation of RIG-I. (**a**,**b**) ELISA of IFN-α production (**a**, left), calcein AM analysis of cell viability (**a**, right) and real-time PCR analysis of the production of EBER-1, EBER-2 and 5*S* (**b**) of Mutu III cells treated for 24 h with ML-60218, presented relative to the expression of *B2M*. (**c**) IFN-β reporter activity in interferon-primed 293T cells transfected for 24 h with the genomic locus encoding EBER-1 and EBER-2 (EBER-1+2) or poly(dA:dT) (120 ng) (left) or decreasing amounts of the genomic locus encoding EBER-1 and EBER-2 or the portions encoding either EBER-1 or EBER-2 (right), together with an IFN-β reporter plasmid. Left, green fluorescent protein construct serves as a negative control (left). (**d**) Transcription of EBER-1, EBER-2, 5*S* rRNA and cyclophilin B in interferon-primed 293T cells treated for 2 h with ML-60218 and transfected for 24 h with the genomic locus encoding EBER-1 and EBER-2, presented relative to the expression of *B2M*. (**e**) Transactivation of the IFN-β promoter in interferon-primed 293T cells treated as described in **d** and transfected with the genomic locus encoding EBER-1 and EBER-2 or with poly(dA:dT) or RIG-I (120 ng); results are presented relative to those obtained with the positive control RIG-I, set as 100%. (**f**) IFN-β reporter activity in 293T cells transfected for 48 h with two individual siRNA molecules targeting RIG-I or IPS-1 or control siRNA, then transfected with an IFN-β reporter plasmid in conjunction with the genomic locus encoding EBER-1 and EBER-2 or with poly(dA:dT) or SEV and assessed after an additional 24 h. Data are from one representative of three (**a**,**e**), two (**b**,**d**,**f**) or four (**c**) experiments (mean and s.e.m.).

tail of 30 nucleotides (30N) containing a specific primer-binding site (AT+30N). Transfection of this synthetic template triggered a type I interferon response in PBMCs and also led to the generation of a stimulatory RNA species, albeit to a lower extent than that obtained with poly(dA:dT) (**Supplementary Fig. 6a**,**b**). Thus, we anticipated that this synthetic poly(dA:dT) construct would be transcribed together with the 30N downstream primer-binding site, which allowed us to use it as a specific tag for a 3′ rapid amplification of cDNA ends (RACE; **Supplementary Fig. 7**). Indeed, after transfection of this template into 293T cells, we were able to detect an RNA transcript containing the specific 3′ RACE tag (**Fig. 6a**), which indicated that the AT+30N dsDNA had been transcribed through its 30N 3′ end. We also assessed 5*S* rRNA, an established RNA polymerase III transcript, by the 3′ RACE PCR method. In addition, we analyzed transcription of β_2-microglobulin as an RNA polymerase II–dependent control (**Fig. 6a**). We obtained similar results when we transfected primary mouse DCs (**Supplementary Fig. 6c**), which indicated that this phenomenon was also operational in cells that responded to poly(dA:dT) in a RIG-I-independent way. Using the same template but with a poly(T) stretch separating the poly(dA:dT) portion from the 30N tag (AT+6T+30N) resulted in much less transcription of the 30N tag (**Fig. 6b**), which indicated that the polymerase activity was terminated before this part of the template. The fact that RNA polymerase III terminates transcription at poly(T) stretches additionally indicates involvement of RNA polymerase III in transcription of the AT+30N template. To address this possibility further, we took advantage of a specific inhibitor of RNA polymerase III, ML-60218. We treated 293T cells with ML-60218 and subsequently transfected the cells with AT+30N. Consistent with the involvement of RNA polymerase III in mediating transcription of the AT+30N template, ML-60218 inhibited transcription of 5*S* rRNA and AT+30N DNA in a dose-dependent way (**Fig. 6c**).

To address the functional consequences of the inhibition of RNA polymerase III on the induction of type I interferon, we treated 293T cells with ML-60218 and then challenged these cells with poly(dA:dT) or SEV. SEV-triggered induction of type I interferon was enhanced at low concentrations of ML-60218 but was suppressed at higher concentrations (**Fig. 6d**). In contrast, poly(dA:dT)-mediated induction of type I interferon was blocked by ML-60218 in a dose-dependent way at concentrations that did not affect cell viability (data not shown). We also used RNA-mediated interference to 'knock down' essential subunits of the RNA polymerase III transcription apparatus to further study the function of RNA polymerase III in this response. We targeted RPC1 and RPC2 (encoded by *Polr3a* and *Polr3b*, respectively), the two core subunits that form the polymerase active center of RNA polymerase III, as well as RPC3 and RPC7 (encoded by *Polr3c* and *Polr3g*, respectively), which are not essential for elongation and termination during transcription with RNA polymerase III but are required for promoter-directed transcription initiation[41] (**Supplementary Fig. 8**). As expected, transcription of 5S rRNA was affected by knockdown of RPC1, RPC2, RPC3 or RPC7 (**Fig. 6e**). However, whereas the core subunits RPC1 and RPC2 were essential for transcription of AT+30N, the RPC3 and RPC7 subunits were dispensable (**Fig. 6f**). In line with those data, induction of type I interferon triggered by poly(dA:dT) was critically dependent on RPC1 and RPC2 but not on RPC3 or RPC7 (**Fig. 6g**). SEV-mediated induction of type I interferon was unaffected by knockdown of any of these components (**Fig. 6g**). Thus, we conclude that promoter-independent transcription of poly(dA:dT) by RNA polymerase III leads to the formation of 3pRNA that in turn activates RIG-I.

RNA polymerase III–transcribed EBER RNA activates RIG-I

To address the physiological relevance of the RNA polymerase III pathway in antiviral host defenses, we examined the function of RNA polymerase III in the regulation of type I interferon responses to a DNA virus. We chose EBV because it encodes small EBER molecules that are transcribed by RNA polymerase III in very large amounts. EBER molecules are nonpolyadenylated, untranslated RNA molecules 167 nucleotides (EBER-1) or 172 nucleotides (EBER-2) in length[42] and are the most abundant viral transcripts in cells with latent EBV infection[43]. Notably, EBV-immortalized lymphoblastoid cell lines and EBV-positive Burkitt lymphoma cell lines produce type I interferons in resting conditions[44,45]. To determine if pattern-recognition receptors are activated constitutively in Burkitt lymphoma cells and to define the involvement of RNA polymerase III in controlling the constitutive production of type I interferons, we treated the EBV-positive human Burkitt lymphoma Mutu III cell line with the RNA polymerase III inhibitor ML-60218. Inhibition of RNA polymerase III blocked IFN-α production in Mutu III cells in a dose-dependent way (**Fig. 7a**). The defect in interferon production correlated with repression of the expression of EBER-1, EBER-2 and 5S rRNA in these cells (**Fig. 7b**). To directly examine the ability of EBER to activate the RIG-I pathway, we cloned the entire EBER gene locus from EBV and transiently overexpressed this construct in interferon-primed 293T cells. Overexpression of EBER molecules led to substantial induction of type I interferon, albeit to a lower extent than did poly(dA:dT) (**Fig. 7c**). Expression of the loci for EBER-1 and EBER-2 separately showed that each EBER molecule could trigger type I interferon responses independently, although EBER-1 was slightly more active at high concentrations (**Fig. 7c**). Notably, when we expressed a dsDNA template encoding a blunt-ended version of EBER-1 RNA, we found more induction of type I interferon (**Supplementary Fig. 9**). This is in line with the finding that RIG-I favors fully blunt-ended 5′-triphosphate dsRNA[37]. As expected, expression of EBER RNA in 293T cells was suppressed by inhibition of RNA polymerase III activity, whereas RNA polymerase II–driven transcription of cyclophilin B was not affected (**Fig. 7d**). In addition, inhibition of RNA polymerase III or expression of RIG-I- or IPS-1-specific siRNA led to less EBER-induced type I interferon (**Fig. 7e**,**f**). Collectively, these results indicate that EBER molecules are transcribed by RNA polymerase III and trigger the induction of type I interferon through RIG-I. In line with those findings, we found that certain synthetic RNA polymerase III genes that encode blunt-ended dsRNA, such as short hairpin RNA, were potent triggers of RIG-I activation (**Supplementary Fig. 10** and data not shown). These findings furthermore establish RIG-I as an important checkpoint in the detection of non-self RNA polymerase III transcripts.

DISCUSSION

Here we have demonstrated a novel mechanism for the sensing of AT-rich dsDNA. The synthetic dsDNA mimetic poly(dA:dT) was converted by host RNA polymerase III into a 3pRNA intermediate, which was in turn recognized by RIG-I. RNA polymerase III–mediated conversion of poly(dA:dT) occurred in mouse and human cells, but at least one additional as-yet-undefined sensing mechanism operates in cells of the mouse immune system; this pathway responds to poly(dA:dT) in an RNA-independent way, presumably as a result of sensing DNA directly. These observations are consistent with published reports showing that mouse cells lacking RIG-I or IPS-1 still produce type I interferons in response to poly(dA:dT)[33,34]. This matter is further complicated by the fact that in the human system, at least one additional DNA-sensing mechanism exists to recognize dsDNA independently of a RIG-I-stimulatory RNA intermediate. Poly(dA:dT) induced the formation of the RIG-I-activating RNA species, but other dsDNA moleules that were not poly(dA:dT)-homopolymeric in nature failed to do so, despite being active when directly transfected into PBMCs. Nevertheless, our data clearly demonstrate that AT-rich DNA transcribed by RNA polymerase III is sensed by RIG-I in the human system in a nonredundant way.

Poly(dA:dT) has been used to study RNA polymerase III–mediated promoter-independent transcription[38–40]. This nonspecific transcriptional activity requires the core polymerase complex of RNA polymerase III, which includes RPC1 and RPC2, yet is independent of subunits used by RNA polymerase III for recruitment to specific promoter sites (RPC3, RPC6 and RPC7)[41]. It is unclear at present if RNA polymerase III has transcriptional activity independent of its characterized promoter sites *in vivo*, as no studies have addressed the RNA polymerase III transcriptome at a global cellular level in an unbiased way. It is plausible that RNA polymerase III also transcribes DNA templates from endogenous sources in a promoter-independent way. Such a mechanism could function as an innate defense strategy by tagging DNA as an RNA intermediate to be detected by RIG-I. Poly(dA:dT) or AT-rich DNA is a 'peculiar' template for RNA polymerase III and thereby indirectly for RIG-I for two main reasons. First, AT-rich sequences might be particularly suited for promoter-independent transcription by RNA polymerase III because of their propensity to form dsDNA regions with low helix stability, which may be particularly accessible as initiation sites for polymerases. However, other DNA templates have also been used to study promoter-independent transcription by RNA polymerase III and thus it is possible that non-AT DNA is also transcribed by RNA polymerase III in a promoter-independent way. Second, and probably more importantly, homopolymeric AT-rich DNA is also transcribed into a homopolymeric RNA molecule that has the propensity to form a complete RNA duplex. RIG-I strongly favors blunt-ended dsRNA over ssRNA or incompletely annealed dsRNA for binding and subsequent activity[37]. Although 5′-triphosphate ssRNA that is not self-complementary is equally active in terms of RIG-I activation when annealed to a complementary ssRNA strand, it shows little or no activity as a single-stranded molecule. Poly(rA:rU) RNA, in contrast, is completely self-complementary and thus has a strong propensity to form dsRNA with complete blunt-end formation, thereby making it ideally suited to be recognized by RIG-I.

Studying the function of host RNA polymerase III–dependent transcription of pathogen-derived DNA in innate immune defense will be important yet technically challenging. During acute infection with DNA viruses, it is likely that several DNA-sensing pathways are triggered in the nucleus or in the cytosol simultaneously, which makes it difficult to study the contribution of a single sensor. Here we focused on cells that were latently infected with EBV and thus contained viral DNA in the nucleus in steady-state conditions. EBV EBER molecules are transcribed in large amounts by RNA polymerase III in latently infected, EBV-positive cells[43]. In these cells, we found an RNA polymerase III–dependent activation of the induction of type I interferon that coincided with EBER RNA expression. Ectopic expression of the EBER locus also induced type I interferon by a mechanism dependent on RIG-I and IPS-1. Published work has also indicated EBER RNAs are endogenous triggers for RIG-I (ref. 46). We speculate that other herpes viruses also encode RNA polymerase III transcripts that can trigger RIG-I activation. For example, the genomes of some γ-herpesviruses contain variable numbers of internal repeats that are highly conserved across different viruses. In this context, it is noteworthy that a highly repetitive region in the genome of murine γ-herpesviruses 68 triggers type I interferon responses[47].

Notably, published work has linked the RIG-like helicase–IPS-1

pathway to the detection of pathogens that replicate in the cytosol but are not RNA viruses. For example, induction of type I interferon triggered by *L. pneumophila*[29] or vaccinia virus[48] is strongly attenuated in cells devoid of IPS-1. It is unclear whether the activation of RIG-like helicases in these cases is due to pathogen-dependent RNA polymerase activity or host-derived RNA generated by an RNA polymerase III–dependent mechanism. Future studies that allow discrimination between host-derived and pathogen-derived RIG-I ligands could help clarify these issues.

METHODS

Methods and any associated references are available in the online version of the paper at http://www.nature.com/natureimmunology/.

Note: Supplementary information is available on the Nature Immunology website.

ACKNOWLEDGMENTS

We thank R. Silverman (Lerner Research Institute, Cleveland Clinic) for *Rnasel*$^{-/-}$ MEFs and their respective controls; and G. Bornkamm and M. Schlee for discussions. Supported by the Deutsche Forschungsgemeinschaft (Ho2783/2-1 V.H.) and the US National Institutes of Health (AI-065483 to E.L.; AI-067497 to K.A.F.; AI-083713 to K.A.F. and E.L.).

AUTHOR CONTRIBUTIONS

A.A., F.B. and V.H. did the experiments; V.H. conceived of and K.A.F. and V.H. supervised the research; G.H. and E.L. provided technical support; E.L., K.A.F. and V.H. sponsored the research; and K.A.F. and V.H. prepared the manuscript.

Published online at http://www.nature.com/natureimmunology/.
Reprints and permissions information is available online at http://npg.nature.com/reprintsandpermissions/.

1. Kawai, T. & Akira, S. Toll-like receptor and RIG-I-like receptor signaling. *Ann. NY Acad. Sci.* **1143**, 1–20 (2008).
2. Takeda, K. & Akira, S. Toll-like receptors in innate immunity. *Int. Immunol.* **17**, 1–14 (2005).
3. Huysamen, C. & Brown, G.D. The fungal pattern recognition receptor, Dectin-1, and the associated cluster of C-type lectin-like receptors. *FEMS Microbiol. Lett.* **290**, 121–128 (2009).
4. Yoneyama, M. & Fujita, T. RIG-I family RNA helicases: cytoplasmic sensor for antiviral innate immunity. *Cytokine Growth Factor Rev.* **18**, 545–551 (2007).
5. Meylan, E., Tschopp, J. & Karin, M. Intracellular pattern recognition receptors in the host response. *Nature* **442**, 39–44 (2006).
6. Takaoka, A. & Taniguchi, T. Cytosolic DNA recognition for triggering innate immune responses. *Adv. Drug Deliv. Rev.* **60**, 847–857 (2008).
7. Takaoka, A. *et al.* DAI (DLM-1/ZBP1) is a cytosolic DNA sensor and an activator of innate immune response. *Nature* **448**, 501–505 (2007).
8. Hornung, V. *et al.* AIM2 recognizes cytosolic dsDNA and forms a caspase-1-activating inflammasome with ASC. *Nature* **458**, 514–518 (2009).
9. Kono, H. & Rock, K.L. How dying cells alert the immune system to danger. *Nat. Rev. Immunol.* **8**, 279–289 (2008).
10. Takeuchi, O. & Akira, S. Innate immunity to virus infection. *Immunol. Rev.* **227**, 75–86 (2009).
11. Takeuchi, O. & Akira, S. MDA5/RIG-I and virus recognition. *Curr. Opin. Immunol.* **20**, 17–22 (2008).
12. Kato, H. *et al.* Differential roles of MDA5 and RIG-I helicases in the recognition of RNA viruses. *Nature* **441**, 101–105 (2006).
13. Pichlmair, A. *et al.* RIG-I-mediated antiviral responses to single-stranded RNA bearing 5′-phosphates. *Science* **314**, 997–1001 (2006).
14. Hornung, V. *et al.* 5′-Triphosphate RNA is the ligand for RIG-I. *Science* **314**, 994–997 (2006).
15. Kato, H. *et al.* Length-dependent recognition of double-stranded ribonucleic acids by retinoic acid-inducible gene-I and melanoma differentiation-associated gene 5. *J. Exp. Med.* **205**, 1601–1610 (2008).
16. Kawai, T. *et al.* IPS-1, an adaptor triggering RIG-I- and Mda5-mediated type I interferon induction. *Nat. Immunol.* **6**, 981–988 (2005).
17. Seth, R.B., Sun, L., Ea, C.K. & Chen, Z.J. Identification and characterization of MAVS, a mitochondrial antiviral signaling protein that activates NF-κB and IRF 3. *Cell* **122**, 669–682 (2005).
18. Xu, L.G. *et al.* VISA is an adapter protein required for virus-triggered IFN-beta signaling. *Mol. Cell* **19**, 727–740 (2005).
19. Meylan, E. *et al.* Cardif is an adaptor protein in the RIG-I antiviral pathway and is targeted by hepatitis C virus. *Nature* **437**, 1167–1172 (2005).
20. Ishii, K.J. *et al.* TANK-binding kinase-1 delineates innate and adaptive immune responses to DNA vaccines. *Nature* **451**, 725–729 (2008).
21. Burckstummer, T. *et al.* An orthogonal proteomic-genomic screen identifies AIM2 as a cytoplasmic DNA sensor for the inflammasome. *Nat. Immunol.* **10**, 266–272 (2009).
22. Fernandes-Alnemri, T., Yu, J.W., Datta, P., Wu, J. & Alnemri, E.S. AIM2 activates the inflammasome and cell death in response to cytoplasmic DNA. *Nature* **458**, 509–513 (2009).
23. Roberts, T.L. *et al.* HIN-200 proteins regulate caspase activation in response to foreign cytoplasmic DNA. *Science* **323**, 1057–1060 (2009).
24. Henry, T., Brotcke, A., Weiss, D.S., Thompson, L.J. & Monack, D.M. Type I interferon signaling is required for activation of the inflammasome during Francisella infection. *J. Exp. Med.* **204**, 987–994 (2007).
25. Charrel-Dennis, M. *et al.* TLR-independent type I interferon induction in response to an extracellular bacterial pathogen via intracellular recognition of its DNA. *Cell Host Microbe* **4**, 543–554 (2008).
26. O'Riordan, M., Yi, C.H., Gonzales, R., Lee, K.D. & Portnoy, D.A. Innate recognition of bacteria by a macrophage cytosolic surveillance pathway. *Proc. Natl. Acad. Sci. USA* **99**, 13861–13866 (2002).
27. Stetson, D.B. & Medzhitov, R. Recognition of cytosolic DNA activates an IRF3-dependent innate immune response. *Immunity* **24**, 93–103 (2006).
28. Stanley, S.A., Johndrow, J.E., Manzanillo, P. & Cox, J.S. The Type I IFN response to infection with *Mycobacterium tuberculosis* requires ESX-1-mediated secretion and contributes to pathogenesis. *J. Immunol.* **178**, 3143–3152 (2007).
29. Opitz, B. *et al. Legionella pneumophila* induces IFNβ in lung epithelial cells via IPS-1 and IRF3, which also control bacterial replication. *J. Biol. Chem.* **281**, 36173–36179 (2006).
30. Roux, C.M. *et al.* Brucella requires a functional type IV secretion system to elicit innate immune responses in mice. *Cell. Microbiol.* **9**, 1851–1869 (2007).
31. Chessler, A.D., Ferreira, L.R., Chang, T.H., Fitzgerald, K.A. & Burleigh, B.A. A novel IFN regulatory factor 3-dependent pathway activated by trypanosomes triggers IFN-β in macrophages and fibroblasts. *J. Immunol.* **181**, 7917–7924 (2008).
32. Yoshida, H., Okabe, Y., Kawane, K., Fukuyama, H. & Nagata, S. Lethal anemia caused by interferon-β produced in mouse embryos carrying undigested DNA. *Nat. Immunol.* **6**, 49–56 (2005).
33. Sun, Q. *et al.* The specific and essential role of MAVS in antiviral innate immune responses. *Immunity* **24**, 633–642 (2006).
34. Kumar, H. *et al.* Essential role of IPS-1 in innate immune responses against RNA viruses. *J. Exp. Med.* **203**, 1795–1803 (2006).
35. Cheng, G., Zhong, J., Chung, J. & Chisari, F.V. Double-stranded DNA and double-stranded RNA induce a common antiviral signaling pathway in human cells. *Proc. Natl. Acad. Sci. USA* **104**, 9035–9040 (2007).
36. Malathi, K., Dong, B., Gale, M., Jr & Silverman, R.H. Small self-RNA generated by RNase L amplifies antiviral innate immunity. *Nature* **448**, 816–819 (2007).
37. Schlee, M. *et al.* Recognition of 5′ triphosphate by RIG-I helicase requires short blunt double-stranded RNA as contained in panhandle of negative-strand virus. *Immunity* published online, doi:10.1016/j.immuni.2009.05.008 (2 July 2009).
38. Huet, J., Riva, M., Sentenac, A. & Fromageot, P. Yeast RNA polymerase C and its subunits. Specific antibodies as structural and functional probes. *J. Biol. Chem.* **260**, 15304–15310 (1985).
39. Zaros, C. & Thuriaux, P. Rpc25, a conserved RNA polymerase III subunit, is critical for transcription initiation. *Mol. Microbiol.* **55**, 104–114 (2005).
40. Thuillier, V., Brun, I., Sentenac, A. & Werner, M. Mutations in the α-amanitin conserved domain of the largest subunit of yeast RNA polymerase III affect pausing, RNA cleavage and transcriptional transitions. *EMBO J.* **15**, 618–629 (1996).
41. Wang, Z. & Roeder, R.G. Three human RNA polymerase III-specific subunits form a subcomplex with a selective function in specific transcription initiation. *Genes Dev.* **11**, 1315–1326 (1997).
42. Rosa, M.D., Gottlieb, E., Lerner, M.R. & Steitz, J.A. Striking similarities are exhibited by two small Epstein-Barr virus-encoded ribonucleic acids and the adenovirus-associated ribonucleic acids VAI and VAII. *Mol. Cell. Biol.* **1**, 785–796 (1981).
43. Lerner, M.R., Andrews, N.C., Miller, G. & Steitz, J.A. Two small RNAs encoded by Epstein-Barr virus and complexed with protein are precipitated by antibodies from patients with systemic lupus erythematosus. *Proc. Natl. Acad. Sci. USA* **78**, 805–809 (1981).
44. Schlee, M., Schuhmacher, M., Holzel, M., Laux, G. & Bornkamm, G.W. c-Myc impairs immunogenicity of human B cells. *Adv. Cancer Res.* **97**, 167–188 (2007).
45. Schlee, M. *et al.* C-myc activation impairs the NF-κB and the interferon response: implications for the pathogenesis of Burkitt's lymphoma. *Int. J. Cancer* **120**, 1387–1395 (2007).
46. Samanta, M., Iwakiri, D., Kanda, T., Imaizumi, T. & Takada, K. EB virus-encoded RNAs are recognized by RIG-I and activate signaling to induce type I IFN. *EMBO J.* **25**, 4207–4214 (2006).
47. Sanchez, D.J. *et al.* A repetitive region of γ-herpesvirus genomic DNA is a ligand for induction of type I interferon. *J. Virol.* **82**, 2208–2217 (2008).
48. Deng, L. *et al.* Vaccinia virus subverts a mitochondrial antiviral signaling protein-dependent innate immune response in keratinocytes through its double-stranded RNA binding protein, E3. *J. Virol.* **82**, 10735–10746 (2008).

ONLINE METHODS

Reagents. Poly(dA:dT) and chloroquine were from Sigma-Aldrich. ML-60218 was from Calbiochem. Human interleukin 4 and granulocyte-macrophage colony-stimulating factor were from ImmunoTools. RNase T1, alkaline phosphatase and DNase I were from Fermentas. RNase III, RNase A, RNA 5′ polyphosphatase and poly(A) polymerase were from Epicentre. The synthetic imidazoquinoline resiquimod (R-848) and CpG oligonucleotide 2216 were from Invivogen.

Cell isolation and culture. Human PBMCs were isolated from whole blood of healthy volunteers by density-gradient centrifugation (Biochrom). Red blood cells were lysed with red blood cell lysis buffer (Sigma). Human monocytes were isolated from PBMCs with anti-CD14 paramagnetic beads (Miltenyi Biotec) and were differentiated for 6 d into MoDCs in the presence of interleukin 4 (800 U/ml) and granulocyte-macrophage colony-stimulating factor (800 U/ml). Mouse bone marrow was cultured for 6 d with 5% (vol/vol) supernatant from J558L cells containing granulocyte-macrophage colony-stimulating factor for the generation of bone marrow–derived DCs. Primary cells were cultured in RPMI medium supplemented with L-glutamine, sodium pyruvate, 10% (vol/vol) FCS (all from Invitrogen) and ciprofloxacin (Bayer Schering Pharma). The 293T cells were cultured in DMEM (Invitrogen) with the same additives described above. *Rnasel*$^{-/-}$ MEFs and their respective controls were provided by R. Silverman. Cell viability was assessed by staining with the fluorescent cell viability indicator calcein AM as described[8]. Experiments involving human and mouse materials were approved by the institutional review board of the University Hospital of the University of Bonn and the University of Massachusetts Medical School.

RNA preparation. If not indicated otherwise, DNA-transfected or SEV-infected 293T cells (2.4×10^5 cells per 12 wells) were collected 16 h after stimulation. The Mini RNA Isolation II kit (Zymo Research) was used for RNA isolation with the following modifications. Cells were lysed with TRIzol (Invitrogen), followed by one round of chloroform extraction. For total RNA extraction, the solution obtained was mixed with 0.7 volumes of ethanol and applied to the separation column and, after washing, column-bound RNA was eluted. For enrichment of small RNA molecules, 0.2 volumes of ethanol were added to the chloroform-extracted solution and applied to the separation column and the flow-through was collected. That fraction was then mixed with 1.0 volume of ethanol and 'passed' to a second column. After washing, column-bound RNA was eluted. For some experiments, the amount of ethanol used in the first binding step was varied to obtain flow-through fractions of different sizes.

Enzymatic reactions. RNA or poly(dA:dT) (2 μg) was treated with alkaline phosphatase (100 U/ml), RNA 5′-polyphosphatase (1,000 U/ml), RNase A (50 μg/ml), RNase III (100 U/ml) or DNase I (1,000 U/ml to 100 U/ml) in the corresponding buffer solution in a volume of 10 μl for 30 min (RNA 5′ polyphosphatase) or 1 h (alkaline phosphatase, RNase A, RNase III or DNase I) at 37 °C. Samples were digested for 30 min at 55 °C with RNase T1 in denaturing conditions in 6 M urea and 17.8 mM sodium citrate, pH 3.5, and 0.9 mM EDTA.

Cell stimulation. For reporter studies, if not indicated otherwise, 293T cells (2×10^4 cells per 96 wells) were transfected with 50 ng IFN-β promoter reporter plasmid pIFN-β–GLuc in conjunction with 50 ng poly(dA:dT) or other nucleic acids using Lipofectamine 2000 (Invitrogen). In some cases, 50 ng expression plasmid (pCMV-hsIRF1, pCMV-hsTBK1, pEF-BOS-RIG-I, pEF-BOS-RIG-IΔCard, pME18-NS3-4A WT or pME18-NS3-4A S139A) was transfected while the total amount of DNA was kept at 200 ng with pcDNA3 as a 'stuffer' plasmid. In some experiments, 293T cells were primed overnight with IFN-β (10 U/ml). Transactivation of the IFN-β promoter was measured 24 h after stimulation in an EnVision 2104 Multilabel Reader (Perkin Elmer). Human PBMCs, human MoDCs and mouse bone marrow–derived DCs (2×10^5 cells per 96 wells) were preincubated with chloroquine (2000 ng/ml), followed by transfection with 200 ng of DNA or RNA using Lipofectamine 2000. Sendai Virus (Cantell strain; Charles River Laboratories) was used at a concentration of 300 hemagglutinating units per ml.

3′ RACE. For 3′ RACE analysis, isolated RNA was 'tailed' with poly(A) polymerase and subsequently reverse-transcribed with the RevertAid First Strand cDNA Synthesis kit (Fermentas) with the 3-RACE-RT primer (5′-CTATAGGCGCGCCACCGGTGTTTTTTTTTTTT TTTTTTTTTTTTTTTTTTTTVN-3′). The cDNA was subsequently amplified by conventional or real-time PCR with a transcript-specific forward primer and the 3-RT-PCR reverse primer (**Supplementary Table 1**).

Quantitative real-time PCR. After cDNA was synthesized from total RNA with the RevertAid First Strand cDNA Synthesis kit (Fermentas), a Roche LC480 with Maxima SYBR Green qPCR Master Mix (Fermentas) was used for quantitative RT-PCR analysis. The specificity of amplification was assessed for each sample by melting-curve and gel analysis. Standard curve analysis was used for relative quantification. Mouse quantification data are presented relative to *Hprt1* expression; human data are presented relative to *B2M* expression. A detailed list of all primer sequences is in **Supplementary Table 1**.

RNA analysis. Enriched small cellular RNA molecules and *in vitro*–transcribed RNA molecules were monitored with the Small RNA kit or RNA 6000 Pico Chip kit with an Agilent Bioanalyzer 2100 (Agilent Technologies).

ELISA. Human IFN-α (Bender Med Systems) and TNF (BD Biosciences) were assessed with commercial ELISA kits according to the manufacturer's instructions.

***In vitro*–transcribed RNA and PCR-generated dsDNA.** *In vitro* transcription was done as described[14] (templates, **Supplementary Table 2**). The 20-, 40-, 77-, 163-, 245-nucleotide dsDNA molecules and EBER dsDNA templates were generated by PCR with pCDNA3 or EBV genomic DNA as the template (primers, **Supplementary Table 3**).

RNA-mediated interference. First, siRNA was reverse-transfected at a concentration of 25 nM into 293T cells (1×10^4 cells per 96 wells) with 0.5 μl Lipofectamine. Then, 48 h after transfection, cells were stimulated and, after an additional period of 24 h, luciferase activity was assessed. Electroporation of human MoDCs and mouse bone marrow–derived DCs was done as described[49] (siRNA sequences, **Supplementary Table 4**).

49. Ablasser, A. *et al.* Selection of molecular structure and delivery of RNA oligonucleotides to activate TLR7 versus TLR8 and to induce high amounts of IL-12p70 in primary human monocytes. *J. Immunol.* **182**, 6824–6833 (2009).

doi:10.1038/ni.1779

Cell

RNA Polymerase III Detects Cytosolic DNA and Induces Type I Interferons through the RIG-I Pathway

Yu-Hsin Chiu,[1] John B. MacMillan,[2] and Zhijian J. Chen[1,3,*]
[1]Department of Molecular Biology
[2]Department of Biochemistry
[3]Howard Hughes Medical Institute
University of Texas Southwestern Medical Center, Dallas, TX 75390-9148, USA
*Correspondence: zhijian.chen@utsouthwestern.edu
DOI 10.1016/j.cell.2009.06.015

SUMMARY

Type I interferons (IFNs) are important for antiviral and autoimmune responses. Retinoic acid-induced gene I (RIG-I) and mitochondrial antiviral signaling (MAVS) proteins mediate IFN production in response to cytosolic double-stranded RNA or single-stranded RNA containing 5′-triphosphate (5′-ppp). Cytosolic B form double-stranded DNA, such as poly(dA-dT)•poly(dA-dT) [poly(dA-dT)], can also induce IFN-β, but the underlying mechanism is unknown. Here, we show that the cytosolic poly(dA-dT) DNA is converted into 5′-ppp RNA to induce IFN-β through the RIG-I pathway. Biochemical purification led to the identification of DNA-dependent RNA polymerase III (Pol-III) as the enzyme responsible for synthesizing 5′-ppp RNA from the poly(dA-dT) template. Inhibition of RNA Pol-III prevents IFN-β induction by transfection of DNA or infection with DNA viruses. Furthermore, Pol-III inhibition abrogates IFN-β induction by the intracellular bacterium *Legionella pneumophila* and promotes the bacterial growth. These results suggest that RNA Pol-III is a cytosolic DNA sensor involved in innate immune responses.

INTRODUCTION

Innate immunity is the first line of host defense against microbial pathogens. Host cells utilize their pattern recognition receptors (PRRs) to detect pathogen-associated molecular patterns (PAMPs). The Toll-like receptor family (TLRs) is one class of PRRs that recognize PAMPs including lipoproteins, lipopolysaccharides (LPS), double-stranded RNA (dsRNA), single-stranded RNA (ssRNA), and unmethylated CpG DNA (reviewed by Akira et al., 2006). Ligand-engaged TLRs recruit the adaptor proteins MyD88 or TRIF to activate downstream kinases including IκB kinase complex (IKK) and IKK-related kinases (TBK1 and IKKε), which activate the transcription factors nuclear factor-kappa B (NF-κB) and interferon regulatory factors (IRFs), respectively. NF-κB and IRFs function together in the nucleus to induce type I interferons (IFNs; e.g., IFN-α and IFN-β) and other cytokines.

In another PRR pathway, cytosolic RNAs are recognized by RIG-I-like receptors (RLRs), which include RIG-I, MDA5, and LGP2 (Yoneyama et al., 2004). RLRs contain RNA helicase domains that recognize viral double-stranded RNA. In addition, RIG-I and LGP2 contain a C-terminal regulatory domain that recognizes single-stranded RNA containing 5′-triphosphate, which distinguishes foreign (e.g., viral) RNAs from self-RNAs that normally contain 5′ modification (e.g., capped mRNA). RIG-I and MDA5 also contain N-terminal tandem caspase activation and recruitment domains (CARD), which interact with the CARD domain of mitochondrial antiviral signaling protein (MAVS, also known as IPS-1, VISA, and CARDIF) (Kawai et al., 2005; Meylan et al., 2005; Seth et al., 2005; Xu et al., 2005). MAVS localizes on the mitochondrial outer membrane through its C-terminal transmembrane domain, and this localization is important for MAVS to activate the cytosolic kinases IKK and TBK1 to induce IFNs (Seth et al., 2005).

Like RNA, accumulation of foreign or self-DNA in the cytosol also triggers potent innate immune responses. DNA can be introduced into the cytosol of mammalian cells after infection with DNA viruses or bacteria, and the detection of cytosolic DNA is important for mounting an immune response against these pathogens. Under certain conditions, self-DNA is inappropriately delivered to the cytosol, resulting in autoimmune responses. For example, DNase II-deficient macrophages lack the ability to digest self-DNA from engulfed apoptotic cells, leading to IFN-β production (Okabe et al., 2005; Yoshida et al., 2005). However, the mechanism by which cytosolic DNA induces IFNs is not well understood. In particular, the sensor that detects cytosolic DNA and triggers IFN production has remained largely unknown. Although DNA-dependent activator of IFN-regulatory factors (DAI) has been proposed to be a potential cytosolic DNA sensor (Takaoka et al., 2007), DAI-deficient mice still produce interferons in response to B form DNA and have similar innate and adaptive immune responses to those of wild-type mice (Ishii et al., 2008). Recent studies identify AIM2 as a cytosolic DNA sensor that activates the inflammasome and caspase-1 (reviewed by Schroder et al., 2009). However, AIM2 is not involved in type I interferon induction by cytosolic DNA.

Genetic studies have shown that cytosolic DNA can induce IFN production in mouse cells lacking RIG-I or MAVS, suggesting that the DNA signaling pathway is distinct from the RIG-I pathway (Ishii et al., 2006; Sun et al., 2006). Nevertheless, there is evidence that in certain human cell lines the induction of IFN-β by transfected double-stranded DNA depends on RIG-I and MAVS (Cheng et al., 2007; Ishii et al., 2006). However, RIG-I binds to RNA but not DNA, raising the question of how DNA might activate the RIG-I pathway.

In this report, we show that the double-stranded DNA (dsDNA) poly(dA-dT)•poly(dA-dT), herein referred to as poly(dA-dT), is converted to an RNA species in the cytosol to trigger the RIG-I pathway in human and mouse cells. This RNA species contains 5′-triphosphate and forms a double-stranded RNA. The conversion of DNA to RNA can be recapitulated in vitro with cytosolic extracts. Biochemical purification led to the identification of DNA-dependent RNA polymerase III (Pol-III) as the enzyme responsible for transcribing the DNA template into an RNA ligand that activates RIG-I. RNA interference (RNAi)-mediated knockdown of Pol-III expression or inhibition of its enzymatic activity impedes interferon induction by transfection of DNA or infection with several DNA viruses, including adenovirus, herpes simplex virus 1 (HSV-1), and Epstein-Barr virus (EBV). Moreover, Pol-III inhibition blocks interferon induction by the intracellular bacterium *Legionella pneumophila.* These results strongly suggest that Pol-III is a cytosolic DNA sensor that triggers type I interferon production through the RIG-I pathway.

RESULTS

Cytosolic DNA Triggers the RIG-I Pathway through an Intermediary RNA

In the course of attempting to identify a cytosolic DNA sensor involved in IFN-β production, HEK293 cells were transfected with various DNA together with a luciferase reporter driven by the IFN-β promoter. The cell lysates were analyzed by luciferase activity assays as well as native gel electrophoresis to detect IRF3 dimerization (Figure 1A). As controls, the cells were also transfected with the synthetic RNA poly(I:C) or infected with Sendai virus (SeV), an RNA virus known to induce IFN-β. Among the DNA tested, including poly(dA-dT), poly(dI-dC)•dpoly(dI-dC) [poly(dI-dC)], calf thymus DNA, PCR fragments of different lengths, and a linearized plasmid (pcDNA3), only poly(dA-dT) could activate IRF3 and induce IFN-β. Silencing the expression of RIG-I or MAVS with two different pairs of small interfering RNA (siRNA) oligos strongly inhibited IRF3 and IFN-β induction by poly(dA-dT) (Figure 1B). Pretreatment of poly(dA-dT) with DNase-I completely abrogated its ability to induce IFN-β, whereas RNase A treatment had no effect (Figure 1C), indicating that RIG-I-dependent induction of IFN-β was not due to some RNA contaminants in poly(dA-dT). Synthetic DNA oligos containing 50 or 100 nucleotides of AT sequence were potent inducers of IFN-β, whereas GCAT or GC sequences of comparable lengths had little activity (Figure S1 available online). Interestingly, insertion of 10 GC nucleotides in the middle of AT50 abolished its IFN-β-inducing activity. Poly-T, poly-A, or the duplex DNA formed between poly-T and poly-A did not induce IFN-β. A duplex DNA containing 80% AT sequence was capable of inducing IFN-β, whereas a DNA containing 50% AT sequence was inactive (Figure S1). Taken together, these results suggest that IFN induction by DNA in HEK293 cells requires AT-rich sequence and certain length (30–50 nucleotides, see below). Poly(dA-dT), but not other DNA tested, also activated IRF3 and induced IFN-β in HeLa cells; the IRF3 activation was inhibited by RNAi of RIG-I or MAVS (Figure S2), indicating that RIG-I-dependent induction of IFN-β by poly(dA-dT) is not restricted to HEK293 cells.

To identify the ligands responsible for RIG-I activation in cells transfected with poly(dA-dT), we extracted nucleic acids from the cell lysates with phenol and chloroform and tested the ability of these nucleic acids to induce IFN-β. The nucleic acids extracted from cells transfected with poly(dA-dT) potently induced IFN-β. Surprisingly, the activity of nucleic acids extracted from poly(dA-dT)-transfected cells was sensitive to RNase A, but not DNase I, suggesting that some intermediary RNAs capable of inducing IFN-β were activated or produced after poly(dA-dT) transfection (Figure 1D).

To test whether the production of IFN-inducing RNA depends on the length and/or composition of cytosolic DNA, we transfected synthetic DNA oligos, as well as longer poly(dA-dT) and poly(dG-dC) (purchased from GE Healthcare), into HEK293-IFNβ-Luc reporter cells to measure IFN-β induction by the DNA. RNA from the transfected cells was extracted, then transfected into the same IFN-β reporter cells to measure IFN-β induction by the RNA (Figure 1E). Interestingly, poly(dA-dT) containing as few as 30 base pairs was capable of directing the production of IFN-inducing RNA in the transfected cells. By contrast, even long poly(dG-dC) and GCAT DNA sequences were unable to produce any IFN-inducing RNA.

Previous studies showed that mouse embryonic fibroblasts (MEFs) lacking RIG-I or MAVS were still capable of producing IFN-β after transfection of DNA, including poly(dA-dT) (Ishii et al., 2006; Sun et al., 2006). To determine whether the transfection of DNA in MEF cells also leads to the generation of IFN-inducing RNA, we transfected MAVS-deficient primary MEF cells with various DNA and then measured IFN-β production by ELISA. Indeed, poly(dA-dT), poly(dI-dC), and calf thymus DNA, but not Sendai virus infection, induced IFN-β production in MAVS-deficient MEF cells (Figure 1F). When RNA extracted from these cells was transfected into HEK293-IFNβ-Luc reporter cells, only the RNA extracted from poly(dA-dT)-transfected and Sendai virus-infected cells was capable of inducing IFN-β (Figure 1G). These results suggest that MEF cells possess two cytosolic DNA-sensing pathways, one detecting DNA irrespective of sequence composition and inducing IFN-β through a MAVS-independent mechanism, and the other recognizing the poly(dA-dT) sequence and producing RNA ligands that trigger the RIG-I-MAVS pathway. Both poly(dA-dT) and poly(dG-dC) DNA induced IFN-β in bone marrow-derived macrophages (BMDMs), but only RNAs extracted from poly(dA-dT)-transfected BMDMs were capable of inducing IFN-β when they were transfected into the HEK293-IFNβ-Luc reporter cells (Figures 1H and 1I). Therefore, poly(dA-dT) leads to the generation of IFN-inducing RNA not only in transformed cells (HEK293 and HeLa), but also in primary fibroblasts (MEFs) and macrophages.

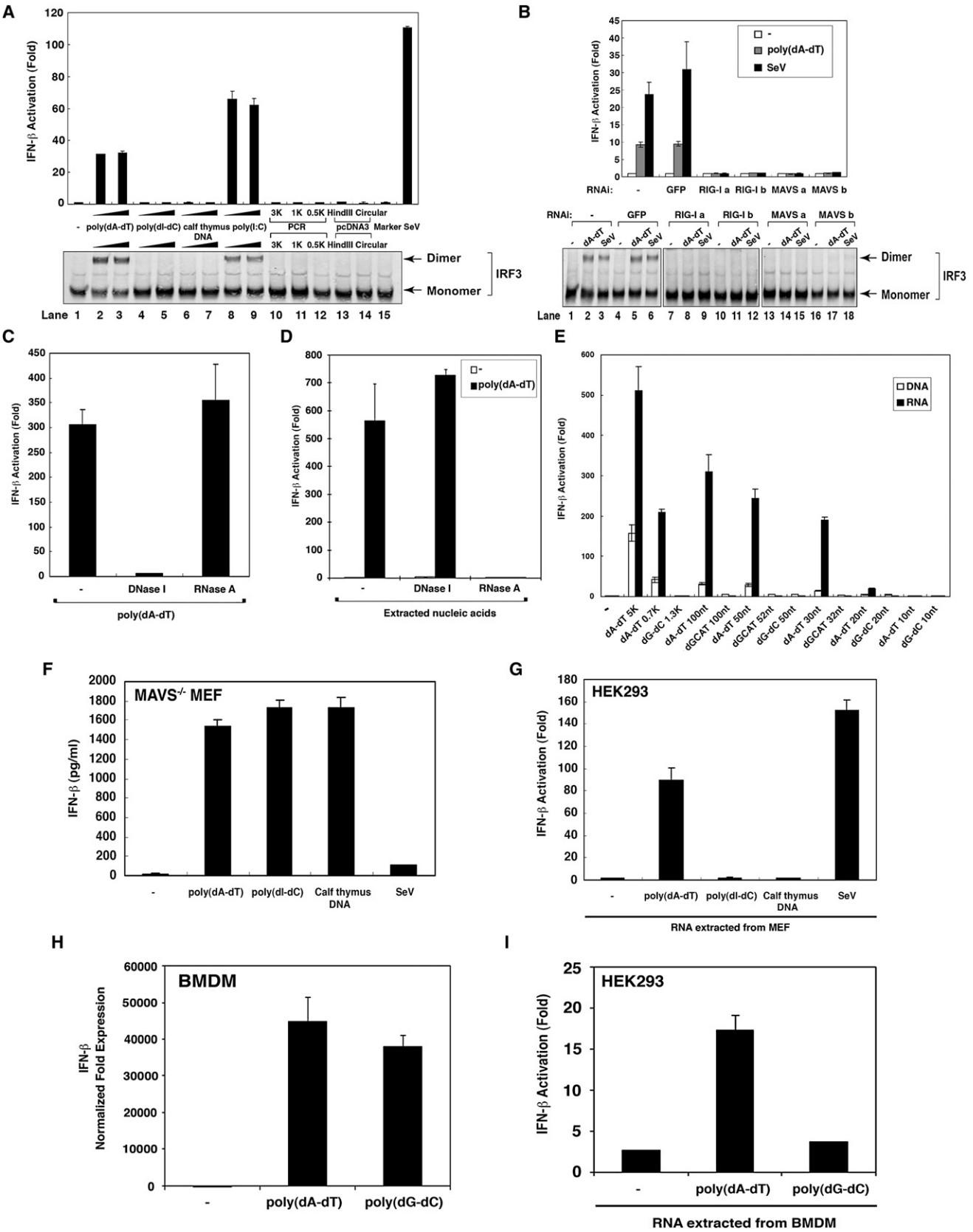
A
IFN-β Activation (Fold)
poly(dA-dT) poly(dI-dC) calf thymus poly(I:C) DNA
3K 1K 0.5K HindIII Circular PCR
pcDNA3 Marker SeV
3K 1K 0.5K HindIII Circular
Dimer
Monomer
IRF3
Lane 1 2 3 4 5 6 7 8 9 10 11 12 13 14 15
B
IFN-β Activation (Fold)
poly(dA-dT)
SeV
RNAi: - GFP RIG-I a RIG-I b MAVS a MAVS b
dA-dT
SeV
Dimer
Monomer
IRF3
Lane 1 2 3 4 5 6 7 8 9 10 11 12 13 14 15 16 17 18
C
IFN-β Activation (Fold)
DNase I
RNase A
poly(dA-dT)
D
IFN-β Activation (Fold)
poly(dA-dT)
DNase I
RNase A
Extracted nucleic acids
E
IFN-β Activation (Fold)
DNA
RNA
dA-dT 5K
dA-dT 0.7K
dG-dC 1.3K
dA-dT 100nt
dGCAT 100nt
dA-dT 50nt
dGCAT 52nt
dG-dC 50nt
dA-dT 30nt
dGCAT 32nt
dA-dT 20nt
dG-dC 20nt
dA-dT 10nt
dG-dC 10nt
F
MAVS-/- MEF
IFN-β (pg/ml)
poly(dA-dT)
poly(dI-dC)
Calf thymus DNA
SeV
G
HEK293
IFN-β Activation (Fold)
poly(dA-dT)
poly(dI-dC)
Calf thymus DNA
SeV
RNA extracted from MEF
H
BMDM
IFN-β Normalized Fold Expression
poly(dA-dT)
poly(dG-dC)
I
HEK293
IFN-β Activation (Fold)
poly(dA-dT)
poly(dG-dC)
RNA extracted from BMDM

Identification of the Intermediary RNA as Double-Stranded RNA Containing 5′-Triphosphate

RIG-I recognizes dsRNA and ssRNA bearing 5′-triphosphate (Hornung et al., 2006; Pichlmair et al., 2006). To determine the features of the IFN-inducing RNA generated in cells transfected with poly(dA-dT), we treated the RNA isolated from HEK293 cells with shrimp alkaline phosphatase (SAP) or polynucleotide kinase (PNK) and then tested its ability to induce IFN-β (Figure 2A). The activity of the RNA was destroyed by SAP, but not PNK treatment. Using PNK to add one phosphate to the SAP-treated RNA did not restore the activity, indicating that RNA containing 5′-monophosphate fails to induce IFN-β. Treatment of the RNA extracted from poly(dA-dT)-transfected cells with terminator exonuclease (Ter Ex), an enzyme that specifically digests RNA containing 5′-monophosphate, did not impair the IFN-inducing activity of the RNA (Figure 2B, lower panel), whereas treatment with RNase If (an RNase sensitive to heat inactivation) destroyed IFN-β induction. Control experiments showed that Ter Ex efficiently degraded 5′-monophosphate (5′-p) RNA generated by the treatment of RNA with SAP followed by PNK (Figure 2B; upper panel). These results show that the IFN-inducing RNA contained more than one phosphate at the 5′ end, most likely 5′-triphosphate (see the Discussion).

Next, to determine the structure of the intermediary RNA, we treated the RNA with RNases known to be specific for ssRNA or dsRNA. The specificity of the RNases was tested with in vitro-synthesized ssRNA or dsRNA (Figure 2C, upper panel). RNase III specifically digests dsRNA, but not ssRNA, whereas RNase T1 has the opposite specificity. ssRNA was more sensitive to digestion by low concentration of RNase A than was dsRNA. When the RNA from poly(dA-dT)-transfected cells was treated with RNase III and a high concentration of RNase A that degrades dsRNA, it lost its ability to induce IFN-β. By contrast, RNase T1 or a low concentration of RNase A, which degrades ssRNA, had no effect on the ability of the RNA to induce IFN-β (Figure 2C, lower panel). These results suggest that the IFN-inducing RNA from poly(dA-dT)-transfected cells is double-stranded RNA containing 5′-triphosphate. To determine whether the RNA is a RIG-I ligand, we immunoprecipitated RIG-I from HEK293 cells stably expressing FLAG-tagged RIG-I using a FLAG-specific antibody (M2). The RNA in the immunoprecipitates was extracted and tested for IFN-β induction (Figure 2D). The RNA extracted from the RIG-I complex immunoprecipitated from poly(dA-dT)-transfected cells induced IFN-β, whereas the RIG-I complex from mock-transfected cells did not contain IFN-inducing RNA. Taken together, these results indicate that poly(dA-dT) instructs or stimulates the production of dsRNA containing 5′-triphosphate, which binds to and activates RIG-I.

There are at least two potential mechanisms by which poly(dA-dT) leads to the generation of IFN-inducing RNA. Poly(dA-dT) might activate certain enzymes such as RNA kinases, which modify endogenous RNAs and convert them into RIG-I ligands. Alternatively, poly(dA-dT) might serve as a template to direct the de novo synthesis of RNA by some enzymes, such as a DNA-dependent RNA polymerase. To determine whether RNA polymerase II (RNA Pol-II) is involved in the synthesis of the IFN-inducing RNA, we transfected poly(dA-dT) into HEK293 cells that were pretreated with the RNA Pol-II inhibitor α-amanitin, and then total RNA was extracted from the cells and transfected into the IFN-β reporter cell line. α-amanitin blocked the transcription of IFN-β induced by poly(dA-dT) (Figure S3A), but did not inhibit the generation of the RNA, which, when extracted from the drug-treated cells and retransfected into HEK293-IFN-β reporter cells, was still capable of inducing IFN-β (Figure S3B). These results indicate that RNA polymerase II is not involved in transcribing the intermediary RNA from poly(dA-dT). Actinomycin D, which intercalates GC-rich double-stranded DNA and blocks transcriptional elongation, also did not prevent the generation of IFN-inducing RNA in poly(dA-dT)-transfected cells (Figure S3B), suggesting that either actinomycin D did not inhibit transcription from poly(dA-dT) or the RNA was not generated through de novo synthesis.

A Cell-free System that Generates IFN-Inducing RNA

To dissect the mechanism by which poly(dA-dT) leads to the production of IFN-inducing RNA, we tested whether the DNA can trigger the RNA generation in a cell-free system. HeLa cytosolic extracts (S100) were incubated with poly(dA-dT),

Figure 1. Poly(dA-dT) Activates RIG-I-Dependent IFN-β Production through Intermediary RNA

(A) HEK293 cells were transfected for 16 hr with the reporter plasmid IFN-β-Luc (25 ng/ml), pCMV-LacZ (50 ng/ml), and various types of DNA or RNA [poly(I:C)] as indicated (1 μg/ml) before cell lysates were prepared for luciferase reporter assay (upper panel) or IRF3 dimerization assay (lower panel). PCR, linear PCR fragments of the indicated size; HindIII, HindIII-linearized fragment of pcDNA3; marker, DNA marker (0.1-10 kB; NEB); SeV, Sendai virus infection.

(B) HEK293 cells were transfected with control siRNA oligos against GFP, two different pairs of siRNA oligos (a and b) against RIG-I, or MAVS. Subsequently, cells were cotransfected with IFN-β-Luc and pCMV-LacZ. After 24 hr, cells were transfected with poly(dA-dT) or infected with SeV before functional assays were performed as described in (A).

(C) HEK293 cells were transfected with poly(dA-dT) that had been predigested with DNase I or RNaseA, and then IFN-β luciferase reporter assay was carried out as described in (A).

(D) HEK293 cells were transfected with or without poly(dA-dT) for 16 hr, and then nucleic acids were prepared, digested with DNase I or RNase A, and transfected into HEK293-IFNβ-luciferase reporter cells to measure IFN-β induction.

(E) HEK293 cells were transfected with DNA of different sizes and compositions as indicated. Total RNA was extracted, then transfected into HEK293-IFNβ-luciferase reporter cells. In parallel experiments, the DNA was directly transfected into the reporter cells.

(F) MAVS-deficient MEF cells were transfected with various DNA or infected with SeV, and then IFN-β in the culture supernatants was measured by ELISA.

(G) MAVS-deficient MEF cells were treated as described in (F), and then total RNAs were extracted and transfected into HEK293-IFNβ-luciferase reporter cells.

(H) Mouse BMDM were transfected with poly(dA-dT) or poly(dG-dC) for 8 hr before total RNAs were extracted for qPCR. The expression level of the *IFN-β* gene was normalized with that of the *β-actin* gene.

(I) BMDM cells were transfected as described in (H), and then total RNAs were extracted and transfected into HEK293-IFNβ-luciferase reporter cells.

Error bars represent the variation range of duplicate experiments (A–G and I) or standard deviation of triplicate (H) experiments.

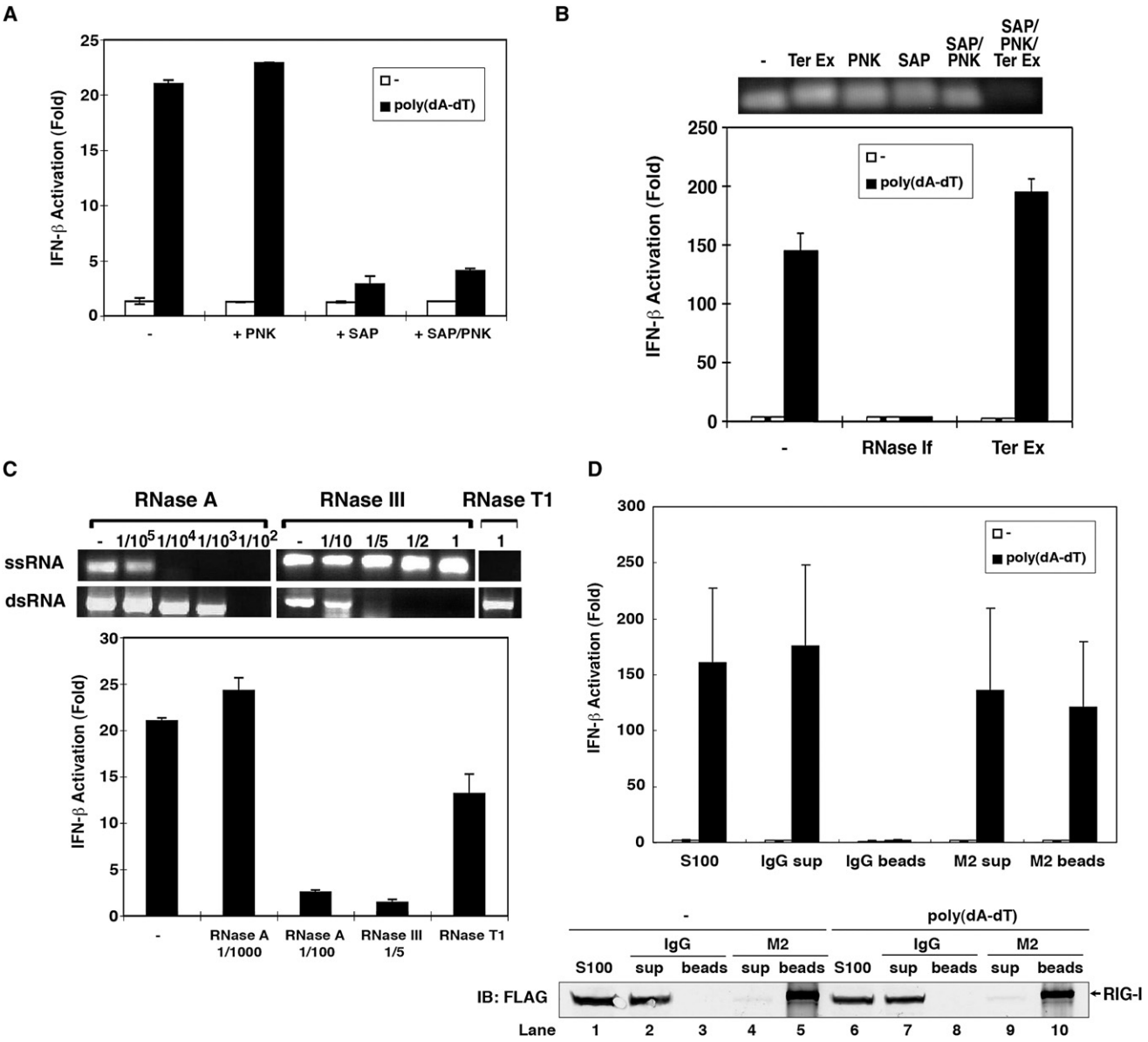

Figure 2. Properties of the IFN-Inducing RNA Derived from Poly(dA-dT)

(A) RNAs extracted from poly(dA-dT)- or mock-transfected cells were treated with shrimp alkaline phosphatases (SAP), polynucleotide kinase (PNK), or SAP followed by PNK at 37°C for 1 hr. The RNAs were then transfected into HEK293-IFNβ-luciferase reporter cells.

(B) Upper panel: poly(A-U) RNA transcribed by T7 polymerase was treated with terminator exonuclease (Ter Ex), PNK, or SAP at 37°C for 1 hr. Two aliquots of SAP-treated RNA were phosphorylated with PNK before one of the aliquots was further treated with Ter Ex. Lower panel: RNAs extracted from poly(dA-dT)- or mock-transfected cells were treated with RNase-If or Ter Ex and then transfected into HEK293-IFNβ-luciferase reporter cells.

(C) Upper panels: single-stranded RNA (ssRNA) or double-strand RNA (dsRNA) generated by T7 polymerase was digested with various amounts of the indicated RNase, separated on agarose gel, and then visualized by ethidium bromide staining. Lower panel: RNAs extracted from poly(dA-dT)-transfected cells were digested with the indicated RNase, then transfected into HEK293-IFNβ-luciferase reporter cells.

(D) Poly(dA-dT) was transfected into HEK293 cells stably expressing FLAG-tagged RIG-I, which was subsequently immunoprecipitated with an anti-FLAG antibody (M2) or control IgG. Nucleic acids in the cell extracts (S100), unbound supernatant (sup), and immunoprecipitates (beads) were extracted and then transfected into HEK293-IFNβ-luciferase reporter cells (upper panel). An aliquot of S100, sup, and beads was separated by SDS-PAGE and immunoblotted with a FLAG antibody (lower panel).

Error bars represent the variation range of duplicate experiments.

ATP, $MgCl_2$, and RNase inhibitors at 30°C for 1 hr, followed by phenol/chloroform extraction and DNase I treatment. The RNA was then tested for IFN-β induction. Remarkably, the RNA generated in this cell-free system potently activated the IFN-β promoter (Figure 3A). This activity was abolished by RNase but not DNase treatment, indicating that the IFN-inducing

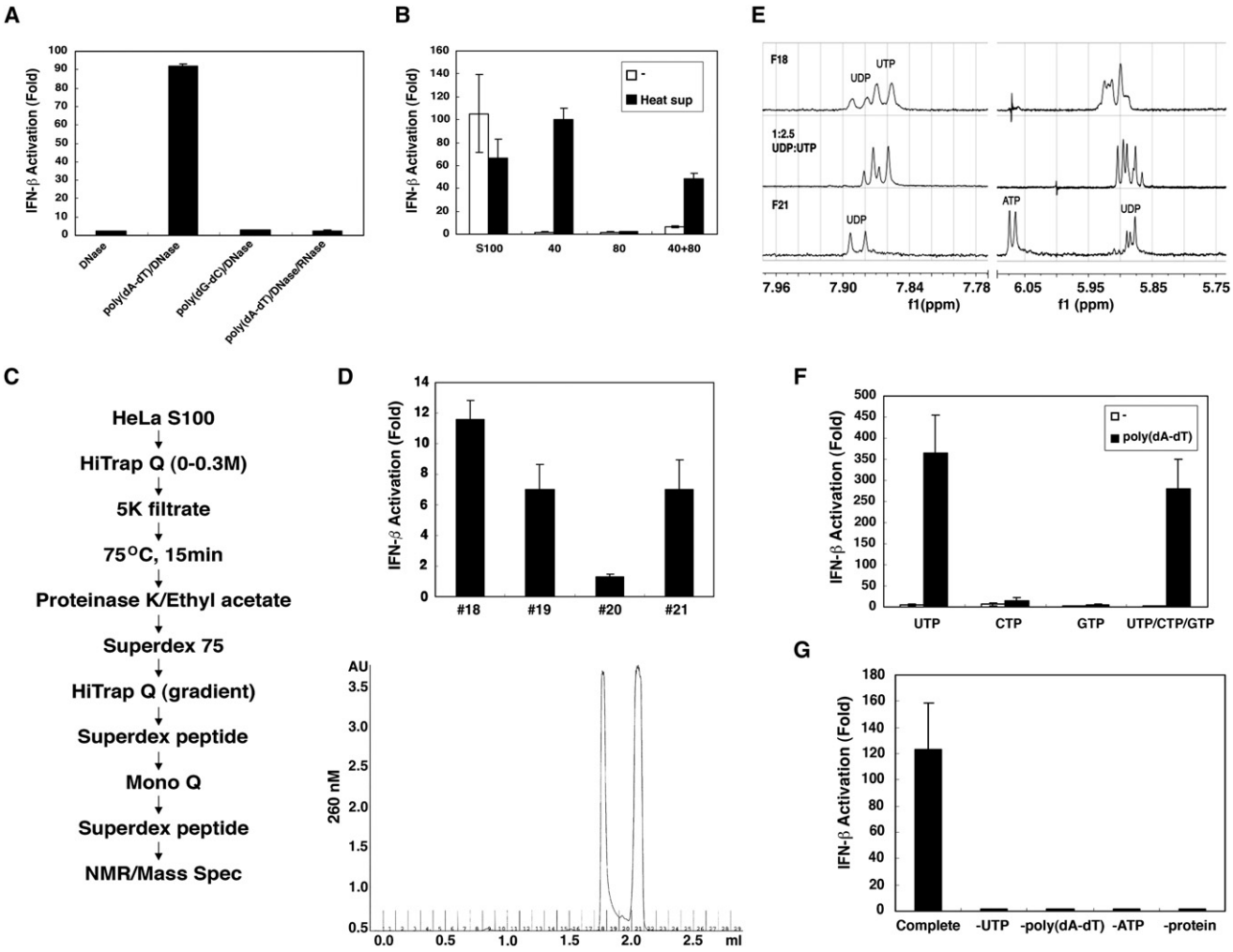

Figure 3. In Vitro Generation of IFN-Inducing RNA Requires ATP and UTP

(A) HeLa S100 was incubated with poly(dA-dT) or poly(dG-dC) and ATP. After DNase I and/or RNase A treatment, RNA was extracted and transfected into HEK293-IFNβ-luciferase reporter cells.

(B) HeLa S100 was precipitated with 40% ammonium sulfate, and then the supernatant was further precipitated with 80% ammonium sulfate. The precipitates were dialyzed and incubated with poly(dA-dT) and ATP in the presence or absence of the supernatant from heat-treated HeLa S100 ("heat sup"). RNA from the in vitro reaction was extracted and transfected into HEK293-IFNβ-luciferase reporter cells.

(C) Scheme of purification of heat-resistant factor required for the generation of IFN-inducing RNA.

(D) Chromatogram (A260) of the small molecules on Superdex peptide column (last step; lower panel). Fractions from the Superdex peptide column were incubated with a protein fraction from 40% ammonium sulfate precipitation, poly(dA-dT), and ATP, and then RNA from the reaction was extracted for IFN-β reporter assays (upper panel).

(E) NMR spectra of fractions 18 (F18; top spectrum) and 21 (F21; bottom). The middle spectrum is a mixture of authentic UDP and UTP standards (1:2.5).

(F) UTP, CTP, GTP, or UTP/CTP/GTP (1.5 mM) was used to substitute for the "heat sup" in the in vitro reaction, then RNA was extracted for IFN-β reporter assays.

(G) Reactions containing a crude protein fraction (40% ammonium sulfate precipitate), poly(dA-dT), ATP, and UTP (complete reaction) or lacking one of the components were carried out in vitro, and then RNA was extracted for IFN-β reporter assays.

Error bars represent the variation range of duplicate experiments.

activity was not due to contaminating poly(dA-dT) (Figure 3A). Similar to the cell-based assays, poly(dG-dC), poly(dI-dC), or calf thymus DNA was incapable of triggering the production of IFN-inducing RNA in the in vitro system (Figure S4A). The cell lysates from human (HEK293 and THP1) and mouse (MEF and Raw264.7) cell lines were also capable of generating IFN-inducing RNA in the presence of poly(dA-dT) (Figure S4B). Furthermore, the RNA generated in vitro lost its ability to induce IFN-β after treatment with SAP or the enzymes that digest dsRNA (RNase III and high concentration of RNase A), but not those that digest ssRNA (RNase T1 and RNase A at low concentration) (Figures S4C and S4D). The in vitro-generated IFN-inducing RNA was also resistant to terminator exonuclease, indicating that it does not contain 5′-monophosphate (Figure S4E). These results indicate that the cell-free system that we established faithfully recapitulates

the generation of IFN-inducing RNA in poly(dA-dT)-transfected cells.

ATP and UTP Are Required for the Generation of IFN-Inducing RNA In Vitro

To identify the factors required for the generation of IFN-inducing RNA, we first divided HeLa cytosolic extracts (S100) into two parts by 40% and 40%–80% ammonium sulfate precipitation. The precipitates were dialyzed (5 kDa cutoff) and then assayed for their ability to generate IFN-inducing RNA in the presence of poly(dA-dT) and ATP. Surprisingly, the 40% and 40%–80% fractions did not have the activity either alone or in combination (Figure 3B), suggesting that some factors were lost during dialysis or were not precipitated by 80% ammonium sulfate. To test whether HeLa S100 contains some small molecules or other heat-resistant factors required for the production of IFN-inducing RNA, we treated HeLa S100 at 75°C for 15 min to precipitate most proteins, and the supernatant ("heat sup") was tested for its ability to support the generation of IFN-inducing RNA in the presence of the dialyzed fractions from ammonium sulfate precipitation. Addition of the "heat sup" to the reaction containing 40% ammonium sulfate-precipitated proteins led to a robust production of IFN-inducing RNA (Figure 3B). The activity in the "heat sup" was resistant to proteinase K, DNase I, and RNase If (Figure S5A) and could penetrate through a filter with 5 kDa molecular weight cutoff (data not shown), suggesting that some small molecules were required for generating IFN-inducing RNA. We purified the small molecules through the purification scheme indicated in Figure 3C and found two distinct peaks of activity in the last step of purification using a gel filtration column (Superdex peptide; Figure 3D). The fractions from both peaks had maximum absorption at 254 nanometer (data not shown), suggesting that they might be nucleotides or derivatives of nucleotides.

Two active fractions (18 and 21) from the Superdex peptide column were further analyzed by LC-MS (Figure S6) and NMR (Figure 3E). LC-MS analysis (see the Supplemental Data for details) of fraction 21 (F21) indicated the presence of UDP with an *m/z* of 403.0 $[M–H]^+$, although the signal was partially masked by the presence of HEPES buffer (Figure S6). The ^{1}H NMR spectrum of F21 measured in D_2O at 600 MHz showed the characteristic signals of a uridine nucleotide: two aromatic doublets at δ 7.89 and 5.91 ppm, an anomeric doublet at 5.87 ppm, and overlapping multiplets of the ribose (Figure 3E). Comparison to an authentic standard of UDP in D_2O with 10 μM HEPES and 40 μM KCl showed an excellent overlap in the ^{1}H NMR spectrum, unequivocally establishing the active component of F21 as UDP.

The second active fraction, F18, was determined to be a 2:1 ratio of UTP to UDP. LC-MS clearly showed the presence of UDP, but under the initial conditions we were unable to detect UTP. ^{1}H NMR analysis showed two doublets at δ 7.85 and 7.89 ppm in a 2:1 ratio and a complex mixture of signals from δ 5.85 to 5.90 ppm (Figure 3E). The close similarity of the two sets of signals between F18 and F21 indicated the presence of a metabolite related to UDP, most likely UTP. ^{1}H NMR of an authentic standard of 1:2.5 UDP:UTP with 10 μM HEPES and 40 μM KCl was nearly identical to F18. The small difference in chemical shift can be attributed to a difference in pH and ionic strength between F21 and the authentic standard. We originally missed the presence of UTP in F18 by LC-MS using our original LC conditions (condition 1 in experimental procedures), but changing the buffer to 0.1 M NH_4OAc as a buffer (condition 2) allowed us to clearly verify the presence of UTP with an *m/z* of 483.0 $[M–H]^+$ (Figure S6).

To verify the requirement of UTP and UDP in the production of IFN-inducing RNA, we replaced the "heat sup" with UTP, CTP, GTP, or a mixture of these three nucleotides in the in vitro assay containing the dialyzed protein (40% ammonium sulfate precipitate), poly(dA-dT), and ATP. Only UTP could support the generation of IFN-inducing RNA (Figure 3F). UDP, UMP, and uridine, but not dNTP, also supported IFN induction in the in vitro assays (Figures S5B and S5C), suggesting that the protein fraction might have nucleotide kinase activity to convert UDP, UMP, or uridine to UTP. As the reaction mixtures always contained ATP, we removed ATP from the reaction and found that this removal abolished the production of IFN-inducing RNA (Figure 3G). Therefore, both ATP and UTP are required for the generation of IFN-inducing RNA in the in vitro system.

DNA-Dependent RNA Polymerase III Catalyzes the Generation of IFN-Inducing RNA

Treatment of HeLa S100 with proteinase K completely destroyed the generation of IFN-inducing RNA in the in vitro system, indicating that one or more proteins in S100 are required for the RNA generation (Figure 4A). We purified the active proteins from HeLa S100 through eight steps of conventional chromatography (Figure 4B, left). Fractions from the last Superdex-200 step were analyzed for their ability to stimulate the generation of IFN-inducing RNA in the presence of poly(dA-dT), ATP, and UTP (Figure 4B, upper right). Aliquots of the fractions were also analyzed by silver staining (Figure 4B, lower right). At least eight visible bands copurified with the activity. Three of these bands, p45, p40, and p23, were identified by nanoelectrospray tandem mass spectrometry. The p45 bands contained subunit D of DNA-directed RNA polymerase III (POLR3D), p40 contained POLR3F, POLR3C, POLR3D, and POLR3H, and p23 contained POLR3H, POLR3G, and POLR3D. Immunoblotting showed that POLR3F and POLR3G copurified with the activity that generates IFN-inducing RNA (Figure S7). As these proteins are subunits of RNA polymerase III, we attempted to identify all the subunits of the Pol-III complex. We established a HEK293 cell line stably expressing FLAG-POLR3F and immunoprecipitated the Pol-III complex with the FLAG antibody. The Pol-III complex was eluted with a FLAG peptide and then immunoprecipitated again with an antibody against POLR3G or a control IgG (Figure 4C). Silver staining of the immunoprecipitated proteins revealed at least 12 distinct bands that were present in the POLR3G complex, but not in the control IgG sample. Nanoelectrospray mass spectrometry of these unique bands identified 11 known Pol-III subunits (POLR3A, POLR3B, POLR3C, POLR3D, POLR3E, POLR3F, POLR3G, POLR3GL, POLR3H, POLR1C, and CGRP-RCP) (Hu et al., 2002) and two other proteins (TRM1-like and RPS4) whose roles in Pol-III-mediated transcription have not been reported (Table S1). Importantly, the purified Pol-III complex immunoprecipitated with anti-POLR3G, but not the control IgG

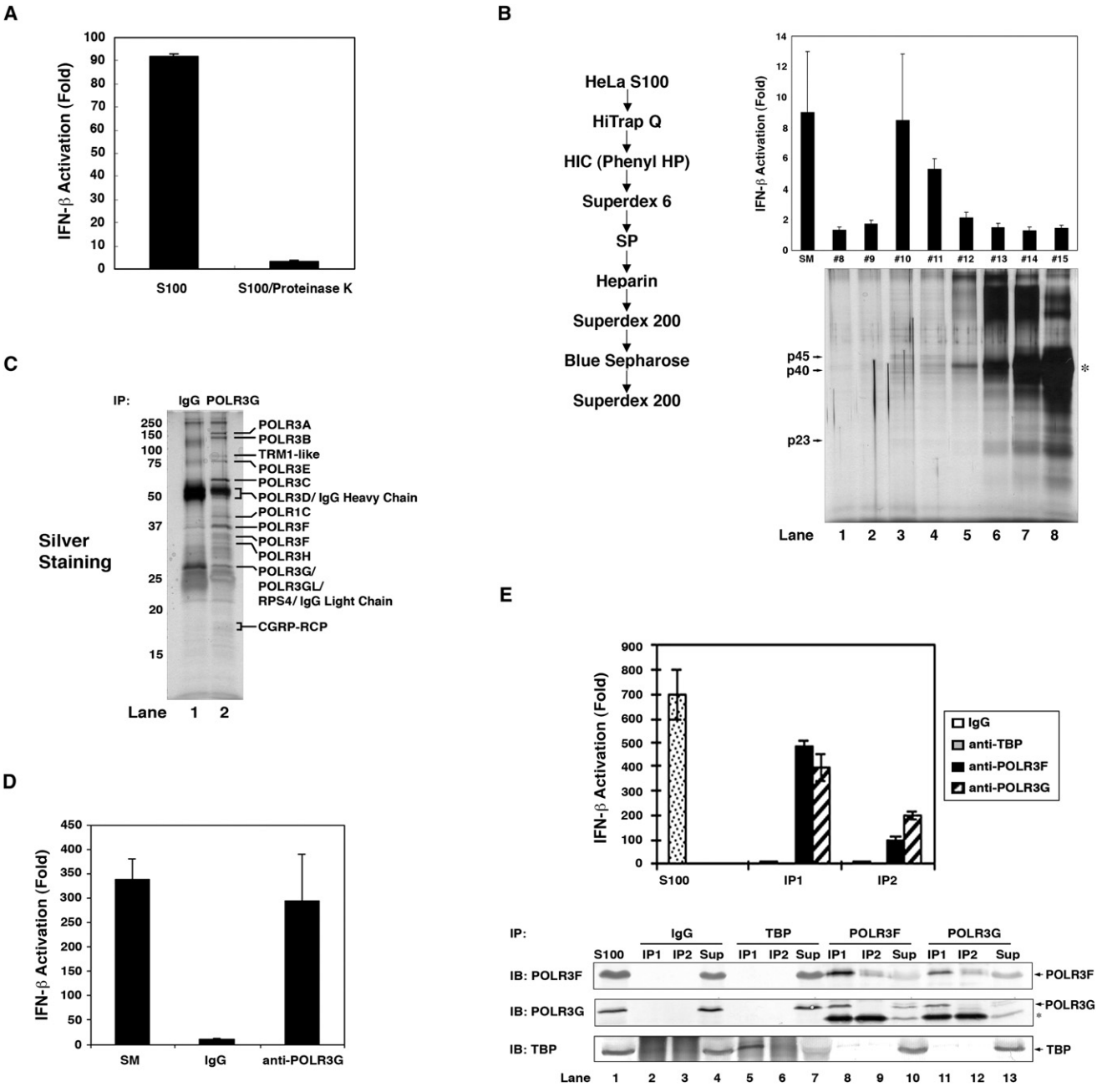

Figure 4. Purification and Identification of Pol-III

(A) HeLa S100 was incubated with or without proteinase K and then incubated with poly(dA-dT) and ATP before RNA was extracted for IFN-β reporter assays.

(B) Protein purification was carried out according to the scheme shown on the left, and fractions from the last Superdex-200 column were analyzed for their activity to produce IFN-inducing RNA (upper panel) and by silver staining (lower panel). Arrows indicate the proteins copurifying with the activity and analyzed by mass spectrometry. The asterisk indicates chicken albumin, which was added as a carrier protein during purification.

(C) Cytosolic extracts from HEK293 cells stably expressing FLAG-POLR3F were used for tandem affinity purification of the Pol-III complex, first with anti-FLAG agarose (M2) and then with an antibody against POLR3G or control IgG. The precipitated proteins were analyzed by silver staining. Unique bands from anti-POLR3G were identified by mass spectrometry.

(D) The immunopurified Pol-III complex from (C) was incubated with poly(dA-dT), ATP, and UTP before RNA was extracted for IFN-β reporter assays. SM, starting material (for IP).

(E) HeLa S100 was immunoprecipitated twice (IP1 and IP2) with an antibody specific for TBP, POLR3F, POLR3G, or control IgG. The precipitated proteins were tested for their activity to produce IFN-inducing RNA (upper panel) and analyzed by immunoblotting.

Error bars represent the variation range of duplicate experiments.

immunoprecipitate, was sufficient to catalyze the synthesis of IFN-inducing RNA in the presence of poly(dA-dT), ATP and UTP (Figure 4D).

To determine whether endogenous Pol-III could catalyze the synthesis of IFN-inducing RNA from poly(dA-dT), we purified the Pol-III complex from HeLa S100 by immunoprecipitation. Proteins immunoprecipitated with the antibodies against POLR3F or POLR3G, but not control IgG, had the ability to generate IFN-inducing RNA (Figure 4E). We also tested the involvement of TATA-binding protein (TBP), which is known to recognize the dT-dA sequence present in most Pol-II and some Pol-III promoters. Proteins precipitated with an antibody against TBP did not contain POLR3F or POLR3G, nor did they catalyze the synthesis of IFN-inducing RNA. Taken together, these results show that the core RNA Pol-III complex catalyzes the generation of IFN-inducing RNA from poly(dA-dT) in vitro.

Pol-III Catalyzes the Synthesis of Poly(A-U) RNA Using Poly(dA-dT) as a Template

Poly(dA-dT), but not poly(dG-dC), leads to the generation of IFN-inducing RNA in transfected cells (Figure 1E) and crude cell lysates (Figure S4A). Similarly, the Pol-III complex purified from HEK293 stable cells expressing FLAG-tagged POLR3D or POLR3F catalyzed the synthesis of IFN-inducing RNA from poly(dA-dT), but not poly(dG-dC) (Figure 5A). Ethidium bromide staining showed that poly(dA-dT), but not poly(dG-dC), served as the template for RNA synthesis in vitro (Figure 5B). In vitro transcription experiments showed that Pol-III catalyzed the incorporation of α-^{32}P-UTP into RNA when poly(dA-dT), but not calf thymus DNA, was used as the template (Figure 5C). Northern blot analysis with a radiolabeled poly(A-U) RNA probe confirmed that the RNA synthesized by Pol-III in the presence of poly(dA-dT) was indeed poly(A-U) (Figure 5D, lane 2).

To test whether poly(dA-dT) directs the synthesis of poly(A-U) RNA in cells, we transfected poly(dA-dT) into HEK293 cells stably expressing FLAG-tagged RIG-I, immunoprecipitated RIG-I with the FLAG antibody, and then analyzed the RIG-I bound RNA by northern blotting using the radiolabeled poly-(A-U) RNA probe (Figure 5D; lanes 4–9). Poly(A-U) RNA was present in the RIG-I complex isolated from poly(dA-dT)-transfected cells but not mock-transfected or Sendai virus-infected cells. These results strongly suggest that poly(dA-dT) serves as a template to direct the synthesis of poly(A-U) RNA by Pol-III. Due to its sequence complementarity, poly(A-U) probably forms a double-stranded RNA, and it apparently retains the 5′-triphosphate, rendering it a strong RIG-I ligand.

Pol-III Is Necessary for the Generation of IFN-Inducing RNA

To determine whether Pol-III is the major enzyme responsible for poly(dA-dT)-dependent RNA synthesis in HeLa S100, we depleted Pol-III from the extract by repeated immunoprecipitation with an antibody against POLR3F. The Pol-III depleted S100 was largely devoid of the activity to synthesize IFN-inducing RNA, whereas mock depletion with a control IgG did not remove the activity (Figure 6A). Consistent with the notion that the cytoplasmic Pol-III generates IFN-inducing RNA in the cytosol, RNA isolated from the cytosol of poly(dA-dT)-transfected cells strongly induced IFN-β, whereas nuclear RNA isolated from the same cells did not (Figure 6B).

To test whether Pol-III is required for the production of IFN-inducing RNA in poly(dA-dT)-transfected cells, we took two independent approaches. In the first approach, we used two different pairs of siRNA oligos against POLR3F to silence the expression of this essential Pol-III subunit in HEK293 cells, then transfected the cells with poly(dA-dT) or infected the cells with Sendai virus. RNA from these cells was extracted and then transfected into the HEK293-IFNβ-luciferase reporter cell line. Both siRNA oligos, but not the control GFP siRNA, strongly inhibited the generation of IFN-inducing RNA in poly(dA-dT)-transfected cells (Figure 6C). In contrast, the production of Sendai virus RNA, which is largely carried out by the viral RNA-dependent RNA polymerase, was not affected by the knockdown of POLR3F. Northern blot analysis showed that RNAi of POLR3F blocked the production of RIG-I-associated poly(A-U) RNA, demonstrating that Pol-III is required for the transcription of poly(dA-dT) in cells (Figure 6D). In the second approach, we treated HEK293 cells with a specific chemical inhibitor of RNA Pol-III, ML-60218 (Wu et al., 2003), before transfection with poly(dA-dT) or infection with Sendai virus. This inhibitor selectively inhibited the production of IFN-inducing RNA in cells transfected with poly(dA-dT) but not in cells infected with Sendai virus (Figures 6E and 6F). The partial blockade of IFN-β induction might be due to incomplete knockdown and partial chemical inhibition of Pol-III in cells. Nevertheless, it is clear from these results that Pol-III is required for the transcription of poly(dA-dT) into poly(A-U) RNA, which induces IFN-β.

Pol-III Is Required for IFN-β Induction by *Legionella pneumophila*

A previous study showed that RNAi of MAVS inhibits IFN-β induction in a human lung epithelial cell line by *Legionella pneumophila* (Opitz et al., 2006), a gram-negative intracellular bacterium that infects macrophages and causes Legionnaires' disease. However, the role of MAVS in immune defense against *Legionella* and the underlying mechanism are largely unknown. We infected BMDM isolated from wild-type and *Mavs*$^{-/-}$ mice with *L. pneumophila* and then measured IFN-β expression by quantitative PCR (qPCR; Figure 7A). The induction of IFN-β by the bacteria was markedly reduced in *Mavs*$^{-/-}$ macrophages. Strikingly, the Pol-III inhibitor ML-60218 strongly inhibited IFN-β induction by *L. pneumophila* in a dose-dependent manner (Figure 7B). When the RNA was extracted from the drug-treated and bacteria-infected cells and then transfected into Raw264.7 macrophages again, IFN-β induction by RNA extracted from Pol-III inhibited cells was reduced to a level similar to that observed with RNA from mock-infected cells (Figure 7C), indicating that Pol-III is required for the generation of IFN-inducing RNA by *Legionella*. The RNA isolated from the cytoplasm of *Legionella*-infected cells contained IFN-inducing activity, whereas the nuclear RNA from the same cells did not induce IFN (Figure 7D). Importantly, ML-60218 treatment significantly increased the bacterial load in the macrophages (Figure 7E), indicating that inhibition of the host Pol-III promotes rather than impedes bacterial growth. IFN-β treatment restored inhibition

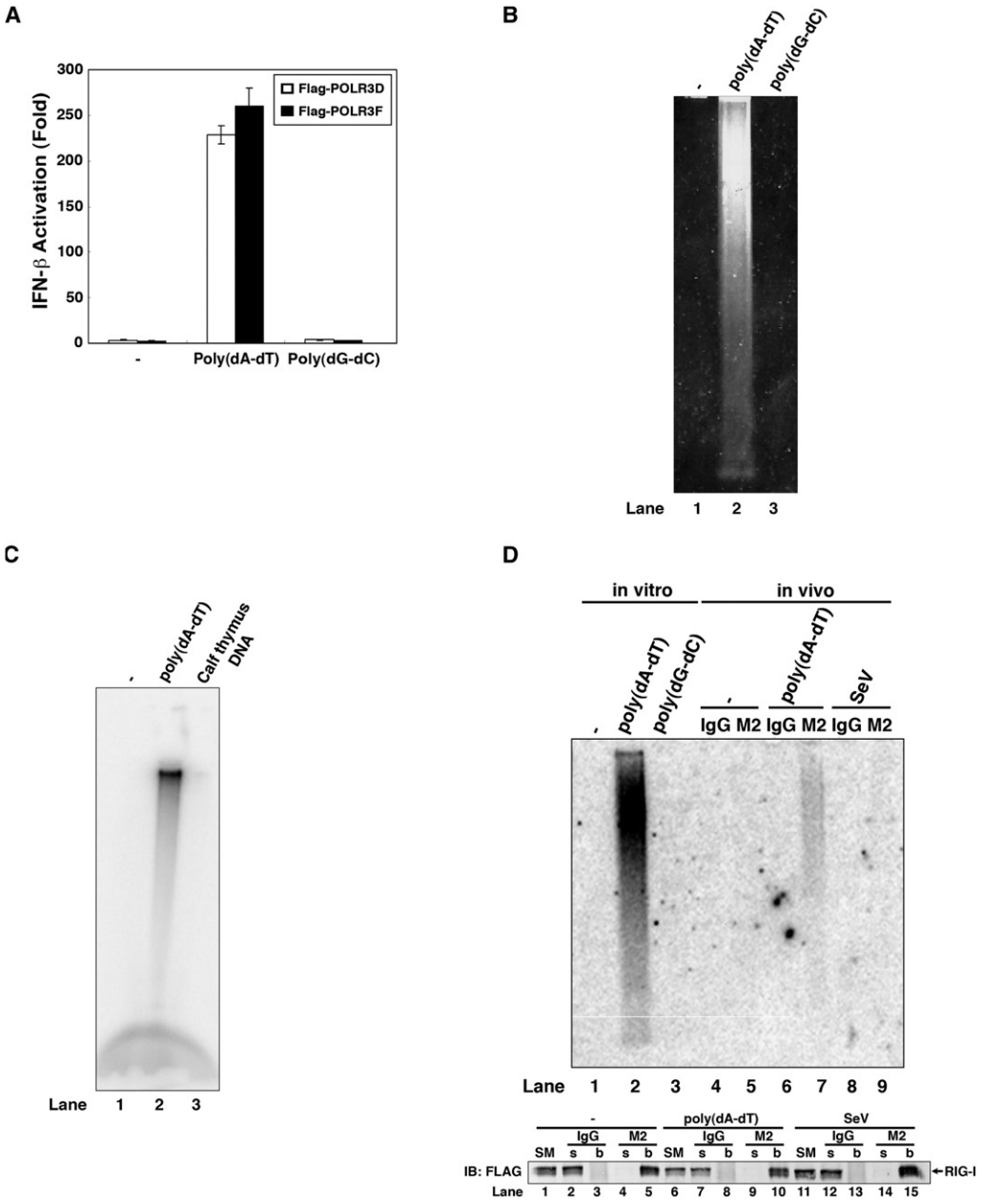

Figure 5. Pol-III Catalyzes the Synthesis of Poly(A-U) RNA Using Poly(dA-dT) as the Template

(A) Pol-III complex was immunopurified from HEK293 cells stably expressing FLAG-tagged POLR3D or POLR3F and then incubated with poly(dA-dT) or poly(dG-dC) in the presence of NTP. RNA was extracted from the reactions for IFN-β reporter assays. Error bars represent the variation range of duplicate experiments.

(B) RNAs synthesized by in vitro transcription of poly(dA-dT) or poly(dG-dC) were separated by agarose gel eletrophoresis followed by ethidium bromide staining.

(C) RNAs synthesized by in vitro transcription of poly(dA-dT) or calf thymus DNA in the presence of α-^{32}P-UTP and NTP were analyzed by agarose gel electrophoresis followed by autoradiography.

(D) HEK293 cells stably expressing FLAG-tagged RIG-I were transfected with poly(dA-dT) (lanes 6 and 7), infected with Sendai virus (lanes 8 and 9), or mock treated (lanes 4 and 5). RIG-I was subsequently immunoprecipitated with the FLAG antibody (M2) or control IgG, and RNA in the precipitates was extracted and analyzed by northern blotting with ^{32}P-labeled poly(A-U) RNA used as a probe. In lanes 1–3, RNAs synthesized by in vitro transcription of poly(dA-dT) or poly(dG-dC) or in the absence of DNA were analyzed by northern blotting. Bottom panel: Immunoprecipitated proteins were analyzed by immunoblotting with a FLAG antibody. SM, starting material (cell lysates); s, supernatant; b, bound proteins on the beads.

of *Legionella* replication in cells treated with the Pol-III inhibitor (Figure 7F), demonstrating that Pol-III-induced IFN-β production is important for suppressing the bacterial replication. Taken together, these results strongly suggest that Pol-III and MAVS mediate interferon induction and immune defense against *Legionella*.

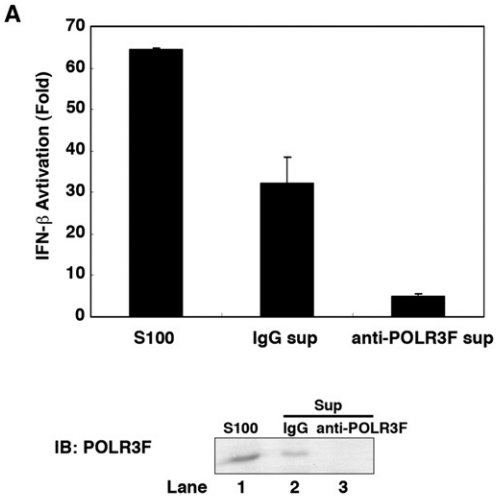
A
IFN-β Avtivation (Fold)
70
60
50
40
30
20
10
0
S100
IgG sup
anti-POLR3F sup
Sup
S100
IgG
anti-POLR3F
IB: POLR3F
Lane 1 2 3

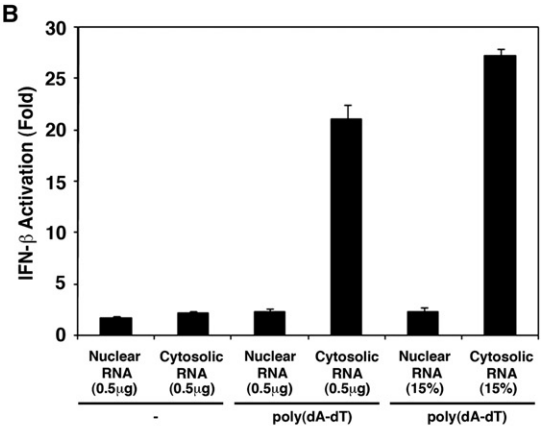
B
IFN-β Activation (Fold)
30
25
20
15
10
5
0
Nuclear RNA (0.5μg)
Cytosolic RNA (0.5μg)
Nuclear RNA (0.5μg)
Cytosolic RNA (0.5μg)
Nuclear RNA (15%)
Cytosolic RNA (15%)
-
poly(dA-dT)
poly(dA-dT)

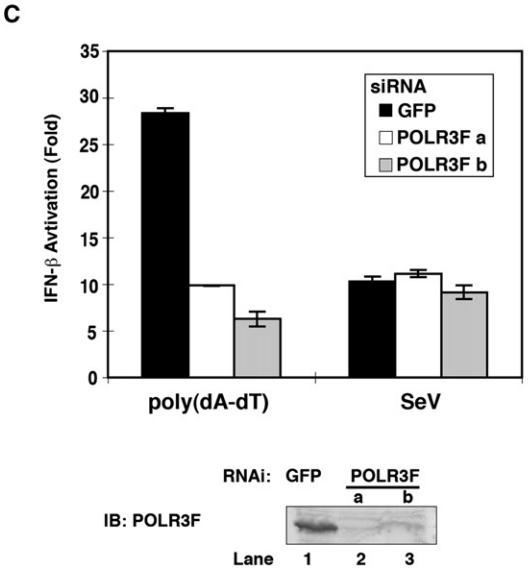
C
IFN-β Avtivation (Fold)
35
30
25
20
15
10
5
0
siRNA
GFP
POLR3F a
POLR3F b
poly(dA-dT)
SeV
RNAi: GFP POLR3F
a b
IB: POLR3F
Lane 1 2 3

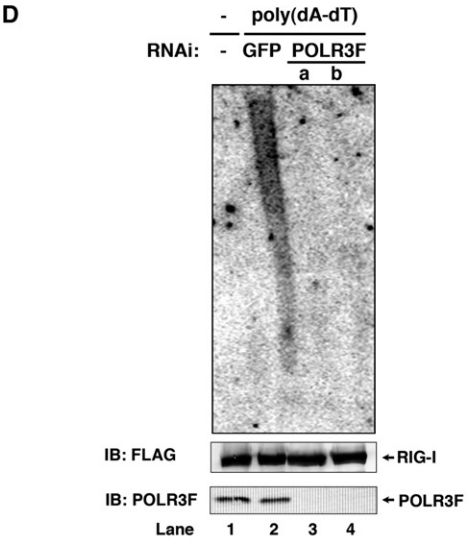
D
- poly(dA-dT)
RNAi: - GFP POLR3F
a b
IB: FLAG
←RIG-I
IB: POLR3F
←POLR3F
Lane 1 2 3 4

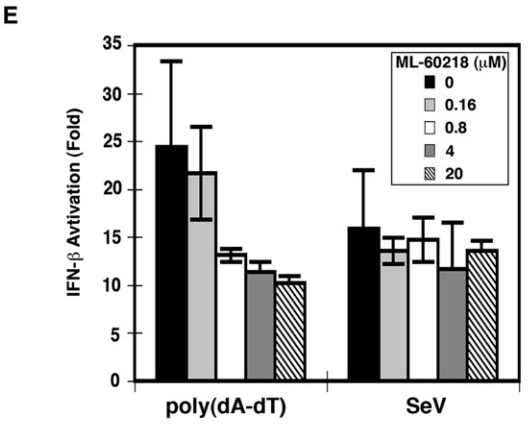
E
IFN-β Avtivation (Fold)
35
30
25
20
15
10
5
0
ML-60218 (μM)
0
0.16
0.8
4
20
poly(dA-dT)
SeV

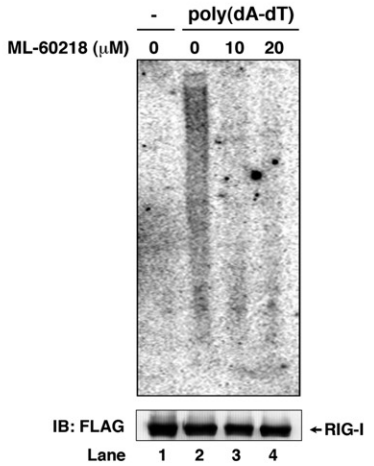
F
- poly(dA-dT)
ML-60218 (μM) 0 0 10 20
IB: FLAG
←RIG-I
Lane 1 2 3 4

Pol-III Mediates IFN-β Induction by DNA Viruses

Some DNA viruses, including adenovirus, HSV-1 and EBV, induce IFN-β production in a RIG-I dependent matter (Cheng et al., 2007; Rasmussen et al., 2007; Samanta et al., 2006). To determine whether Pol-III plays a role in IFN induction by DNA viruses, we treated Raw264.7 cells with ML-60218 and then infected the cells with adenovirus, HSV-1, or Sendai virus (RNA virus as a control). IFN-β induction by adenovirus (Figure 7G) and HSV-1 (Figure 7H) was markedly reduced by ML-60218 treatment. By contrast, ML-60218 treatment had no effect on IFN-β induction by Sendai virus (Figure 7I), suggesting that the effect of ML-60218 was not due to general inhibition of IFN-β synthesis. ML-60218 also inhibited the production of IFN-inducing RNA in macrophages infected with HSV-1 but not Sendai virus (Figures S8A and S8B).

IFN induction by EBV has been linked to human autoimmune diseases, including systemic lupus erythematosus (SLE) (Ronnblom and Pascual, 2008). Interestingly, EBV-encoded small RNA 1 and 2 (EBER1 and EBER2) are noncoding, nonpolyadenylated RNAs that form dsRNA-like stem-loop structures (Lerner et al., 1981). These abundant small RNAs, which contain 5′-triphosphate, are present in RNP particles that can be precipitated with anti-La antibody from the SLE patients. We tested the effects of the Pol-III inhibitor on IFN-β production in an EBV-producing human B cell line, B95-8. These cells were treated with different amounts of ML-60218 before total RNA was extracted for qPCR. The levels of EBER1, EBER2, and IFN-β RNA were reduced by the treatment with ML-60218 (Figure 7J). By contrast, the expression of a Pol-II dependent gene, α-*actin*, was not affected by the Pol-III inhibitor. ML-60218 also inhibited the production of IFN-inducing RNA in EBV-infected cells (Figure S8C). Collectively, these results suggest that Pol-III mediates IFN-β induction in EBV-infected B cells, possibly through transcription of EBV-encoded small RNAs.

DISCUSSION

In this report, we delineate a mechanism by which AT-rich cytosolic DNA induces IFN-β production in human and mouse cell lines. We found that poly(dA-dT) serves as a template for the de novo synthesis of poly(A-U) RNA by DNA-dependent RNA polymerase III. The IFN-inducing activity of the RNA is resistant to terminal exonuclease and RNase T1 but sensitive to alkaline phosphatase and RNase III, indicating that this is a double-stranded RNA containing more than one phosphate at the 5′ ends. Although at present we cannot definitively determine whether the RNA contains 5′-triphosphate or 5′-diphosphate, Pol-III is known to synthesize RNA containing 5′-triphosphate. Our results that Pol-III is responsible for the synthesis of the RNA from poly(dA-dT) (Figures 4 and 6), which binds directly to RIG-I (Figures 2D and 5D), strongly suggest that the RNA contains 5′-triphosphate.

The RNA Pol-III complex is both necessary and sufficient to catalyze the synthesis of poly(A-U) from poly(dA-dT) in vitro. By employing RNAi and a specific inhibitor of Pol-III, we show that Pol-III is required for the production of IFN-inducing RNA by poly(dA-dT) in cells. Furthermore, Pol-III inhibition significantly reduced the induction of IFN-β by intracellular bacteria (*Legionella pneumophila*) and DNA viruses (adenovirus, HSV-1, and EBV), but not RNA viruses (Sendai virus). Pol-III inhibition also led to a significant increase of bacterial replication (*Legionella pneumophila*). These results strongly suggest that Pol-III plays a key role in sensing and limiting infection by intracellular bacteria and DNA viruses.

Cytosolic RNA Pol-III Is a DNA Sensor that Triggers Innate Immune Response

Pol-III was purified from cytosolic extracts (Figure 4), consistent with its role as a cytosolic DNA sensor. Cytosolic RNA isolated from cells transfected with poly(dA-dT) or infected with Legionella strongly induced IFN-β, whereas RNA isolated from the nucleus of the same cells did not (Figures 6B and 7D), further supporting our model that cytosolic Pol-III is responsible for production of IFN-inducing RNA, which is then recognized by RIG-I in the cytosol. Previous studies utilizing in vitro transcription assays showed that two-thirds of the Pol-III activity is in the cytoplasm, whereas only 16% and 11% of the Pol-I and Pol-II activities are in the cytoplasm, respectively (Jaehning and Roeder, 1977). These pioneering studies divided Pol-III into two chromatographic forms (III_A and III_B). Only Pol-III_A is present in the nucleus, while approximately equal amounts of Pol-III_A and Pol-III_B are found in the cytoplasm. It has been a long-standing mystery why the majority of Pol-III activity is present in the cytosol, where DNA should be avoided. Our

Figure 6. Pol-III Is Required for the Production of IFN-Inducing RNA

(A) HeLa S100 was immunodepleted five times with a POLR3F antibody or control IgG. S100 and the immunodepleted supernatants were incubated with poly(dA-dT), UTP, and ATP before RNA was extracted for IFN-β reporter assays (upper panel). The efficiency of immunodepletion was analyzed by immunoblotting with the POLR3F antibody (lower panel).

(B) HEK293 cells were transfected with or without poly(dA-dT) for 4 hr. Nuclear and cytosolic lysates were prepared for RNA extraction. HEK293-IFNβ-luciferase reporter cells were transfected with 0.5 μg or 15% of nuclear or cytosolic RNAs, followed by measurement of IFN-β induction.

(C) Two siRNA oligos against POLR3F (a and b) or a control GFP siRNA were transfected into HEK293 cells. The cells were subsequently transfected with poly(dA-dT) or infected with Sendai virus for 2 hr before RNAs were extracted for IFN-β reporter assays.

(D) HEK293/RIG-I-FLAG stable cells were transfected with siRNA as described in (C) and then transfected with poly(dA-dT) for 3 hr. The RIG-I complex was immunoprecipitated with a FLAG antibody, and then the RNAs associated with RIG-I were extracted and analyzed by northern blotting with α-^{32}P-poly(A-U) RNA used as a probe. RIG-I in the immunoprecipitates and POLR3F in cell lysates were analyzed by immunoblotting.

(E) HEK293 cells were treated with the indicated concentrations of the Pol-III inhibitor ML-60218 for 10 hr before transfection with poly(dA-dT) or infection with Sendai virus for 2 hr. RNAs were extracted for IFN-β reporter assays.

(F) HEK293/RIG-I-FLAG stable cells were treated with ML-60218 and then transfected with poly(dA-dT). RNAs associated with the RIG-I complex were analyzed by northern blotting as described in (D).

Error bars represent the variation range of duplicate experiments.

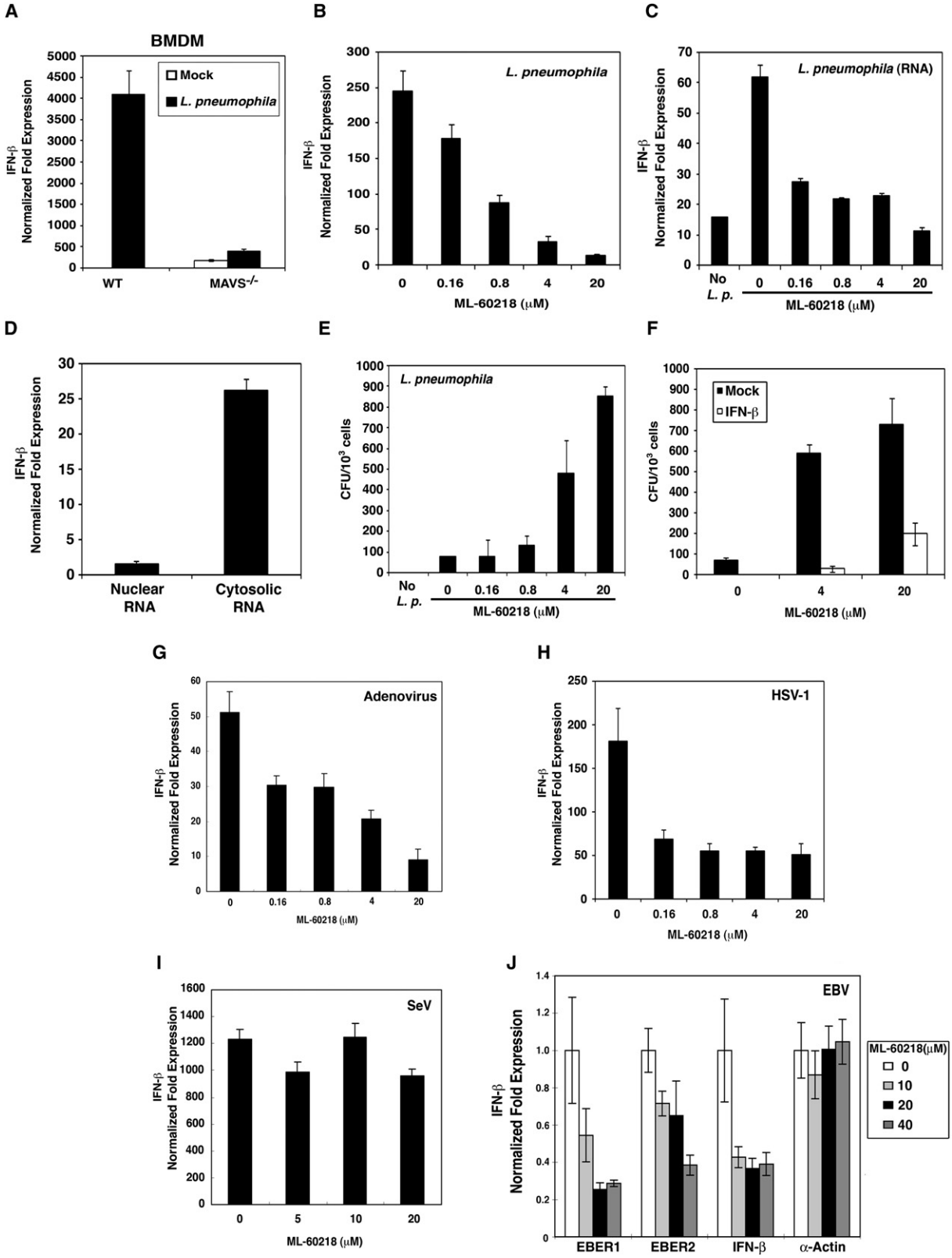
A
BMDM
Mock
L. pneumophila
IFN-β Normalized Fold Expression
WT
MAVS-/-
B
L. pneumophila
IFN-β Normalized Fold Expression
ML-60218 (μM)
C
L. pneumophila (RNA)
IFN-β Normalized Fold Expression
No L. p.
ML-60218 (μM)
D
IFN-β Normalized Fold Expression
Nuclear RNA
Cytosolic RNA
E
L. pneumophila
CFU/10³ cells
No L. p.
ML-60218 (μM)
F
Mock
IFN-β
CFU/10³ cells
ML-60218 (μM)
G
Adenovirus
IFN-β Normalized Fold Expression
ML-60218 (μM)
H
HSV-1
IFN-β Normalized Fold Expression
ML-60218 (μM)
I
SeV
IFN-β Normalized Fold Expression
ML-60218 (μM)
J
EBV
IFN-β Normalized Fold Expression
ML-60218(μM)
0
10
20
40
EBER1
EBER2
IFN-β
α-Actin

finding that cytosolic Pol-III is a DNA sensor that mediates innate immune response provides a potential answer to this conundrum. The cytosol is a strategic location for Pol-III to function in immune defense, because RNA synthesized in the cytosol contains 5′-triphosphate that can be detected by RIG-I, whereas RNA synthesized in the nucleus is likely to be modified by enzymes such as the capping enzymes (e.g., mRNA) or processed to generate 5′-monophosphate (e.g., tRNA), which escapes detection by RIG-I. Therefore, we propose that nuclear and cytoplasmic RNA polymerases serve opposing functions: while the nuclear polymerases produce the host RNA that should be modified to avoid triggering autoimmune response through the RIG-I pathway, the cytosolic Pol-III is specialized to detect foreign and aberrant DNA to mount an immune response to defend the integrity of the host cytoplasm.

Recognition of AT-Rich DNA Sequences by RNA Pol-III

At least three different complexes have been identified as transcription factors for polymerase III (TFIIIA, TFIIIB, and TFIIIC) (Schramm and Hernandez, 2002). TBP is one of the subunits in TFIIIB, and it binds to the TATA box. The nature of the poly(dA-dT) sequence might provide the TATA motifs for TBP binding. However, TBP is not present in the highly purified Pol-III complex that catalyzes in vitro transcription of poly(dA-dT), and TBP immunoprecipitated from cytosolic extracts does not have the transcription activity (Figures 4C and 4E). Therefore, TBP may not be responsible for the preferential recognition of dA-dT-rich sequences by Pol-III, although our results cannot rule out the possibility that TBP might play a role in DNA sequence recognition by cytosolic Pol-III in vivo. The Pol-III complex we purified contains at least 13 subunits; some of these subunits may determine the optimal sequences that permit transcription by Pol-III.

A recent study suggests that homopolymeric ribonucleotide composition, such as A-U rich sequence, is required for RNA to bind and activate RIG-I (Saito et al., 2008). Thus, it is possible that a GC-rich DNA could still be transcribed into an RNA, but the RNA lacks the ability to activate RIG-I. However, we found that Pol-III could not transcribe poly(dG-dC) or poly(dG-dC-dA-dT) DNA (Figure 5). Moreover, if we used T7 RNA polymerase to transcribe an RNA containing a GCAU sequence or a random sequence with 50% GC composition, this RNA could efficiently induce IFN-β (Figure S9), indicating that the failure of GC-rich DNA to induce IFN-β was due to the lack of the production of the RNA rather than the inability of the GC-rich RNA to induce IFN-β.

Detection of Viral and Bacterial DNA by Cytosolic RNA Pol-III

Although many DNA viruses encode DNA-dependent RNA polymerases and some use the cellular RNA polymerases for viral gene transcription, the majority of the viral RNA is modified by cellular and virus-encoded modification enzymes such as the capping enzymes. However, some viral RNAs, such as the VA-I and VA-II RNAs from adenovirus and EBER1 and EBER2 RNAs from EBV, are noncoding small RNAs containing 5′-triphosphate (Lerner et al., 1981; Rosa et al., 1981). Our results and those of previous studies suggest that these viral RNAs are transcribed by cellular Pol-III. *EBER* genes contain internal control sequence motifs (box A and B) that are recognized by TFIIIB and TFIIIC, which direct Pol-III transcription (Schramm and Hernandez, 2002). In addition, the upstream promoters of *EBER* genes contain a TATA-like sequence that specifies Pol-III, but not Pol-II, transcription (Howe and Shu, 1993). Thus, the transcription of cytosolic DNA, some of which is derived from bacteria and viruses, is controlled not only by recognition of dA-dT rich sequence by Pol-III, but also by other transcription factors associated with Pol-III, such as TFIIIA, TFIIIB, and TFIIIC.

While the VA and EBER small RNAs are abundant Pol-III transcripts that contain 5′-triphosphate, they are normally in complex with cellular proteins to form RNP particles that predominantly reside in the nucleus (Lerner et al., 1981). Therefore, these viral RNAs are segregated from RIG-I in the cytosol, providing an explanation for why cells containing these abundant viral RNAs do not produce copious amounts of IFN. This may be a mechanism by which the virus evades the host immune system, and it may also be a mechanism by which the host avoids excessive autoimmune responses. However, the VA and EBER RNP particles react with antibodies from SLE patients (Lerner et al., 1981; Rosa et al., 1981). Both the sera from SLE patients and cells chronically infected with EBV have elevated

Figure 7. Pol-III Is Required for IFN-β Induction by Intracellular Bacteria and DNA Viruses

(A) Wild-type or MAVS-deficient BMDM cells were infected with *Legionella pneumophila* for 8 hr. Total RNAs were extracted for qPCR. The expression level of *IFN-β* was normalized with that of *β-actin*.

(B) Raw264.7 cells were treated with the indicated concentrations of ML-60218 for 10 hr and then infected with *L. pneumophila*. Total RNAs were extracted after 8 hr of infection for qPCR of *IFN-β* and *β-actin*.

(C) RNAs extracted from ML-60218-treated and *L. pneumophila*-infected Raw264.7 cells as described in (B) were transfected into Raw264.7 cells to induce IFN-β.

(D) Raw264.7 cells were infected with *L. pneumophila* for 8 hr before nuclear and cytosolic lysates were prepared to extract RNAs. The RNAs were transfected into Raw264.7 cells to induce IFN-β.

(E) Raw264.7 cells were treated with ML-60218 for 10 hr and infected with *L. pneumophila* for 24 hr. The bacterial colonies were counted and shown as CFU per 1000 cells.

(F) Raw264.7 cells were treated with ML-60218 in the presence or absence of mouse IFN-β and subsequently infected with *L. pneumophila*. Bacterial colonies were determined as described in (E).

(G–I) Raw264.7 cells were treated with ML-60218 for 10 hr and then infected with adenovirus (AdV; G), Herpes Simplex Virus-1 (HSV-1; H) or Sendai virus (SeV; I). Total RNAs were extracted for qPCR of *IFN-β* and *β-actin*.

(J) The Epstein-Bar virus (EBV)-producing B95-8 cells were treated with ML-60218 for 24 hr, and then total RNAs were prepared for qPCR. The expression levels of *EBER1*, *EBER2*, *IFN-β*, and *α-actin* genes were normalized with that of the *β-actin* RNA.

Error bars represent standard deviations of triplicate experiments.

levels of type I interferons, and epidemiology studies have suggested a link between EBV infection and SLE (Ronnblom and Pascual, 2008). It is possible that under certain pathological conditions, some of the viral RNA gains access to RIG-I, triggering IFN production that contributes to autoimmune diseases.

Like viruses, intracellular bacteria are potent inducers of type I interferons. However, the mechanisms by which bacteria induce interferons are largely unknown. Interestingly, Mavs-deficient macrophages are severely defective in producing IFN-β in response to infection by *Legionella pneumophila*. Our finding that Pol-III is required for IFN-β induction by *L. pneumophila* provides a mechanism for the Mavs-dependent innate immune response against this bacterium. Our results suggest that Pol-III detects some segments of the bacterial DNA and transcribes them into RNA ligands that induce IFN-β through the RIG-I-MAVS pathway. The utilization of Pol-III as a DNA sensor for bacteria and DNA viruses may allow the host to take advantage of the RIG-I-MAVS pathway to defend against a much larger spectrum of microbial pathogens.

MAVS-Dependent and -Independent Pathways Triggered by Cytosolic DNA

Our results that deletion of MAVS or inhibition of Pol-III blocked IFN-β production in response to *Legionella* infection suggest that the Pol-III-MAVS pathway is the major pathway responsible for interferon induction by this bacterium (Figures 7A and 7B). Future research should reveal whether the MAVS-dependent DNA-sensing pathway is the major pathway for immune defense against other pathogens, including bacteria, DNA viruses, or even parasites such as malaria. However, the Pol-III-MAVS pathway is unlikely to be the only cytosolic DNA-sensing pathway that induces type I IFNs. While the human cell lines HEK293 and HeLa solely rely on the Pol-III-MAVS pathway to induce IFN in response to poly(dA-dT), primary MEF cells possess both MAVS-dependent and -independent pathways to detect cytosolic DNA. Interestingly, we noticed that spontaneous immortalization of MEF cells by repeated passages led to a loss of the MAVS-independent pathway (Y.C. and Z.J.C., unpublished data). It is not clear why immortalized or transformed cells lose the MAVS-independent pathway, but it is interesting to note that the loss of IFN induction by DNA transfection in some transformed cells such as HEK293 and HeLa may allow the widespread use of these cells in molecular cell biology. The MAVS-independent pathway appears to recognize DNA structure rather than its sequence. Although the DNA-binding protein DAI (ZBP1) has been proposed as a DNA sensor that induces type I IFNs, DAI-deficient mice and cells from these mice do not have apparent defects in producing type I IFNs in response to DNA stimulation (Ishii et al., 2008; Takaoka et al., 2007). The recently discovered DNA-binding protein AIM2 is clearly a cytosolic DNA sensor that activates the inflammasome and caspase-1, but it does not induce type I IFNs (Schroder et al., 2009). It is possible that multiple sensors exist to detect the invasion of cytosol by foreign or aberrant self DNA. The identification of these DNA sensors, including Pol-III, should provide critical insights into the mechanism of innate immune responses against a large variety of microbial pathogens including bacteria and viruses. Furthermore, this line of research will lead to a deeper understanding of the mechanism underlying debilitating autoimmune diseases such as lupus.

EXPERIMENTAL PROCEDURES

Nucleic Acid Extraction

Total RNAs were extracted by TRIzol (Invitrogen) from cells according to the manufacturer's instructions. For preparation of nuclear and cytoplasmic RNA, cells were lysed in buffer A (10 mM HEPES [pH 7.5], 10 mM KCl, and 1.5 mM $MgCl_2$) by douncing and centrifuged at 100 × g for 5 min to remove cell debris. The supernatant was centrifuged at 500 × g for 5 min to collect the nuclear pellet. The supernatant was further centrifuged at 20,000 × g for 10 min to collect the cytosolic supernatant. Nucleic acids were extracted from the nuclear and cytosolic lysates with phenol and chloroform, followed by isopropanol precipitation.

In Vitro Reconstitution Assay

Cell extracts (S100) were prepared as described previously (Deng et al., 2000). S100 (2 mg/ml) was incubated with poly(dA-dT) or poly(dG-dC) (20 μg/ml) together with ATP (2 mM), $MgCl_2$ (5 mM), and RNase inhibitor (0.4U/μl, Invitrogen) in a 50 μl reaction mixture at 30°C for 1 hr. After incubation, 50 μl of buffer A was added, and then nucleic acids were extracted by phenol/chloroform, followed by isopropanol precipitation and DNase I digestion. The extracted RNA was tested for IFN-β induction. For reconstitution experiments, dialyzed proteins from ammonium sulfate precipitation or column fractions and heat supernatant (heat sup) were used in the reactions in lieu of S100. Heat sup was obtained by incubating HeLa S100 at 75°C for 15 min followed by centrifugation at 20,000 × g to collect the supernatant. For purification of small molecules from the heat sup, the reaction mixtures contain 40% dialyzed ammonium sulfate precipitates from S100, column fractions from heat sup, poly(dA-dT), ATP, $MgCl_2$, and RNase inhibitor. For purification of Pol-III, the reaction mixtures contain column fractions from S100, UTP (0.2 mM), poly(dA-dT), ATP, $MgCl_2$, and RNase inhibitor.

Purification of the Enzyme that Converts DNA into IFN-Inducing RNA

HeLa S100 (440 mg) was applied to a HiTrap Q column (10 ml bed volume, GE Healthcare) pre-equilibrated with buffer B (10 mM HEPES [pH 8.0], 10 mM KCl, and 1.5 mM $MgCl_2$), and eluted with a 100 ml linear gradient KCl (0–500 mM). Fractions (380–500 mM) were dialyzed against buffer C (10 mM HEPES [pH 8.0], 1 M $(NH_4)_2SO_4$, 10 mM KCl, and 1.5 mM $MgCl_2$) and loaded onto a hydrophobic interaction chromatography (HIC) column (Phenyl-Sepharose High Performance, 1 ml bed volume, GE Healthcare) pre-equilibrated with buffer C. Bound proteins were eluted with a 10 ml linear reverse gradient of $(NH_4)_2SO_4$ (1.0–0 M). The active fractions (700–300 mM) were applied to a Superose-6 gel filtration column (24 ml bed volume, GE Healthcare) pre-equilibrated with buffer D (10 mM HEPES [pH 6.5], 10 mM KCl, 1.5 mM $MgCl_2$, and 0.02% CHAPS). After elution with buffer D, fractions containing the activity were pooled and loaded onto a SP cation exchange column (1 ml bed volume, GE Healthcare) pre-equilibrated with buffer D. Bound proteins were eluted with a 10 ml linear gradient of KCl (0–500 mM). The active fractions (100–250 mM KCl) were dialyzed against buffer E (10 mM HEPES [pH 8.0], 10 mM KCl, 1.5 mM $MgCl_2$, and 0.02% CHAPS) and applied to a Heparin column with chicken ovalbumin (10 μg) as a carrier protein (1 ml bed volume, GE Healthcare) pre-equilibrated with buffer E. The active fractions (300–450 mM KCl) were eluted with a 10 ml linear gradient of KCl (0–500 mM) and loaded onto a Superdex-200 gel filtration column (0.1 ml bed volume). The SMART system was used for this and subsequent steps of purification, and ovalbumin was used as a carrier. After elution with buffer E, the fractions were applied to a Blue-Sepharose column (0.1 ml bed volume, GE Healthcare). The column was washed with 1M KCl, and the fraction containing the activity was eluted with 2 M KCl. This fraction was further separated on a Superdex-200 gel filtration column (0.1 ml bed volume). The fractions corresponding to the peak of the activity were analyzed by 12% SDS-PAGE and silver staining. The bands that copurified with the activity were excised for in-gel digestion with trypsin and identified by nano-high-pressure liquid chromatography/tandem mass spectrometry.

Viral and Bacterial Infection

Raw264.7 cells were pretreated with the Pol-III inhibitor, ML-60218 (Calbiochem), for 10 hr and then infected with an engineered adenovirus type 5 (Ad-CMV-GFP from Vector Biolabs; this virus lacks the *E1* and *E3* genes) at 100 multiplicity of infection (MOI), HSV-1 at 100 MOI, or *Legionella pneumophila* (serogroup 1 strain AA100, from ATCC) at 50 MOI for 8 hr. Cells were rinsed with PBS and lysed in Trizol for total RNA extraction.

SUPPLEMENTAL DATA

Supplemental Data include Supplemental Experimental Procedures, nine figures, and one table and can be found with this article online at http://www.cell.com/supplemental/S0092-8674(09)00714-4.

ACKNOWLEDGMENTS

We thank Xiang Chen and Xiao-Dong Li for assistance in preparing BMDM, Hon-Ren Huang (Harvard University) for technical advice, and Brian Skaug for critical reading of the manuscript. This work was supported by grants from the National Institutes of Health and the Welch Foundation (Z.J.C.) and by the Chilton Foundation (J.M.). Z.J.C. is an Investigator of Howard Hughes Medical Institute.

Received: February 8, 2009
Revised: April 13, 2009
Accepted: June 3, 2009
Published online: July 23, 2009

REFERENCES

Akira, S., Uematsu, S., and Takeuchi, O. (2006). Pathogen recognition and innate immunity. Cell *124*, 783–801.

Cheng, G., Zhong, J., Chung, J., and Chisari, F.V. (2007). Double-stranded DNA and double-stranded RNA induce a common antiviral signaling pathway in human cells. Proc. Natl. Acad. Sci. USA *104*, 9035–9040.

Deng, L., Wang, C., Spencer, E., Yang, L., Braun, A., You, J., Slaughter, C., Pickart, C., and Chen, Z.J. (2000). Activation of the IkappaB kinase complex by TRAF6 requires a dimeric ubiquitin-conjugating enzyme complex and a unique polyubiquitin chain. Cell *103*, 351–361.

Hornung, V., Ellegast, J., Kim, S., Brzozka, K., Jung, A., Kato, H., Poeck, H., Akira, S., Conzelmann, K.K., Schlee, M., et al. (2006). 5′-Triphosphate RNA is the ligand for RIG-I. Science *314*, 994–997.

Howe, J.G., and Shu, M.D. (1993). Upstream basal promoter element important for exclusive RNA polymerase III transcription of the EBER 2 gene. Mol. Cell. Biol. *13*, 2655–2665.

Hu, P., Wu, S., Sun, Y., Yuan, C.C., Kobayashi, R., Myers, M.P., and Hernandez, N. (2002). Characterization of human RNA polymerase III identifies orthologues for Saccharomyces cerevisiae RNA polymerase III subunits. Mol. Cell. Biol. *22*, 8044–8055.

Ishii, K.J., Coban, C., Kato, H., Takahashi, K., Torii, Y., Takeshita, F., Ludwig, H., Sutter, G., Suzuki, K., Hemmi, H., et al. (2006). A Toll-like receptor-independent antiviral response induced by double-stranded B-form DNA. Nat. Immunol. *7*, 40–48.

Ishii, K.J., Kawagoe, T., Koyama, S., Matsui, K., Kumar, H., Kawai, T., Uematsu, S., Takeuchi, O., Takeshita, F., Coban, C., et al. (2008). TANK-binding kinase-1 delineates innate and adaptive immune responses to DNA vaccines. Nature *451*, 725–729.

Jaehning, J.A., and Roeder, R.G. (1977). Transcription of specific adenovirus genes in isolated nuclei by exogenous RNA polymerases. J. Biol. Chem. *252*, 8753–8761.

Kawai, T., Takahashi, K., Sato, S., Coban, C., Kumar, H., Kato, H., Ishii, K.J., Takeuchi, O., and Akira, S. (2005). IPS-1, an adaptor triggering RIG-I- and Mda5-mediated type I interferon induction. Nat. Immunol. *6*, 981–988.

Lerner, M.R., Andrews, N.C., Miller, G., and Steitz, J.A. (1981). Two small RNAs encoded by Epstein-Barr virus and complexed with protein are precipitated by antibodies from patients with systemic lupus erythematosus. Proc. Natl. Acad. Sci. USA *78*, 805–809.

Meylan, E., Curran, J., Hofmann, K., Moradpour, D., Binder, M., Bartenschlager, R., and Tschopp, J. (2005). Cardif is an adaptor protein in the RIG-I antiviral pathway and is targeted by hepatitis C virus. Nature *437*, 1167–1172.

Okabe, Y., Kawane, K., Akira, S., Taniguchi, T., and Nagata, S. (2005). Toll-like receptor-independent gene induction program activated by mammalian DNA escaped from apoptotic DNA degradation. J. Exp. Med. *202*, 1333–1339.

Opitz, B., Vinzing, M., van Laak, V., Schmeck, B., Heine, G., Gunther, S., Preissner, R., Slevogt, H., N'Guessan, P.D., Eitel, J., et al. (2006). Legionella pneumophila induces IFNbeta in lung epithelial cells via IPS-1 and IRF3, which also control bacterial replication. J. Biol. Chem. *281*, 36173–36179.

Pichlmair, A., Schulz, O., Tan, C.P., Naslund, T.I., Liljestrom, P., Weber, F., and Reis e Sousa, C. (2006). RIG-I-mediated antiviral responses to single-stranded RNA bearing 5′-phosphates. Science *314*, 997–1001.

Rasmussen, S.B., Sorensen, L.N., Malmgaard, L., Ank, N., Baines, J.D., Chen, Z.J., and Paludan, S.R. (2007). Type I interferon production during herpes simplex virus infection is controlled by cell-type-specific viral recognition through Toll-like receptor 9, the mitochondrial antiviral signaling protein pathway, and novel recognition systems. J. Virol. *81*, 13315–13324.

Ronnblom, L., and Pascual, V. (2008). The innate immune system in SLE: type I interferons and dendritic cells. Lupus *17*, 394–399.

Rosa, M.D., Gottlieb, E., Lerner, M.R., and Steitz, J.A. (1981). Striking similarities are exhibited by two small Epstein-Barr virus-encoded ribonucleic acids and the adenovirus-associated ribonucleic acids VAI and VAII. Mol. Cell. Biol. *1*, 785–796.

Saito, T., Owen, D.M., Jiang, F., Marcotrigiano, J., and Gale, M., Jr. (2008). Innate immunity induced by composition-dependent RIG-I recognition of hepatitis C virus RNA. Nature *454*, 523–527.

Samanta, M., Iwakiri, D., Kanda, T., Imaizumi, T., and Takada, K. (2006). EB virus-encoded RNAs are recognized by RIG-I and activate signaling to induce type I IFN. EMBO J. *25*, 4207–4214.

Schramm, L., and Hernandez, N. (2002). Recruitment of RNA polymerase III to its target promoters. Genes Dev. *16*, 2593–2620.

Schroder, K., Muruve, D.A., and Tschopp, J. (2009). Innate immunity: cytoplasmic DNA sensing by the AIM2 inflammasome. Curr. Biol. *19*, R262–R265.

Seth, R.B., Sun, L., Ea, C.K., and Chen, Z.J. (2005). Identification and characterization of MAVS, a mitochondrial antiviral signaling protein that activates NF-kappaB and IRF 3. Cell *122*, 669–682.

Sun, Q., Sun, L., Liu, H.H., Chen, X., Seth, R.B., Forman, J., and Chen, Z.J. (2006). The specific and essential role of MAVS in antiviral innate immune responses. Immunity *24*, 633–642.

Takaoka, A., Wang, Z., Choi, M.K., Yanai, H., Negishi, H., Ban, T., Lu, Y., Miyagishi, M., Kodama, T., Honda, K., et al. (2007). DAI (DLM-1/ZBP1) is a cytosolic DNA sensor and an activator of innate immune response. Nature *448*, 501–505.

Wu, L., Pan, J., Thoroddsen, V., Wysong, D.R., Blackman, R.K., Bulawa, C.E., Gould, A.E., Ocain, T.D., Dick, L.R., Errada, P., et al. (2003). Novel small-molecule inhibitors of RNA polymerase III. Eukaryot. Cell *2*, 256–264.

Xu, L.G., Wang, Y.Y., Han, K.J., Li, L.Y., Zhai, Z., and Shu, H.B. (2005). VISA is an adapter protein required for virus-triggered IFN-beta signaling. Mol. Cell *19*, 727–740.

Yoneyama, M., Kikuchi, M., Natsukawa, T., Shinobu, N., Imaizumi, T., Miyagishi, M., Taira, K., Akira, S., and Fujita, T. (2004). The RNA helicase RIG-I has an essential function in double-stranded RNA-induced innate antiviral responses. Nat. Immunol. *5*, 730–737.

Yoshida, H., Okabe, Y., Kawane, K., Fukuyama, H., and Nagata, S. (2005). Lethal anemia caused by interferon-beta produced in mouse embryos carrying undigested DNA. Nat. Immunol. *6*, 49–56.